DASA-13.018

AD 644823

R 502

Technical Report

DYNAMIC SHEAR STRENGTH OF

REINFORCED CONCRETE BEAMS

PART II

January 1967

NAVAL FACILITIES ENGINEERING COMMAND

U. S. NAVAL CIVIL ENGINEERING LABORATORY

Port Hueneme, California

D D C

JAN 1 1 1967

B

DYNAMIC SHEAR STRENGTH OF REINFORCED CONCRETE BEAMS - PART II

Technical Report R-502

Y-F008-08-02-110, DASA-13.018

by

Richard H. Seabold

ABSTRACT

A series of reinforced concrete beams was tested to study shear and diagonal tension in beams under dynamic load. The tests constitute the second phase of a continuing program to determine criteria for the minimum amount of web reinforcement required for developing the ultimate flexural resistance of beams, and to determine the difference between these criteria for static and dynamic loading.

The primary objectives of this Part II series of tests were (1) to determine the minimum amount of web reinforcement necessary to force flexural failures; (2) to confirm, under uniformly distributed loads, a formula for shear resistance recommended by a joint committee of the American Concrete Institute (ACI) and the American Society of Civil Engineers (ASCE), which is based on the analysis of data from tests with concentrated loads; (3) to confirm the coefficients suggested in Part I of this program for the dynamic increase in shearing strength; and (4) to study the influence of stirrup arrangement and type of loading on the location of the critical diagonal tension crack.

Fifteen beams were tested, eight loaded dynamically and seven statically. Each beam was simply supported and all loads were uniformly distributed. Twelve beams contained web reinforcement in the region of the critical section, and three had none there. Major variables were type of loading (static and dynamic), magnitude of dynamic load, and stirrup spacing.

It was found that the shear strength of reinforced concrete beams is greater under dynamic load than under static load, and that a formula for designing simply supported beams subjected to concentrated static loads recommended by the joint ACI-ASCE committee could be modified for designing simply supported beams subjected to uniformly distributed dynamic loads.

Design recommendations are given (1) for determining the maximum applied dynamic shearing force, (2) for determining the location of the critical section where cracking and yielding occur in shear, and (3) for determining the usable ultimate shear strength.

CONTENTS

INTRODUCTION

Objectives of the Program

In order to meet the Navy requirement for development of design criteria for protective construction, there is a need for knowledge of the resistance and behavior in shear of reinforced concrete beams under dynamic load. Although many investigators have studied the static shear resistance of beams, this continuing program being conducted by the Naval Civil Engineering Laboratory (NCEL) is the first known effort to study the dynamic shear resistance. The objectives of the program are to determine criteria for the minimum amount of web reinforcement required for developing the ultimate flexural resistance of beams and to determine the difference between these criteria for static and dynamic loading.

Previous Work

NCEL Technical Report R-395, Dynamic Shear Strength of Reinforced Concrete Beams - Part I[1] covers the first phase of the program. The work reported in Part I consisted of a literature search, a theoretical study, and the testing of nine reinforced concrete beams.

The literature search did not yield any information regarding dynamic shear resistance. It did yield information regarding static shear resistance, much of which is summarized by the report of the ACI-ASCE Joint Committee 326, "Shear and Diagonal Tension."[2] The following equations, the first empirical and the second semi-empirical, were selected by Committee 326 as the basis for design criteria for statically loaded beams:

$$v_c = \frac{V_c}{bd} = 1.9 \sqrt{f_c'} + 2,500\, p\left(\frac{Vd}{M}\right) \qquad \leq 3.5 \sqrt{f_c'} \qquad (1)$$

$$v_u = \frac{V_u}{bd} = Krf_y + v_c \qquad \leq 10 \sqrt{f_c'} \qquad (2)$$

where
v_c = shearing strength at critical section contributed by concrete

v_u = usable ultimate shearing strength at critical section

V_c = total shear resistance at critical section contributed by concrete

V_u = usable total shear resistance at critical section

b = width of beam

d = effective depth of beam

f_c' = compressive strength of concrete at 28 days

Krf_y = shearing strength at critical section contributed by web reinforcement

K = $(\sin \alpha + \cos \alpha) \sin \alpha$

α = angle of inclination of web reinforcement

p = ratio of cross-sectional areas of longitudinal tension steel and effective concrete

$\dfrac{V}{M}$ = ratio of shear to moment at critical section

f_y = static yield strength of steel

1

Equation 1 is intended for designing beams without web reinforcement in the critical section and is based on the following concepts and observations: (1) Diagonal tension is a combined stress involving horizontal tensile stress due to bending as well as shearing stress. (2) Since failure due to shear can occur with the formation of the critical diagonal crack if redistribution of internal forces is not accomplished in design, the load causing the formation of the critical diagonal tension crack is generally considered as the ultimate load-carrying capacity of a reinforced concrete member without web reinforcement. (3) Distribution of shear and flexural stress over a cross section of reinforced concrete is not known. Committee 326 studied the data from more than 440 beam tests and concluded that the three significant parameters are percentage of longitudinal reinforcement, p, the dimensionless quantity, M/Vd, and the quality of the concrete, f_c'. The empirical equation was obtained by fitting the parameters to the data from 194 tests on beams with simple supports and concentrated loads. At a later time, data from other tests with different conditions of loading and restraint correlated well with values computed using the equation.

Equation 2 is intended for designing beams with web reinforcement at the critical section, and is based on the following concepts and observations: (1) Failure can occur in diagonal tension upon diagonal cracking, in shear-compression upon yielding of the web reinforcement, or in compression prior to yielding of the web reinforcement; shear-compression is the most common mode of failure in normally proportioned beams. (2) The ultimate shearing capacity is the sum of the shearing capacity at diagonal cracking plus a contribution from the web reinforcement at the point where yielding of the web reinforcement occurs. (3) The concept of truss analogy can be used to analyze the stress in the web reinforcement. The semi-empirical equation was obtained by summing the empirical terms for the cracking resistance and the rational truss analogy term for the contribution from web reinforcement. From the above concepts and observations, Keenan[1] concludes that the effective amount of web reinforcement required to produce a flexural failure is a function of the difference between the shears corresponding to the ultimate flexural resistance and the diagonal tension cracking resistance. Tests on beams with web reinforcement to support Equation 2 were limited both in number and scope.[2]

A rigorous modal analysis of a simply supported beam under a uniformly distributed dynamic load is given in Appendix G of Reference 1, with selected data plotted. Constant mass and stiffness with respect to position along the span, a linear decaying load with respect to time, and zero rise time were assumed. Damping was considered. Equations were derived for the deflection, moment, and shear along the span; the maximum dynamic shear factor at the supports; and the shear-moment ratio along the span. Plots of computed data indicated that the shear distribution and shear-moment ratio along the span for dynamic loading did not vary widely from those for static loading. Therefore, it seemed logical that for design criteria, Equations 1 and 2 can be modified to include the effects of dynamic loading. The shearing stresses at the critical section corresponding to diagonal tension cracking and yielding of the web steel may be expressed as

$$v_c = C_1\left(1.9\sqrt{f_c'}\right) + 2,500\, pd\left(\frac{V}{M}\right) \qquad \therefore\ C_1\left(3.5\sqrt{f_c'}\right) \tag{3}$$

$$v_u = C_2\left(Krf_y\right) + v_c \qquad \leq C_1\left(10\sqrt{f_c'}\right) \tag{4}$$

where C_1 is a coefficient for the dynamic increase in concrete tensile strength and C_2 is a coefficient for the dynamic increase in web steel tensile strength. For static loading, $C_1 = C_2 = 1$.

2

Nine beams were tested by Keenan,[1] three loaded statically and six dynamically. Each beam was simply supported at its ends, all loads were uniformly distributed, and all web reinforcement consisted of vertical stirrups made from No. 2 deformed reinforcing bars. Four of the dynamically loaded beams did not fail under the first loading. These were subjected to repeated loading until failure occurred. The following conclusions were made by Keenan from the results of the tests:

(1) The maximum dynamic shear at the supports was greater than the shear produced by the same peak load applied statically and increased with peak load and load duration. If the tension steel did not yield at midspan, the maximum shear occurred when the midspan deflection first reached a maximum value. If the tension steel did yield at midspan, the maximum shear occurred at that yielding. (2) Under both static and dynamic loading, the web reinforcement was effective only after the formation of the critical diagonal crack. When the crack formed there was a pronounced increase in the magnitude and rate of straining in stirrups located near the crack. (3) There was no apparent change in the location of the critical diagonal crack under dynamic load; the variation in crack location was about the same for static and dynamic loads. (4) Yielding of the stirrups did not trigger collapse of the beam. In general, the first stirrup to yield was located a distance from the support equal to about one-tenth the span length. (5) The strain rates in the stirrups crossed by the critical diagonal crack were greater than the strain rates in the longitudinal tension steel at midspan. (6) A stirrup arrangement with values of Krf_y 69% less than the value required by the ACI-ASCE formula for static beams forced flexural failure at midspan under both static and dynamic loads. (7) The proposed ACI-ASCE formula for the ultimate shear resistance yielded values which were consistently less than the measured values. (8) The shears at the supports corresponding to diagonal cracking and first yielding of the stirrups were greater under dynamic load and were predictable from the following equations:

$$\frac{V_c'}{bd} = \frac{L}{L - 2x_c}\left[1.7\left(1.9\sqrt{f_c'}\right) + 2,500\ pd\left(\frac{V}{M}\right)_c\right] \tag{5}$$

$$\frac{V_u'}{bd} = \frac{L}{L - 2x_c}\left[1.7\left(1.9\sqrt{f_c'}\right) + 2,500\ pd\left(\frac{V}{M}\right)_c + 1.4\ rf_y\right] \tag{6}$$

where
V_c' = total shear resistance at support contributed by concrete

V_u' = usable total shear resistance at support

L = length of span, center to center of supports

x_c = distance from center of support to critical section

1.7 = C_1, coefficient for dynamic increase in concrete tensile strength

1.4 = C_2, coefficient for dynamic increase in web steel tensile strength

$\left(\frac{V}{M}\right)_c$ = shear-moment ratio at critical section

Shears were computed at the supports rather than at the critical section for convenience in comparing measured and computed results, shear being easily measured at the supports. It should be noted that Equations 5 and 6 apply to uniformly distributed loads only, since the multiplier $L/(L - 2x_c)$ derives from the assumption of linear shear distribution along the span.

Theory

In designing reinforced concrete beams to resist diagonal tension under dynamic or static loading, the designer has three distinct problems: (1) to determine how much shear will be imposed at the critical section by a given load, (2) to determine how much shear can be resisted by the beam at the critical section, and (3) to determine the location of the critical section.

Classical methods, which are well established, give the designer a means of solving the first problem with considerable accuracy for static loading. For dynamic loading, inertia forces complicate the problem. Rigorous modal analysis methods have been used to plot curves or provide tabulated data for various conditions of loading and restraint in dynamic design, but these methods usually produce shear values at the supports instead of at the critical section. Since the shear is a complicated function of both time and position along the span, it is difficult to obtain easily used design data for the applied shear at points other than at the supports. Equations and computed data from methods such as presented in Appendix G of Reference 1 must undergo considerable simplification before they can be applied to practical design problems.

For the second problem - determining how much shear can be resisted by the beams at the critical section - a lack of knowledge about the shear distribution over a cross section, about the stress trajectories, the formation and propagation of cracks, and the failure mechanism has resulted in the rejection of rigorous and rational approaches. Recommended design criteria for static loading are empirical equations based on observation of a large number of tests, but these tests are mostly limited to static concentrated loads. Therefore, a question arises as to whether these criteria can be modified for application to other conditions of load distribution and restraint, and to dynamic loading. Equations 3 and 4 are suggested for modifying Equations 1 and 2.

The ACI-ASCE Joint Committee 326 [2] did not recommend a method for determining the location of the critical section which is needed to use Equations 1 and 2. The Committee concluded that for simple supports and static concentrated loads, the designer will be conservative in assuming the critical section to be a distance from the support equal to the effective depth of the beam. The application of this rule to other conditions of loading and restraint is questionable. Keenan's data [1] indicate that the distance to the critical section of those beams tested with simple supports, uniformly distributed load, and both static and dynamic loading was equal to approximately one-tenth the span length. A method is presented in Appendix A of this report for approximating the position of the critical section for both static and dynamic loads using the static shear distribution and Equation 3. Accurate results cannot be expected because of the simplifying assumption regarding shear distribution and the fact that this empirical equation was primarily intended for predicting stress rather than location.

Definitions

Terminology and notation in this report follow as closely as practical those of Committee 326 [2] and Keenan. [1] However, for the evaluation of experimental data, it is necessary to define in specific detail certain terms which might conflict or might have been given general connotations in the past.

Flexural cracks are caused by bending forces only. Diagonal tension cracks, also called shear cracks, are caused by diagonal tension forces which are combined shear and bending forces. The critical diagonal tension crack, also called the critical diagonal crack, is a shear crack which forms at the critical section. The critical section is the transverse cross section with the smallest ratio of resisting shear to applied shear. Therefore, the location of the critical section depends on the conditions of loading and restraint as well as the cross section along the beam. In the experiments reported herein, unless otherwise noted, the location of the critical section is measured from the center of the support along the longitudinal tension steel to the critical diagonal crack.

4

For under-reinforced beams like those in the tests reported herein, yielding of the longitudinal steel at midspan constitutes flexural yielding. Yielding of one stirrup in tension or the concrete in compression near the critical section constitutes yielding in shear. Since redistribution of internal stresses can occur after flexural yielding and yielding in shear, it is possible for both types of yielding to occur prior to failure. Either type of yielding constitutes yielding of the beam.

Rupture of any component, excluding cracking of the concrete, constitutes failure of the beam. Flexural failure occurs upon crushing of the concrete at midspan. Shear failures are of three types: diagonal tension failure, which results from diagonal tension cracking if redistribution of internal forces is not accomplished; shear-compression failure, from crushing of the concrete near the critical section after a stirrup has yielded; and compression failure, which results from crushing of the concrete near the critical section prior to yielding of a stirrup. A beam is said to have failed in shear or flexure depending on which type of rupture occurs first.

The ultimate shear strength of a reinforced concrete beam is the average unit shearing stress at the critical section upon the incidence of shear failure. Committee 326 states: "The load causing formation of a critical diagonal tension crack must ordinarily be considered in design as the usable ultimate load-carrying capacity of a reinforced concrete member without web reinforcement."[2] Therefore, in this report, the usable ultimate shear strength of reinforced concrete beams without web reinforcement is considered as the average unit shearing stress at the critical section corresponding to formation of a critical diagonal tension crack. As inferred by Equation 2, the usable ultimate shear strength of reinforced concrete beams with web reinforcement is considered as the average unit shear stress at the critical section corresponding to yielding in shear.

A few notations in this report are different from those in Part I. Such changes were made in the interest of simplicity, order, standardization, and conformance with ACI designation. In general, uppercase letters are used to indicate forces while lowercase letters indicate forces per unit area. For example, V_u is the usable ultimate shear resistance (total force), while v_u is the usable ultimate unit shearing stress (force per unit area). Where it is necessary to indicate location at the support rather than at the critical section, primed symbols are used to specify location at the support. For example. V_u' is the ultimate shear resistance at the support while V_u is the usable ultimate shear resistance at the critical section. In this report, a d is added to the subscripts of symbols to denote the dynamic case. For instance, f_y is the yield strength of steel and f_{dy} denotes the dynamic yield strength of steel.

Notations in Appendix C, Instrumentation, conform to manufacturer symbology.

In Part I, the beam ends were designated left and right, designations which depend on the direction from which the beams are photographed or observed. In Part II, the beam ends are designated east and west to indicate the precise position of the beams during the test. Shear failures in both series of tests were anticipated at the weaker end: these correspond to the left end in Part I and the east end in Part II.

EXPERIMENT

Objectives

The primary objectives of this Part II investigation were (1) to determine the minimum amount of web reinforcement required to force flexural failures, (2) to confirm the validity of the Committee 326 formulas[2] in the case of uniformly distributed loads, (3) to confirm the coefficients suggested by Keenan[1] for the dynamic increase in shear strength, and (4) to study the influence of stirrup arrangement and type of loading on the location of the critical diagonal crack. A subordinate objective was to study the effectiveness of stirrups through a range of small values of Krf_y.

Experiment Plan

To pursue the objectives, a series of tests on reinforced concrete beams was planned as shown in Table 1. The variable parameters were type of loading (static and dynamic), magnitude of the load, and stirrup spacing. The dominant parameters held constant were distribution of the load, duration of the dynamic loads, restraint condition, geometry of the beam, flexural cross section, strength of materials, and stirrup diameter. All 15 beams were doubly reinforced, simply supported, and subjected to uniformly distributed loads. Three beams with stirrups were planned for each combination of type of loading and stirrup spacing, plus one beam without stirrups for each type of loading. Two changes to the plan were made during the experiment. The test for beam OE3 was added to pursue the objectives of the test for OE1 after the success of the latter became limited by difficulties in controlling and measuring the load. The type of loading for test of beam WE12 was changed from static to dynamic to replace data lost during the test for WE4 when the recording system failed.

Table 1. Experiment Plan

Constant test parameters:

L = 12 ft 0 in.	A_s = 2 No. 9 bars	f_c' = 3,000 psi
b = 7.75 in.	A_s' = 2 No. 7 bars	f_y = 70,000 psi
d = 12.94 in.	p = 0.0199	A_v = 0.0346 in.^{2}
d' = 1.50 in.	p' = 0.0120	f_y = 40,000 psi for stirrups

Beam No.	Type of Load	Amount of Load [1] (lb/in.)	Stirrup Spacing (in.)
WE1	Dynamic	607	5
WE2	Dynamic	486	5
WE3	Dynamic	486	5
WE4	Dynamic	486	3
WE5	Dynamic	486	3
WE6	Dynamic	486	3
WE7	Static	To collapse	5
WE8	Static	To collapse	5
WE9	Static	To collapse	5
WE10	Static	To collapse	3
WE11	Static	To collapse	3
WE12	Dynamic	607	3
OE1	Static	To collapse	∞
OE2	Dynamic	486	∞
OE3	Static	To collapse	∞

[1] Static test loads to be increased slowly from zero to collapse. Dynamic test loads to be of long duration, with peak overpressure as shown.

With all other parameters constant, the stirrup spacing can be varied to obtain both shear and flexural failures. Interpolation of data over the interval where mode of failure changes can then be used to determine the minimum amount of web reinforcement required to force flexural failures, thus satisfying the first objective of the experiment. Theory and experience indicated that, for the statically designed beam selected for testing, a stirrup spacing of about 3.5 inches would provide equal probability of failure in shear or flexure. Thus, spacings of 5 inches and 3 inches were planned to insure the occurrence of both shear and flexural failures. Identical beams were provided in the plan to be tested under two different dynamic loadings so that a study could be made on the effect of both the type of loading and the magnitude of dynamic loading on the minimum amount of web reinforcement required to force flexural failures.

All the statically loaded beams were to be used in satisfying the second objective, to confirm the validity of the Committee 326 formulas in the case of uniformly distributed loads. The test with the statically loaded beam without stirrups was planned to indicate whether the stirrups have any effect on the critical diagonal cracking strength, and to aid in determining the portion of the ultimate usable shear strength provided by the stirrups.

All the beams were to be used in satisfying the third objective, to confirm the coefficients suggested by Keenan for the dynamic increase in shear strength. Comparison between dynamic and static tests and between beams with and without web reinforcement, and information obtained from dynamic tests on stirrup coupons were used for determining the coefficients C_1 and C_2 in Equations 3 and 4.

None of the beams were specifically planned for accomplishment of the fourth objective, to study the location of the critical diagonal crack, but all contributed toward fulfilling that objective.

It was desired to keep the same beam cross section as used in Part I[1] and vary only Krf_y so as not to change too many parameters at once, and to permit rapid comparison of Part I and Part II data. Using the cross section of the Part I beams, very small values of Krf_y were required to insure shear failures; therefore, the subordinate objective, to study small values of Krf_y, was happenstance and not necessarily a planned study.

Test Specimens

Description. Fifteen specimens with a 12-foot span between supports were fabricated. All had rectangular cross sections of 7.75-inch width, 12.94-inch effective depth, and 15-inch total depth. The distance from the top surface to the center of the compression steel was 1.5 inches. All beams were doubly reinforced with two No. 9 deformed bars in tension and two No. 7 bars in compression. All had vertical box-type stirrups hooked to the compression steel. Beams with stirrups in the region of the critical section were designated WE1 through WE12, and those without stirrups in this region, OE1 through OE3. Termed the E Series, the specimens were identical to those of the D Series of Part I[1] except for stirrup material, size, and spacing. There were three types of beams: Type I - those with 5-inch spacing between stirrups in the critical region, Type II - those with 3-inch spacing there, and Type III - beams without stirrups in the critical region. Details are shown in Figures 1, 2, and 3. The ends of each beam were supported on and bolted to 10-inch-long by 1-inch-thick bearing plates which were free to translate horizontally and to rotate.

The beams were intended to fail in shear near the east end or in flexure at midspan; therefore, the stirrups were spaced closer together near the west end. The departure from symmetry in the design was not large enough to cause unsymmetrical flexural response, but large enough to preclude shear failure near the west end. Stirrups made from No. 2 bars were utilized to hold the longitudinal bars firmly in place during fabrication.
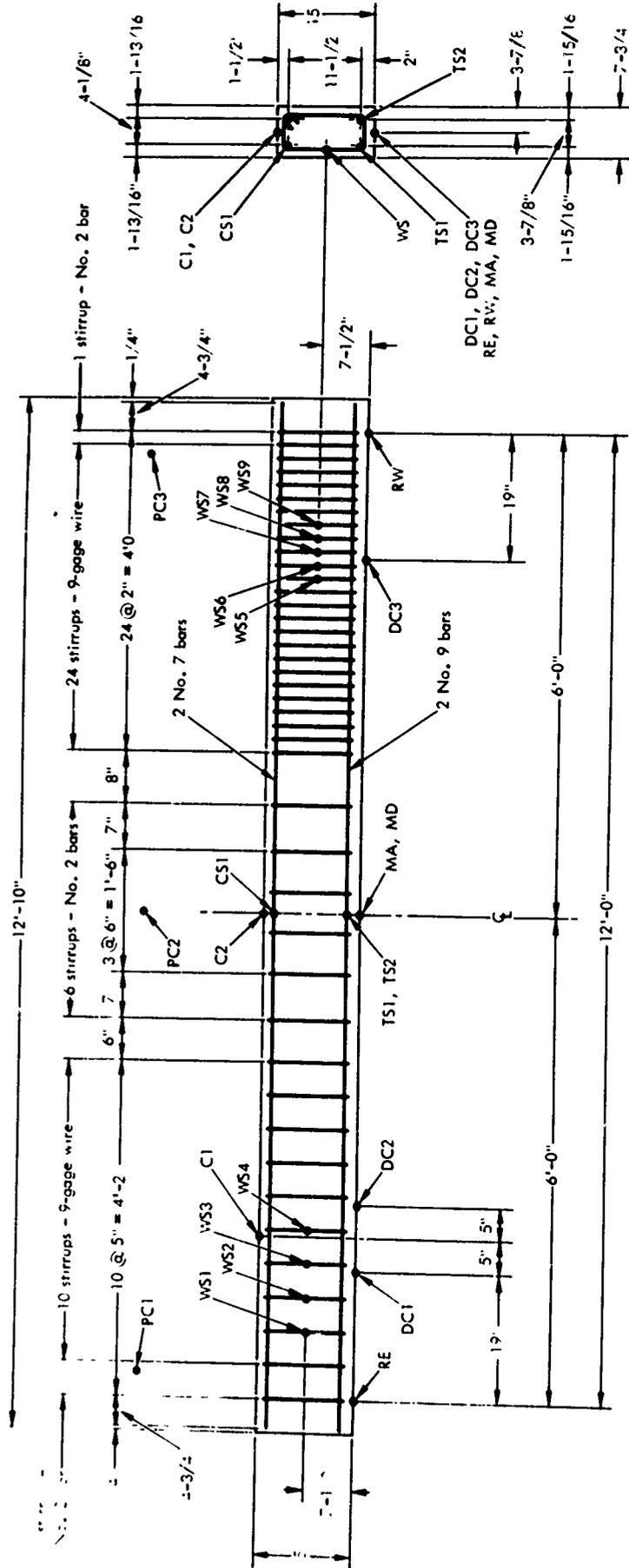
7

Figure 1. Details and instrumentation, beam Type I – 5-inch spacing between stirrups in the critical region.
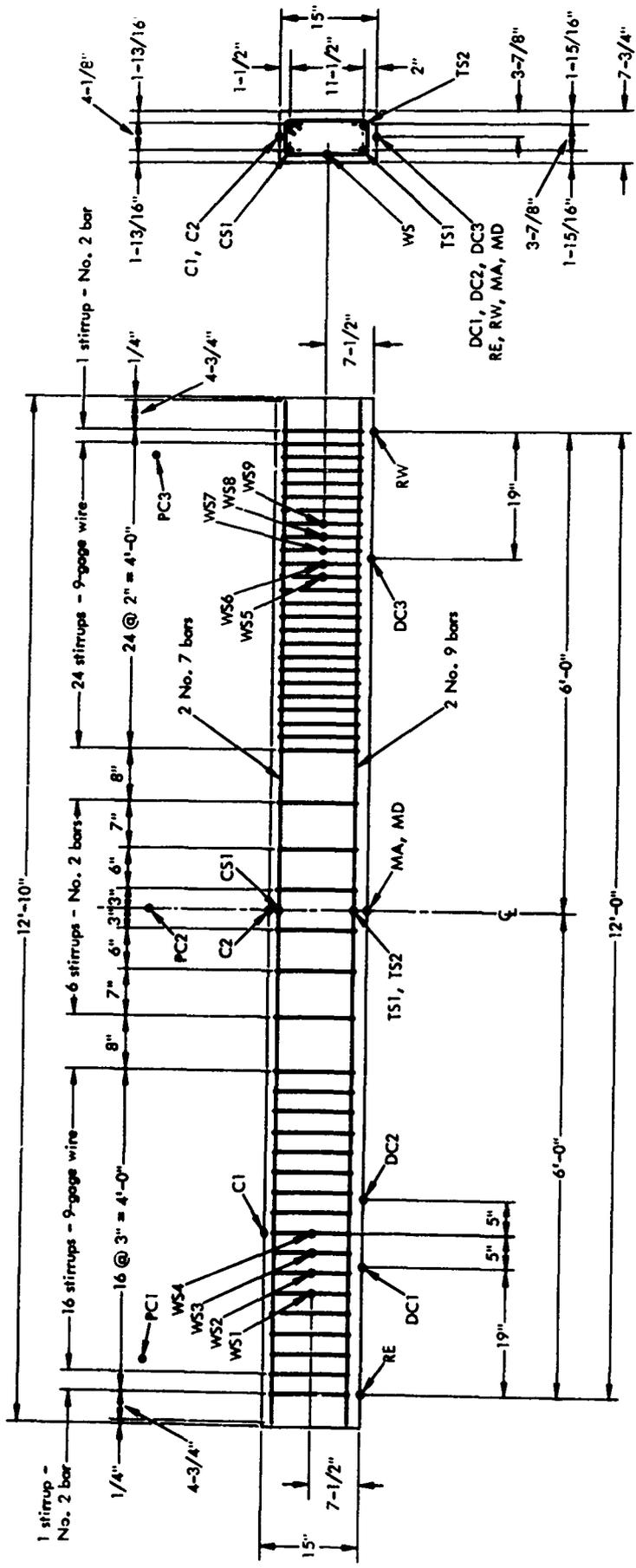
Mark	Measurement
C1, C2	Concrete strain
CS1	Compression steel strain
DC1, DC2, DC3	Depth change
MA	Midspan acceleration
MD	Midspan deflection

Mark	Measurement
PC1, PC2, PC3	Overpressure
RE	Reaction, east
RW	Reaction, west
TS1, TS2	Tension steel strain
WS1...WS9	Stirrup (web steel) strain

8

Figure 2. Details and instrumentation, beam Type II – 3-inch spacing between stirrups in the critical region.
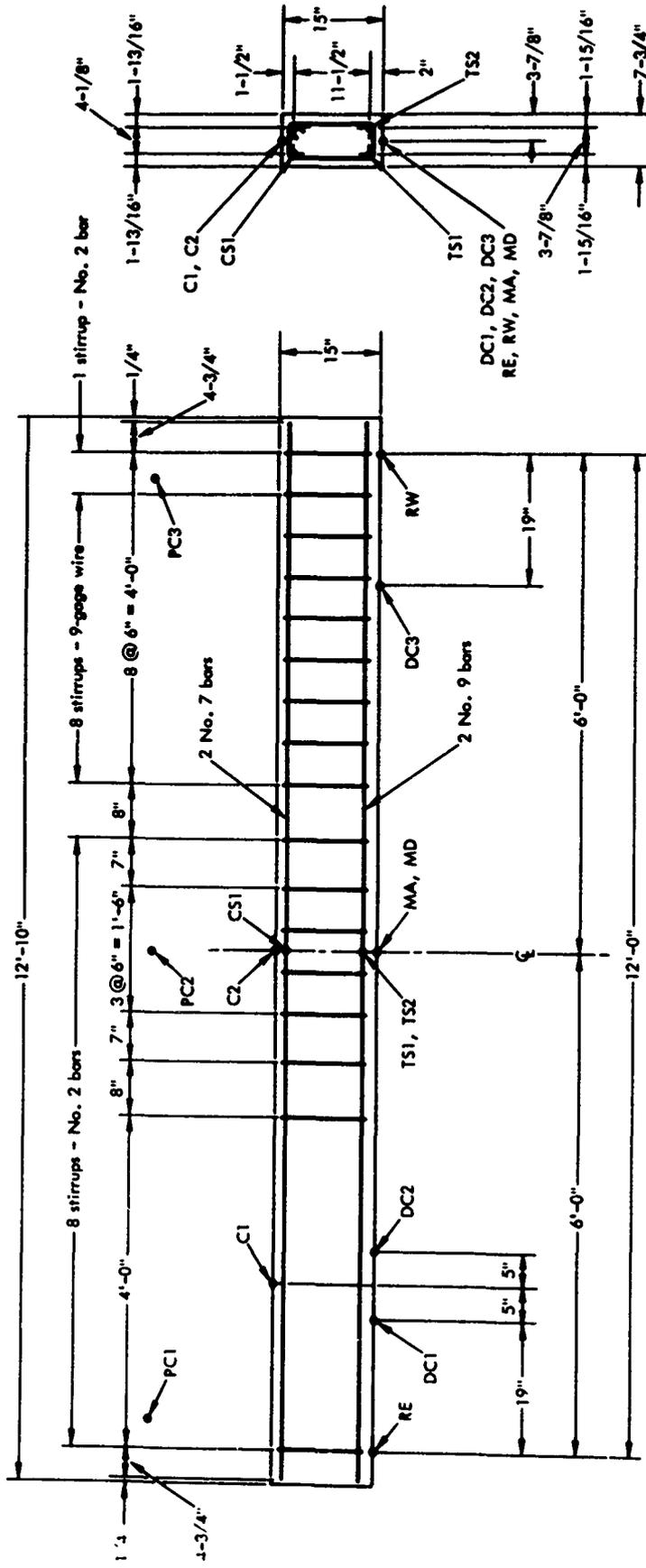
9

Figure 3. Details and instrumentation, beam Type III – without stirrups in the critical region.

Mark	Measurement
C1, C2	Concrete strain
CS1	Compression steel strain
DC1, DC2, DC3	Depth change
MA	Midspan acceleration
MD	Midspan deflection

Mark	Measurement
PC1, PC2, PC3	Overpressure
RE	Reaction, east
RW	Reaction, west
TS1, TS2	Tension steel strain

Material Properties. Tests on concrete control cylinders and steel coupons to determine the static and dynamic material properties of the beams are discussed and the results given in Appendix B. Also, the static material properties are summarized in Table 2. The concrete mix proportions were $1.00:3.82:3.66$ by weight, with a water-cement ratio of 0.71 by weight, cement factor of 4.7, maximum aggregate size of 3/4 inch, and sand fineness modulus of 2.82. The average static strength at 28 days was 3,660 psi in compression and 410 psi in tension. The dynamic tensile splitting strength increased about 70% when the concrete cylinders were stressed at a rate of 300,000 psi per second. The longitudinal reinforcing steel satisfied the strength requirements of Specification A432 and the deformation requirements of Specification A305-56T of the American Society for Testing and Materials (ASTM). The average static upper yield strength was 67,600 psi for No. 9 bars and 65,900 psi for No. 7 bars. For both sizes, the tangent modulus of elasticity was 29×10^6 psi. The dynamic upper yield strength increased by 24% when coupons were strained at a rate of 0.3 in./in./sec. The stirrups used in the region of the critical section were made from 9-gage bright annealed plain wire. The average static upper yield strength was 36,000 psi, and the secant modulus of elasticity taken to a point between the proportional limit and the upper yield point was 29×10^6 psi. The modulus was obtained from the idealized stress-strain relationship shown in Figure B-4 of Appendix B. Under dynamic loading, the increase in upper yield strength varied logarithmically with respect to strain rate from about 50% at a strain rate of 0.2 in./in./sec to 100% at 3.0 in./in./sec. The increase was about 80% at a strain rate of 1 in./in./sec.

Table 2. Static Material Properties of Beams

Material properties common to all beams:

$E = 29 \times 10^6$ psi for compression steel, tension steel, and stirrups $p' = 0.0119$ $f_y = 36,000$ psi

$p = 0.0198$ $A_v = 0.0346$ sq in. for stirrups

Beam No.	Concrete			Longitudinal Steel		Stirrups			
				Tension	Compression	East End		West End	
	Age (days)	f_c' (psi)	f_t (psi)	f_y (ksi)	f_y (ksi)	s (in.)	rf_y (psi)	s (in.)	rf_y (psi)
WE1	32	3,010	365	70.6	65.3	5	32.2	2	80.5
WE2	30	4,090	390	68.7	67.5	5	32.2	2	80.5
WE3	35	3,450	403	65.0	66.6	5	32.2	2	80.5
WE4	27	3,580	423	67.4	64.0	3	53.7	2	80.5
WE5	30	3,910	395	68.3	67.7	3	53.7	2	80.5
WE6	33	4,120	452	66.0	68.3	3	53.7	2	80.5
WE7	26	3,320	370	69.5	64.0	5	32.2	2	80.5
WE8	28	3,720	440	67.8	64.9	5	32.2	2	80.5
WE9	23	3,920	447	66.6	67.1	5	32.2	2	80.5
WE10	27	3,930	422	66.2	65.1	3	53.7	2	80.5
WE11	20	3,420	397	67.1	68.0	3	53.7	2	80.5
WE12	27	3,380	393	68.0	64.4	3	53.7	2	80.5
OE1	28	3,400	405	68.8	66.0	∞	0	6	26.8
OE2	27	3,640	432	66.0	65.9	∞	0	6	26.8
OE3	28	4,000	--	--	--	∞	0	6	26.8

Equipment

Loading Machine. The beams were tested in the NCEL blast simulator (Figure 4), which is capable of applying a uniformly distributed static or dynamic load.[3] Dynamic loads are applied by generating expanding gases in the simulator from the detonation of Primacord by means of two blasting caps. The peak pressure is controlled by the amount of Primacord, and the decay time by opening valves which vent the gases to the atmosphere. Static loads are applied by admitting compressed air into the simulator by means of a compressor. The design capacity of the simulator is 185 psi.

Supports. The support configuration is shown in Figures 4 and 5. The test specimens were bolted to the bearing plate, which was free to translate horizontally and to rotate. The beams had a 5-inch overhang measured from the center of the bolt pattern to the end of the beam. Each of the two supports contained a 60-kip-capacity load cell.

Measurements

Instrumentation. The locations of the measurements for each type of beam are shown in Figures 1, 2, and 3. A detailed description of the transducers, strain gages, circuitry, timing equipment, and recording equipment is given in Appendix C. Measurements were taken to study the applied load, shear at the supports, shear behavior at the critical section including propagation of the diagonal tension crack, flexural behavior at midspan, and motion at midspan.

Overpressure. The applied load (overpressure) was measured about 20 inches above the top surface of the beam at three locations along the span. Pressure transducer PC2 was positioned directly above the center of the span, PC1 4 inches from the center of the east support, and PC3 was positioned 4 inches from the center of the west support.

Force. The reactions at the supports (forces) were measured by load cells RE and RW located in the supports (Figure 5). These force measurements, corrected for the effects of the 5-inch overhang, were used to determine the total shearing force at the supports.

Acceleration. In the dynamic tests only, accelerometer MA was attached to the underside of the beam to measure the motion of the beam at midspan. The values obtained were integrated once to obtain velocity and twice to obtain deflection.

Distance. Linear potentiometer MD was located on the underside of the beam to measure the deflection at midspan. Also, a rotating drum operating in conjunction with paper and pencil was used to corroborate measurement MD. The spring-loaded pencil was attached to an insert in the side of the beam 6 inches up from the bottom at midspan, and recorded on paper taped to the rotating drum which was attached to the bottom edge of the simulator wall and powered by an electric motor. In the static tests only, a scale (100 parts to the inch) oriented in the vertical direction was attached with masking tape to the side of the beam at midspan, and a surveyor's transit with the telescope in a fixed position was used to measure the midspan deflection. Linear potentiometers DC1, DC2, and DC3 were used to measure the change in distance between the top and bottom surfaces of the beam in the region of the diagonal tension crack. A 2-inch-square aluminum plate was anchored to the top surface of the beam with hooks. A rod threaded into the plate extended down through a small vertical hole in the beam to the linear potentiometer mounted on the bottom surface of the beam (Figure 6). The measured change in total depth of the beam is the sum of the vertical components of the average concrete strain and the crack widths. This measurement was used mainly as a detector and indicator of crack propagation.

Figure 4. Schematic of beam in NCEL blast simulator.
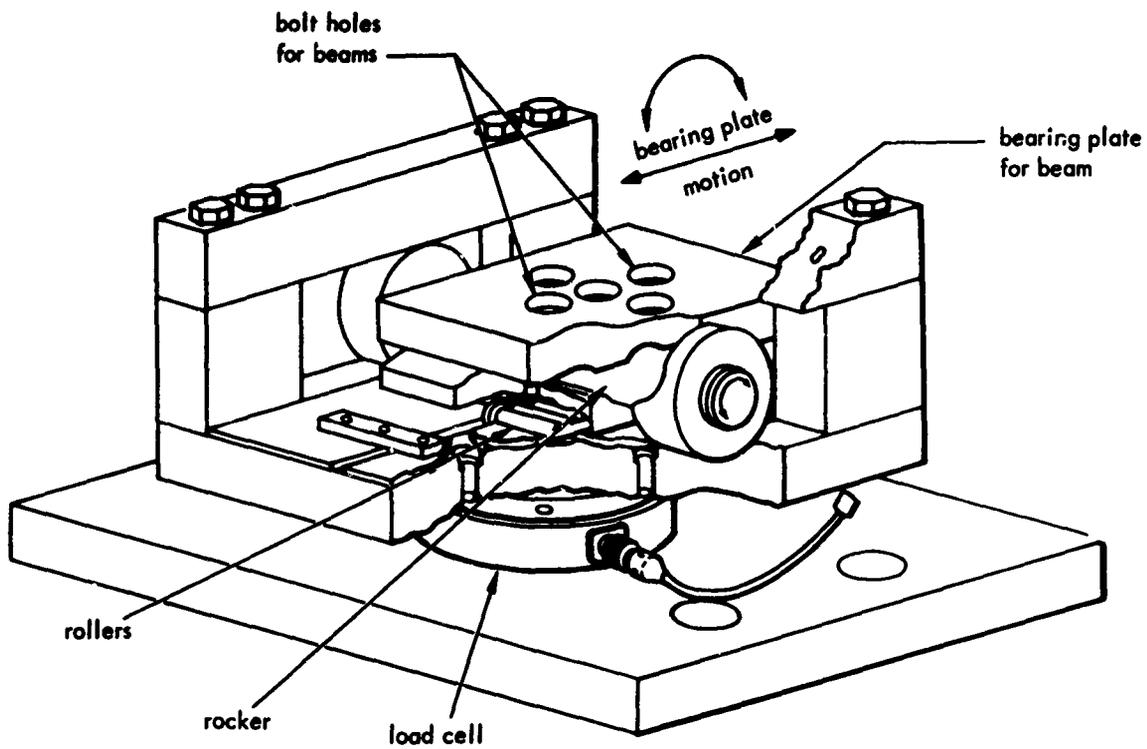
Figure 5. Support configuration.
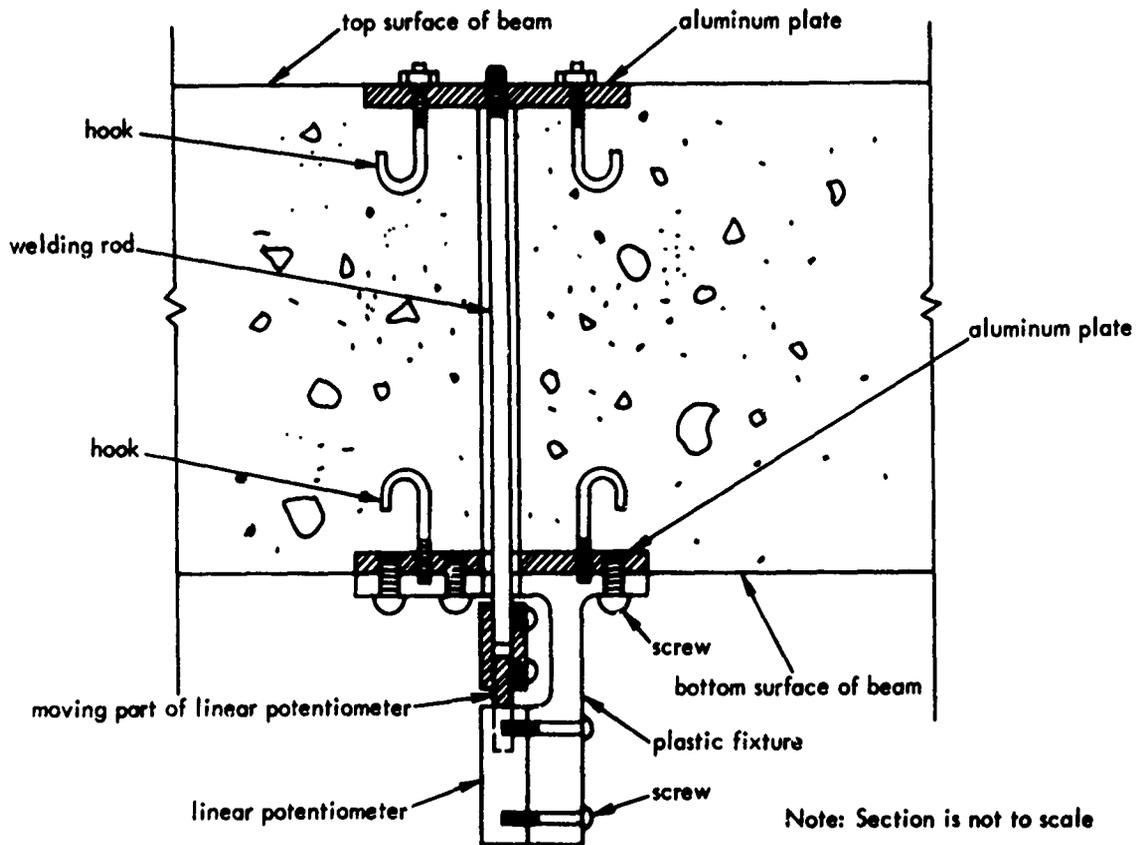
Figure 6. Details of depth change measuring device.

<u>Strain</u>. Strains TS1, TS2, and CS1 in the longitudinal steel at midspan were measured with electronic foil strain gages placed diametrically opposite each other on the bar and wired to form opposite arms of a Wheatstone bridge circuit. Strains C1 and C2 were measured with electronic strain gages bonded to the top surface of the concrete in the longitudinal direction, one at midspan and one in the region of the critical section. Stirrup strains, WS1 through WS9, were measured with one electronic strain gage at each location, bonded to the wire in the vertical direction, and positioned at mid-depth of the beam. The stirrup strain measurements were used to detect cracking, trace crack propagation, and indicate yielding of the stirrups.

Procedure

<u>Fabricating Reinforcing Steel Cages</u>. One cage for each beam was made from the longitudinal reinforcing and the stirrups using the following procedure:

1. The 9-gage wire, received in a 2-foot-diameter coil, was straightened by drawing it by hand through a hole in a wooden block.

2. Samples of the wire were tested to determine the material properties.

3. The wire was formed into box-shaped stirrups by cutting it to the required length and bending it around a pin.

4. The No. 2 bars were formed into stirrups with the step 3 technique.

5. Nine wire stirrups were selected and one strain gage was applied to each, the gage being oriented along the axis of the wire and positioned 6-1/8 inches from the bottom of the stirrup.

6. The longitudinal steel (No. 9 and No. 7 bars) was labeled for identification, cut to the required length, and the coupons were tested to determine the material properties.

7. Deformations were filed from all the No. 9 bars and half of the No. 7 bars at midlength, and two strain gages attached to each filed location; these gages were oriented along the axis of the bar and placed diametrically opposite each other.

8. The longitudinal steel bars (two gaged No. 9 bars, one gaged No. 7 bar, and one ungaged No. 7 bar) were placed on a wooden form which positioned them.

9. The No. 2 stirrups were positioned, and tied with wire to the longitudinal steel. The purpose of the No. 2 stirrups was to hold the longitudinal steel firmly in position during the remainder of steel cage fabrication and concrete casting.

10. The 9-gage wire stirrups were positioned and tied.

11. In the final step, lifting eyes made from No. 2 bars were tied to the longitudinal steel at each end of the beam.

<u>Casting</u>. Thirteen cubic feet of concrete per batch was made of the mix described in Appendix B at the test site in a diesel-powered mixer of 16-cubic-foot capacity. A small quantity of water was added, if necessary, to obtain a slump of about 2 inches. One batch was sufficient to cast one beam and six associated control cylinders.

The reinforcing steel cage was positioned in the steel form by means of small hydrostone cubes wired to the longitudinal bars as spacers against the form sides. Steel sleeves were installed to create the holes for the tiedown bolts at the supports. The small aluminum plates and wires associated with depth change measurements DC1, DC2, and DC3 were set in place. The lead wires from the strain gages were inserted outward through small holes drilled into the side of the form. Finally, a metal insert was positioned for holding the pencil which would record deflection.

The beam and the six test cylinders were cast by shoveling the concrete into the forms and vibrating it with an electric probe-type vibrator. Special care was taken to prevent damage to the wires and fixtures. Finally, the top surfaces of the beam and cylinders were troweled smooth.

Curing. The beam and associated cylinders were removed from the forms about one day after casting and cured under wet burlap until about 2 days before testing. The burlap was watered once a day, five days a week.

Preparing Specimens. The following steps were taken to prepare each beam for testing:

1. The beam was set out to dry for 2 days.

2. Strain gages C1 and C2 were bonded to the top face of the concrete.

3. The wires used to form holes for measurements DC1, DC2, and DC3 were withdrawn and replaced with smaller diameter wires, to prevent bonding between the wire and concrete.

4. Transducers DC1, DC2, and DC3 were fastened to the beam.

5. The sides of the beam were whitewashed to emphasize the crack pattern in the concrete during the test and lined with black paint to indicate the location of the stirrups and longitudinal reinforcement.

6. After the beam was positioned and bolted on the support devices, the lifting eyes were cut off and the entire assembly was wheeled into position in the blast simulator and anchored to the concrete foundation.

7. A strip of neoprene was placed over the top of the beam to seal the pressure chamber of the simulator.

8. Transducer MD was fastened to the beam, and the rotating drum and pencil were installed. For dynamic tests only, transducer MA was fastened. For static tests only, the scale for visually measuring midspan deflection was taped to the beam.

9. Finally, all electrical connections were made and the beam was ready for testing as shown in Figure 4.

Testing. In the static tests, a uniformly distributed load on the beam was gradually and continuously increased to the point of beam collapse. The uniform load was applied by injecting air pressure into the blast simulator with an air compressor. The amount of overpressure was monitored visually with an Emery pressure gage of 375-psi capacity. Measurements of load, reaction, deflection, and strain were recorded with the Budd digital recorder (Appendix C) at each 5-psi increment of overpressure until an overpressure of 30 psi was attained; then an increment of 2 psi was used until the beam collapsed. At each increment, midspan deflection was automatically recorded on the rotating drum, and transit readings of midspan deflection were recorded by hand, as was the overpressure indicated by the Emery pressure gage.

In the dynamic tests, first the firing tube of the simulator was loaded with the amount of Primacord required to obtain the desired peak overpressure, and the sequence and delay time of the simulator valves were set to obtain the desired overpressure decay rate. A blasting cap was then inserted in each end of the firing tube and wired to the master control circuit. Finally, a switch was closed to start an electromechanical programmer which in turn started the recording equipment, ignited the explosive charge, controlled the opening of the simulator valves, and stopped the recording equipment. Continuous measurements of load, reaction, deflection, and strain were recorded on magnetic tape (Appendix C).

After the test, the beam was inspected and removed from the simulator. The transducers were removed, the cracks lined with black ink for contrast, and the beam was photographed.

RESULTS AND DISCUSSION

Data Reduction and Presentation

The data from the dynamic tests were recorded on magnetic tape, played through an analog-to-digital converter, and then reduced on a digital computer. The computer output consisted of plots, many of which are presented in Appendix D, and punched cards. The punched cards provided digitized data recorded for each channel of electronic instrumentation at time intervals of 1/4 millisecond.

The data from the static tests were recorded on a digital recorder and reduced by hand. Plots of the data were made by hand, many of which are given in Appendix D.

The distance between the walls of the blast simulator is 8.10 inches; therefore, loads expressed in pressure units (psi) must be multiplied by 8.10 to be expressed in terms of force per unit length (lb/in.).

Failure Mode

All the beams failed in shear except two. The two which failed in flexure were WE10 and WE11; both were loaded statically and had 3-inch stirrup spacing at the weak (east) end. Four identical beams (WE4, WE5, WE6, and WE12), which were loaded dynamically, had higher shear strength under dynamic load, but failed in shear. This behavior indicates that a beam with adequate web reinforcement to force flexural failure under static conditions might not have sufficient web reinforcement to force flexural failure under dynamic conditions. Post-test photographs of the various beams are shown in Figures 7, 8, and 9.

Beam OE2, which had no stirrups in the region of the critical section at one end and 6-inch stirrup spacing at the other, failed in shear at both ends without yielding at midspan.

Beam failure was detected by strain gages on the top face of the beam. Concrete strain of 0.0035 in./in. in compression or 0.00015 in./in. in tension was selected as a quantitative definition of failure. A strain value of 0.003 in./in. in compression is used by the American Concrete Institute [4] to define yield strain for concrete, and rupture follows almost immediately thereafter; hence, 0.0035 in./in. was assumed to be the crushing strain. The average tensile strength of the concrete cylinders (Appendix B) was 410 psi. Therefore, if the secant modulus of elasticity for concrete in tension is assumed to be about 3×10^6 psi, the yield strain would be about 0.000137 in./in. Since rupture in tension occurs immediately after yielding, 0.00015 in./in. was assumed to be the approximate failure strain in tension.

Flexural Failures

Beams WE10 and WE11 each had 3-inch stirrup spacing and were subjected to a slowly increasing static load. The first shear crack formed at a load of approximately 280 lb/in., the beam yielded in shear by yielding of stirrup WS2 at about 390 lb/in., then yielded in flexure by yielding of the longitudinal tension steel at about 575 lb/in., and finally failed in flexure by crushing of the concrete at midspan under a load of 625 lb/in. Yielding of the compression steel did not occur until after failure of the beam. Figure 10 is a diagram of the measured and idealized static flexural resistance for beams WE10 and WE11.

Shear Failures

All three types of shear failure occurred: diagonal tension, shear-compression, and compression. Table 3 gives the type of failure for each beam.

Three beams without stirrups were tested. They failed in diagonal tension, but collapse was retarded or prevented by dowel action. In the test on beam OE3, in which a static load was increased slowly, the first diagonal crack formed at a load of 310 lb/in.; failure occurred at 325 lb/in. when the crack propagated into the upper portion of the beam, but collapse did not occur until a load of 420 lb/in. was reached. Beam OE2, which was loaded dynamically, behaved similarly, but the effects of dowel action were less apparent. Table 4 is a list of the events leading to diagonal tension failure during the test on beam OE2.

Figure 7. Post-test photographs of dynamically loaded beams WE1 through WE6.

Figure 8. Post-test photographs of statically loaded beams WE7 through WE11 and dynamically loaded beam WE12.
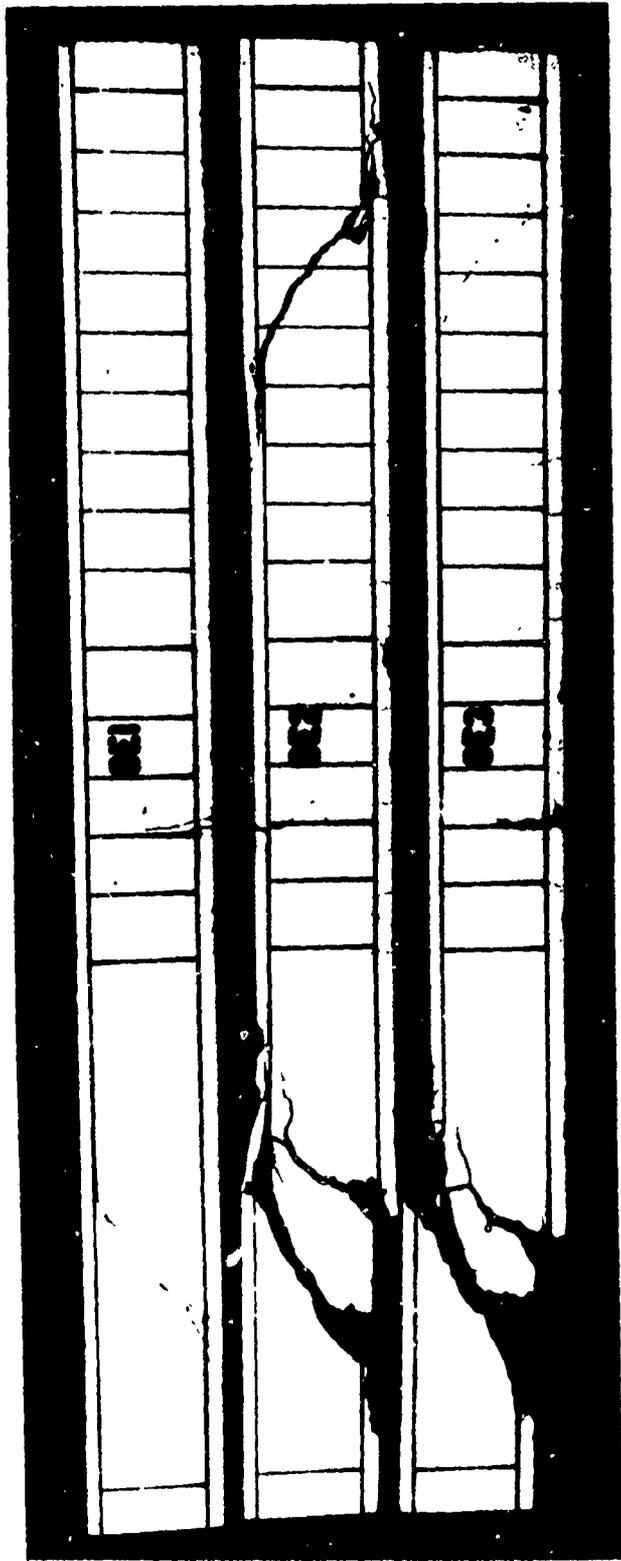
Figure 9. Post-test photographs of statically loaded beams OE1 and OE3 and dynamically loaded beam OE2.
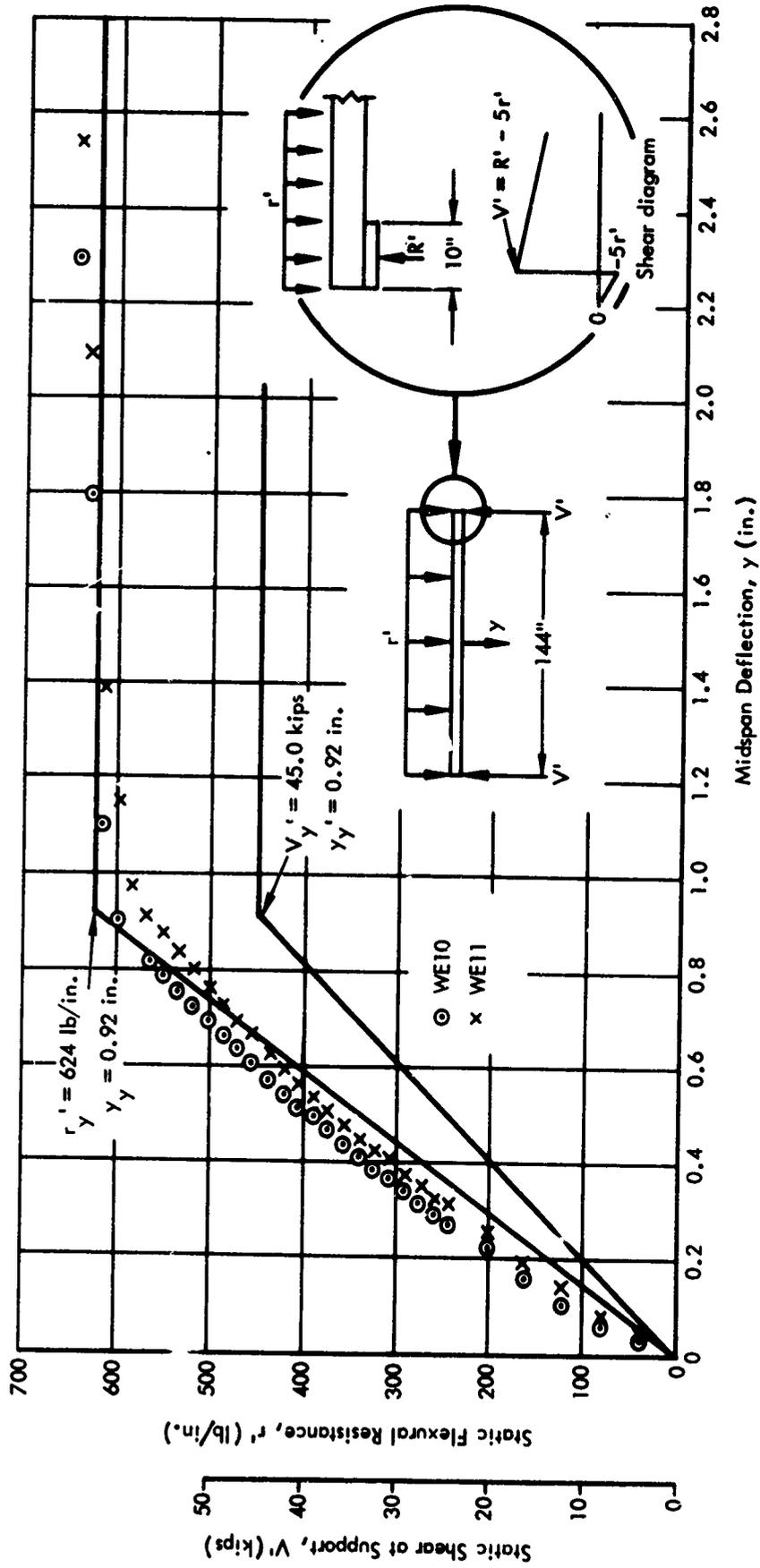
Figure 10. Measured and idealized static flexural resistance diagrams, beams WE10 and WE11.

Table 3. Failure Mode of Beams Tested

Beam No.	Stirrup Spacing (in.)	Load Type	Failure Mode (General)	Failure Mode (Specific)	Beam Collapse
WE1	5	Dynamic	Shear	Shear-compression	Yes
WE2	5	Dynamic	Shear	Compression	No
WE3	5	Dynamic	Shear	Compression	Yes
WE4	3	Dynamic	Shear	Compression	No
WE5	3	Dynamic	Shear	Compression	No
WE6	3	Dynamic	Shear	Compression	No
WE7	5	Static	Shear	Shear-compression	Yes
WE8	5	Static	Shear	Shear-compression	Yes
WE9	5	Static	Shear	Shear-compression	Yes
WE10	3	Static	Flexure	(Ductile)	No
WE11	3	Static	Flexure	(Ductile)	No
WE12	3	Dynamic	Shear	Shear-compression	No
OE1	∞	Static	Shear	Diagonal tension	No [1]
OE2	∞	Dynamic	Shear	Diagonal tension	Yes [2]
OE3	∞	Static	Shear	Diagonal tension	Yes [2]

[1] Collapse was prevented by dowel action.
[2] Collapse was retarded by dowel action.

Table 4. Sequence of Events Leading to Diagonal Tension Failure
During Test of Beam OE2

Time (msec)	Event
-0.75	Detonation of the Primacord
0.00	Impingement of the load on the beam
0.25	Significant midspan acceleration and small shock wave in the beam
0.75	Significant reactions at the supports
1.00	Maximum midspan acceleration greater than 150 g (beyond the range of the transducer) and significant midspan deflection
2.00	Peak load of the initial pulse, 524 lb/in., and significant compressive strain in the remote fiber at midspan
2.75	Significant compressive and tensile strains in the longitudinal steel at midspan
3.00	Significant compressive strain in the remote fiber near the critical section
6.25	Absolute maximum load, 525 lb/in.
7.75	Maximum midspan velocity, 23 ft/sec
9.50	Formation of diagonal tension cracks at both ends of the beam
10.25	Maximum dynamic reaction at the weak end, 43.3 kips
11.50	Maximum midspan deceleration, -99 g
11.75	Marked increase in compressive strain at the remote fiber near the critical section accompanied by decrease in all strains measured at midspan
12.50	Beam failure in diagonal tension by rapid crushing of the concrete at the remote fiber near the critical section
13.50	Collapse

The beams with 5-inch stirrup spacing subjected to a slowly increasing static load definitely failed in shear-compression. Formation of the first shear crack occurred at a load of about 290 lb/in., followed by yielding and rupture of the stirrups crossed by the propagating crack. Failure occurred by crushing of the concrete at about 470 lb/in., and collapse with rupture of the last stirrup crossed by the crack at a load of approximately 570 lb/in.

The dynamically loaded beams behaved differently. The stirrups yielded at almost the same time as the concrete crushed, making the specific mode of failure difficult to establish. After a careful study of the data, it was determined that two beams failed in shear-compression and five in compression. This behavior indicates that beams failing in shear-compression under static conditions might fail in compression under dynamic conditions. With the exception of beam WE12, yielding did not occur at midspan. Table 5 is a list of events leading to shear-compression failure of beam WE1, and Table 6 of events leading to compression failure in beam WE5.

Table 5. Sequence of Events Leading to Shear-Compression Failure During Test of Beam WE1

Time (msec)	Event
-0.75	Detonation of the Primacord
0.00	Impingement of the load of the beam
1.00	Significant midspan acceleration
2.00	Significant compressive strain in the remote fiber near the critical section and small shock wave in the beam
2.25	Peak load of the initial pulse, 621 lb/in., significant reactions at the supports, and significant midspan deflection
3.00	Significant compressive and tensile strains at midspan
4.25	Acceleration greater than 150 g (beyond the range of the transducer)
6.00	Peak load of the second major pulse, 668 lb/in.
7.25	Formation of a diagonal tension crack at the weak end near stirrup WS3
7.75	Formation of a diagonal tension crack at the strong end near stirrup WS8
9.25	Formation of a second diagonal tension crack at the weak end near stirrup WS2, marked increase in strain rates of stirrups WS1 and WS2 to about 0.90 in./in./sec, and decrease in strain rate in the longitudinal tension steel at midspan from about 0.35 in./in./sec to about 0.06 in./in./sec
10.75	Large compressive strain at the remote fiber near the critical section, 1,060 μin./in., accompanied by rapid increase in crack width indicating rapid crack propagation into the compression zone
11.50	Yielding of stirrup WS2
12.25	Yielding of stirrup WS1
12.75	Yielding of stirrup WS3
13.50	Beam failure in shear-compression
15.25	Maximum dynamic reaction at the weak end, 61.2 kips
18.25	Absolute maximum load, 671 lb/in.
	Collapse

Table 6. Sequence of Events Leading to Compression Failure
During Test of Beam WE5

Time (msec)	Event
-0.75	Detonation of the Primacord
0.00	Impingement of the load on the beam
0.25	Significant midspan acceleration
0.50	Significant reactions at the supports
1.00	Maximum midspan acceleration, 72 g, and small shock wave in the beam
1.25	Significant midspan deflection
2.00	Peak load of the initial pulse, 494 lb/in.
2.25	Significant compressive and tensile strains at midspan
3.25	Significant compressive strain in the remote fiber near the critical section
6.50	Peak load of the second major pulse, 495 lb/in.
7.50	Maximum midspan velocity, 7.8 ft/sec
8.00	Decrease in strain rate in the longitudinal tension steel at midspan from about 0.31 in./in./sec to about 0.05 in./in./sec with large increase in shearing forces
8.50	Formation of a diagonal tension crack at the strong end near stirrup WS7
9.00	Formation of a diagonal tension crack at the weak end near stirrup WS4, and maximum tensile strain at midspan, 1,800 μin./in.
9.25	Formation of a second diagonal tension crack at the weak end near stirrup WS2 with reduction of tensile strains at midspan
10.00	Marked increase in the strain rates of stirrups WS1, WS2, and WS3 to about 1.10 in./in./sec, indicating acceleration of crack propagation and rapid redistribution of the shearing forces from the concrete to the stirrups
10.25	Peak load of the third major pulse, 499 lb/in.
10.50	Marked increase in compressive strain in the remote fiber near the critical section
11.25	Beam failure in compression by rapid crushing of the concrete at the remote fiber near the critical section
11.50	Yielding of stirrup WS2 (after failure of the beam), and maximum midspan deceleration, -31 g
14.25	Absolute maximum load, 500 lb/in.
17.00	Maximum dynamic reaction at the weak end, 53.8 kips
19.50	Maximum midspan deflection, 1.09 in.
	Collapse did not occur

Critical Diagonal Tension Crack

The critical diagonal tension cracks formed and propagated in the same manner as those in the D Series tests of Part I.[1] After the first diagonal tension crack formed and propagated partway up into the beam, a second diagonal tension crack formed nearer the support. The second crack propagated much faster than the first, up through the beam to the compression reinforcement, and finally to the top face of the beam. The two cracks are shown in Figure 11, crack A being the first to form and crack B the critical one at failure. The measured distances from the center of the support to the critical diagonal crack at both ends of each beam are given in Table 7. The distances measured along the longitudinal tension steel and also at mid-depth of the beam are listed. The theoretical distances to the critical sections, also given in the table, were computed using the equation developed in Appendix A, and compared with the measured values. In every instance, at both ends of all the beams, the theoretical distance fell in the zone between the two measured distances; therefore, it seems that the method in Appendix A is adequate for predicting the location of the critical section. The rule of thumb recommended by the ACI-ASCE Joint Committee 326, that the distance is approximately equal to the effective depth of the beam, also seems to be adequate. The equation developed in Appendix A predicts a location of the critical section nearer to the support for dynamic conditions than for static conditions. However, the difference is too small to be confirmed one way or the other by the measured data.

Shear Resistance at the Support

At the support and for each beam tested, the measured and computed unit shearing stresses which correspond to diagonal tension cracking and to yielding of a stirrup are given in Table 8. The measured values which correspond to failure of the beam also are presented.
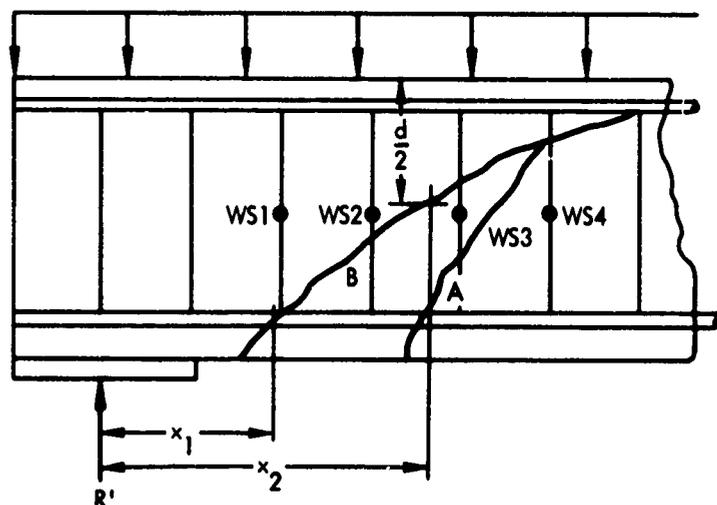
Figure 11. Critical diagonal tension crack.

Table 7. Location of the Critical Tension Crack

Beam No.	Computed Location			Measured Location [1]												Value Measured ÷ Computed			
				Weak (East) End						Strong (West) End						Weak End		Strong End	
	x_c (in.)	$\frac{x_c}{d}$	$\frac{x_c}{L}$	x_1 (in.)	$\frac{x_1}{d}$	$\frac{x_1}{L}$	x_2 (in.)	$\frac{x_2}{d}$	$\frac{x_2}{L}$	x_1 (in.)	$\frac{x_1}{d}$	$\frac{x_1}{L}$	x_2 (in.)	$\frac{x_2}{d}$	$\frac{x_2}{L}$	$\frac{x_1}{x_c}$	$\frac{x_2}{x_c}$	$\frac{x_1}{x_c}$	$\frac{x_2}{x_c}$
									Dynamic Tests										
WE1	13.3	1.03	0.09	7.5	0.58	0.05	12.5	0.97	0.09	6.5	0.50	0.05	17.0	1.31	0.12	0.56	0.94	0.49	1.28
WE2	12.5	0.97	0.09	9.0	0.70	0.06	20.0	1.54	0.14	11.5	0.89	0.08	21.0	1.62	0.15	0.72	1.60	0.92	1.68
WE3	12.9	1.00	0.09	9.0	0.70	0.06	19.0	1.47	0.13	6.5	0.50	0.05	18.5	1.43	0.13	0.70	1.47	0.50	1.43
WE4	12.8	0.99	0.09	8.5	0.66	0.06	19.0	1.47	0.13	8.0	0.62	0.06	16.0	1.24	0.11	0.66	1.48	0.62	1.25
WE5	12.6	0.97	0.09	9.0	0.70	0.06	15.0	1.16	0.10	8.5	0.66	0.06	19.5	1.51	0.14	0.71	1.19	0.67	1.55
WE6	12.4	0.96	0.09	12.0	0.93	0.08	22.0	1.70	0.15	14.0	1.08	0.10	21.0	1.62	0.15	0.97	1.77	1.17	1.70
WE12	13.0	1.00	0.09	13.0	1.04	0.09	19.0	1.47	0.13	7.5	0.58	0.05	21.0	1.62	0.11	1.00	1.46	0.58	1.61
OE2	12.8	0.99	0.09	11.0	0.85	0.08	19.0	1.47	0.13	10.0	0.77	0.07	17.0	1.31	0.12	0.86	1.48	0.78	1.33
Average	12.8	0.99	0.09	9.9	0.77	0.07	18.2	1.41	0.12	9.1	0.70	0.06	18.9	1.46	0.13	0.77	1.42	0.72	1.48
									Static Tests										
WE7	16.0	1.24	0.11	8.0	0.62	0.06	19.5	1.51	0.14	7.0	0.54	0.05	19.5	1.51	0.14	0.50	1.22	0.44	1.22
WE8	15.7	1.21	0.11	9.0	0.70	0.06	18.0	1.39	0.12	8.5	0.66	0.06	16.0	1.24	0.11	0.57	1.15	0.54	1.02
WE9	15.5	1.20	0.11	9.0	0.70	0.06	17.0	1.31	0.12	6.0	0.46	0.04	15.0	1.16	0.10	0.58	1.10	0.39	0.97
WE10	15.5	1.20	0.11	7.0	0.54	0.05	16.5	1.27	0.11	9.5	0.73	0.07	15.0	1.16	0.10	0.45	1.06	0.61	0.97
WE11	16.0	1.24	0.11	6.5	0.50	0.05	17.5	1.35	0.12	6.0	0.46	0.04	15.5	1.20	0.11	0.41	1.09	0.38	0.97
OE1	16.0	1.24	0.11	15.0	1.16	0.10	22.5	1.74	0.16	—[2]	--	--	--	--	--	0.94	1.41	--	--
OE3	15.5	1.20	0.11	6.5	0.50	0.05	18.0	1.39	0.12	11.0	0.85	0.08	15.0	1.16	0.10	0.42	1.16	0.71	0.97
Average	15.7	1.22	0.11	8.7	0.67	0.06	18.4	1.42	0.13	8.0	0.62	0.06	16.0	1.50	0.11	0.55	1.17	0.51	1.02
Average [3]	14.2	1.10	0.10	9.3	0.72	0.06	18.3	1.41	0.13	8.6	0.66	0.06	17.6	1.36	0.12	0.67	1.31	0.62	1.28

1/ x_1 is measured along the tension reinforcement; x_2 is measured at mid-depth of the beam.
2/ No crack occurred at strong end.
3/ All tests.

Table 8. Comparison of Measured and Computed Results for
Shear Resistance at East Support

Beam No.	Unit Shearing Stress at East Support, v' (psi)						
	Cracking, v_c'			Yielding, v_u' [1]			Failure, v_f' (Measured)
	Measured	Computed	Ratio	Measured	Computed	Ratio	
Dynamic Tests							
WE1	313	291	1.08	469	353	1.33	525
WE2	248	312	0.80	397	375	1.06	398
WE3	394	294	1.34	498	357	1.40	498
WE5	314	308	1.02	386	412	0.94	366
WE6	284	310	0.92	392	419	0.94	392
WE12	300	284	1.06	427	396	1.08	540
OE2	340	295	1.15	--	--	--	360
Static Tests							
WE7	204	204	1.00	239	240	1.00	338
WE8	233	210	1.11	257	248	1.04	420
WE9	192	213	0.90	227	251	0.90	251
WE10	204	232	0.88	297	291	1.02	Flexure
WE11	198	222	0.89	256	282	0.91	Flexure
OE3	221	231	0.96	--	--	--	233

[1] Yielding of stirrups or crushing of concrete, whichever occurred first.

Computed values of the unit shearing stresses at the critical section, v_c and v_u, were obtained by using Equations 3 and 4. All computed values of the cracking strength were lower than the limiting value given in Equation 3, and all computed values of the usable ultimate shearing strength were lower than the limiting value given in Equation 4. The following measured values were used in the formulas: (1) compressive concrete strength, f_c', obtained from cylinder tests, (2) distance to the critical section, x_c, measured to the critical diagonal crack at the elevation of the tension reinforcement, and (3) dynamic increase coefficient, C_2, for the stirrups. Nominal values were used for the other parameters.

The dynamic increase coefficient for the stirrups loaded dynamically was found to be 1.7 from the results shown in Table 9 and Figure B-6 of Appendix B. In the table, a footnote number is used to indicate which stirrup was the first to yield in each beam, placed beside the strain rate in that stirrup prior to yielding. The rates varied from 0.81 in./in./sec in beam WE12 to 1.22 in./in./sec in beam WE3. For determining the dynamic increase coefficient, the most conservative strain rate (0.81 in./in./sec) was chosen. In the figure, the corresponding increase in upper yield stress is 77%. Again conservatism was applied by rounding this number to the next lower increment of 10% (70%). Thus a coefficient of 1.7 was found. The upper yield point was used instead of the lower yield point because first yielding of a stirrup is defined as the usable ultimate and, therefore, the remainder of the stress-strain relationship was not used. The conservatism of the selection of 1.7 is discussed further in the subsequent paragraph where correlation between measured and computed shears is presented.

Table 9. Measured Strain Rates in Stirrups and Longitudinal Tension Steel

Beam No.	Measured Strain Rate, $\dot{\epsilon}$ (in./in./sec)					
	Stirrup WS1	Stirrup WS2	Stirrup WS3	Stirrup WS4	Bar TS1	Bar TS2
WE1	0.90	0.86 [1/]	0.33	0.31	0.35	0.36
WE2	0.90	1.33	1.07 [1/]	0.47	0.28	0.30
WE3	1.45	0.97	1.22 [1/]	--	0.29	0.31
WE5	0.90	1.05 [1/]	0.89	1.02	0.32	0.32
WE6	1.05	0.70	0.91 [1/]	0.82	0.28	0.30
WE12	0.67	0.81 [1/]	0.72	0.73	0.34	0.31

[1/] First stirrup to yield.

The dynamic increase coefficient for the concrete is given in Reference 5 as 1.7. This value is discussed in Part I[1] and shown in Figure B-1 of Appendix B along with results of dynamic split cylinder tests performed by Keenan.

Therefore, for the static tests, $C_1 = C_2 = 1$, and for the dynamic tests, $C_1 = C_2 = 1.7$. Computed values of the unit shearing stresses at the support, v_c' and v_u', were obtained from the values at the critical section assuming linear shear distribution along the span. These equations are given as

$$v_c' = \left(\frac{L}{L - 2x_c}\right) v_c \tag{7}$$

$$v_u' = \left(\frac{L}{L - 2x_c}\right) v_u \tag{8}$$

The measured values of the shearing stresses at the supports were obtained from the measured reactions, which were corrected for the influence of the overhang.

The correlation between the measured and computed values listed in Table 8 is shown in Figure 12. The data from the static tests indicate that the ACI-ASCE Joint Committee 326 formula is satisfactory for predicting the shearing resistance at cracking and yielding in the case of the simply supported beams which were subjected to uniformly distributed static loads. The correlation between measured and computed values was about the same for cracking and yielding. Of the eleven data points compared, 73% of the measured values were within ±10% of the computed values, and all the values were within ±12%. This correlation is believed to be within the limits that can be expected due to control requirements for quality of the concrete, placement of the reinforcing steel, and application of the load.
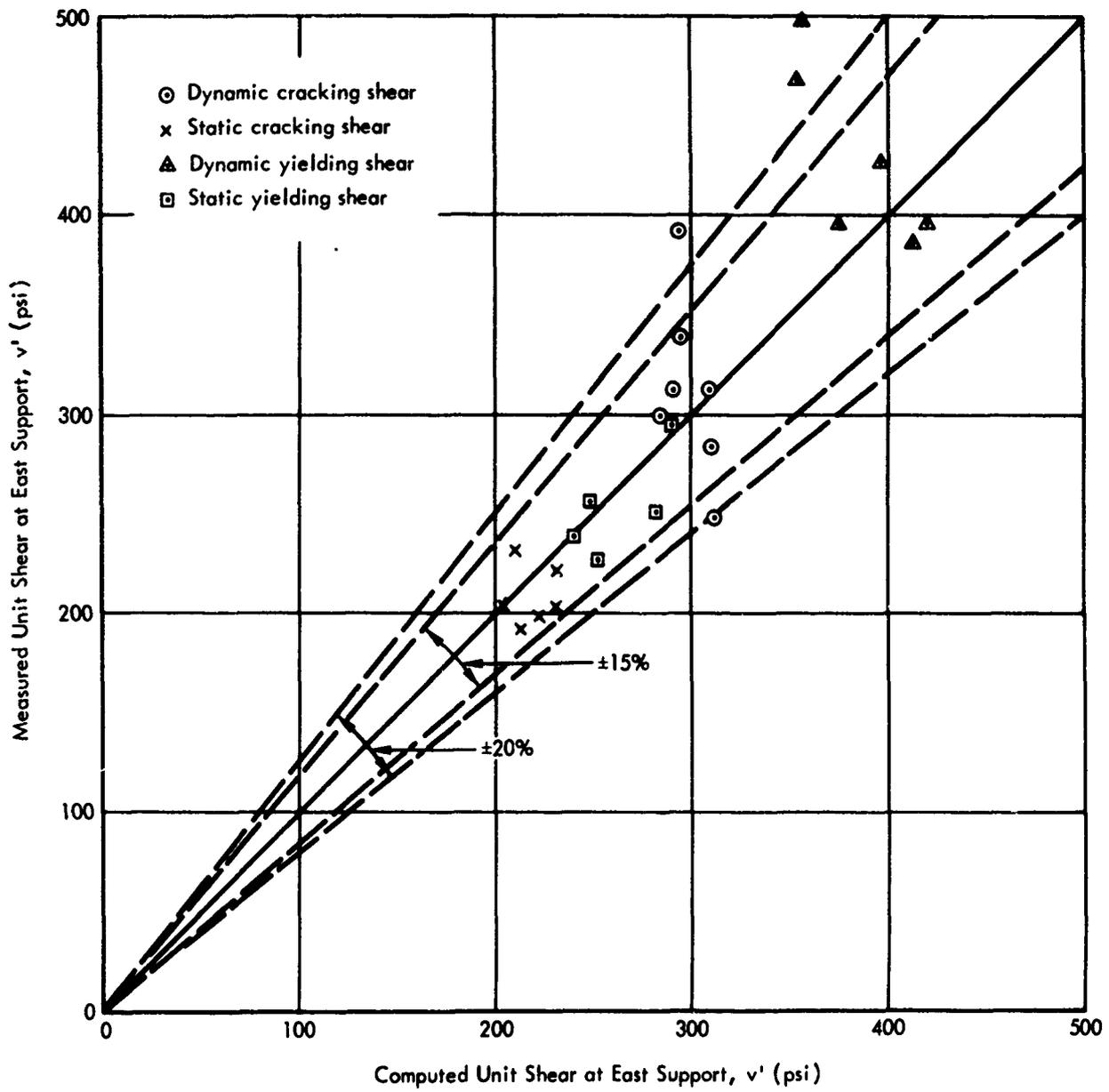
Figure 12. Correlation of measured and computed results for shear resistance at east support.

The data from both static and dynamic tests indicate that the formula as modified by Keenan[1] and further modified in this report is satisfactory for predicting the shearing resistance at cracking and yielding in the case of the simply supported beams which are subjected to uniformly distributed static and dynamic loads. In general, the correlation between measured and computed values is about the same for static and dynamic conditions, but more scatter exists in the measured dynamic data. Computed values of the dynamic yielding shear strength tend to be more conservative than other data because a conservative value of the strain rate (0.81 in./in./sec) was selected from Table 9 in determining a value for the dynamic increase coefficient for stirrups, C_2. Of the 24 data points compared, 67% of the measured values were within ±10% of the computed values, 83% within ±15%, and 88% were within ±20%.

Shear Resistance Beyond Yielding in Shear

From the data listed in Tables 8 and 10, it can be seen that the dynamically loaded beams had a much smaller percentage of resistance beyond yielding of the stirrups than the statically loaded beams. The statically loaded beams with 5-inch stirrup spacing had from 11% to 63% additional strength after yielding and prior to failure in shear; identical beams loaded dynamically had very little or none. In fact, beams WE2 and WE3, which also had 5-inch spacing (Table 10), failed before yielding of the stirrups. This difference in behavior under dynamic loading is caused by the large increase in stirrup contribution which is not accompanied by a comparable increase in the flexural capacity of the cross section reduced by propagation of the diagonal tension crack. In this type of failure, the ratio of applied moment to resisting moment becomes greater in the region of high shear than in the region of high moment. Also, these results suggest that the limiting value in Equation 3 might not be low enough for the design of dynamically loaded beams.

The statically loaded beams with 5-inch stirrup spacing had additional shear resistance after yielding and prior to collapse equal to 70% of the yield strength. This additional shear resistance resu' s mainly from the ductility of the stirrups and longitudinal reinforcement in the region of the critical section, and from the dowel action of the longitudinal bars. The magnitude of' additional strength was not determined in dynamic tests, where collapse is not defined i ɛrms of time and st 'n.

The sta.. :ally loaded beams with 3-inch stirrup spacing had sufficient resistance after yielding in shear to force flexural failure. ⌐his created the interesting situation where the usable ultimate shear strength, as defined earlier, was exceeded although the failure mode was flexure.

Effectiveness of Stirrups

The stirrup effectiveness, ψ, is the percentage of the usable ultimate shear resistance provided by the stirrups. Therefore, from Equation 4

$$\psi = \frac{100\, C_2 \left(Krf_y \right)}{v_u} = \frac{100 \left(v_u - v_c \right)}{v_u} = 100 \left(1 - \frac{v_c}{v_u} \right) \tag{9}$$

Measured and computed values of ψ are listed and compared in Table 11. Eleven beam tests with web reinforcement were analyzed. Six of the beams were loaded dynamically and five statically. In all tests, the stirrups were sufficiently effective to accomplish internal stress redistribution after cracking. Computed values of the effectiveness were conservative in 9 of the 11 tests. In general, the computed values were more conservative in the dynamic than the static tests; also, more scatter existed in the dynamic tests. In the static tests, the stirrup effectiveness was greater in the beams with 3-inch spacing than those with 5-inch spacing as predicted. In the dynamic tests, the amount of scatter in the data was large enough to prevent making a judgment. This scatter is believed to be due to premature cracking in beam WE2 and the higher dynamic loads which were applied to beams WE1 and WE12, these factors resulting in higher measured effectiveness.

Table 10. Shear Resistance Beyond Yielding in Shear

Beam No.	Stirrup Spacing (in.)	Unit Shearing Stress Measured at East Support, v' (psi)					Shear Resistance Beyond Yielding (%)	
		Yielding in Shear	Yielding in Flexure	Failure in Shear	Failure in Flexure	Collapse in Shear	To Failure	To Collapse
Dynamic Tests								
WE1	5	469	None	525	--	$1/$	12	$1/$
WE2	5	426	None	398	--	None	0	--
WE3	5	498	None	498	--	$1/$	0	$1/$
WE5	3	386	None	386	--	None	0	--
WE6	3	421	None	392	--	None	0	--
WE12	3	427	542	540	--	None	26	--
Static Tests								
WE7	5	239	None	338	--	396	41	66
WE8	5	257	420	420	--	437	63	70
WE9	5	227	None	251	--	402	11	77
WE10	3	297	420	--	449	None	51	--
WE11	3	256	408	--	449	None	75	--

$1/$ Not well defined in dynamic tests.

The ACI Building Code[4] places the following limit on the amount of web reinforcement: "Where web reinforcement is required, its area shall not be less than 0.15 percent of the area, bs, computed as the product of the width of the web and the spacing of the web reinforcement along the longitudinal axis of the member." This limit would require a value of Krf_y equal to or greater than 54 psi in the beams tested. In three dynamic tests and three static tests, stirrups with Krf_y values equal to 32.2 psi were effective.

Dynamic Loading and Response

A modal analysis of a simply supported beam under a uniformly distributed dynamic load is developed in Appendix G of Reference 1. The correlation of this theory with the results of the D Series beam tests is discussed on page 25 of Reference 1. The theory was used to obtain the curves plotted in Figure 13 for obtaining the maximum dynamic shear factor, DSF_m. This multiplier was applied to the ratio of the dynamic peak load and the dynamic flexural resistance to determine the maximum dynamic shear at the supports. In the D Series correlation was good, indicating that yielding in shear did not greatly alter the maximum applied shear and the deflection for the beams tested, all of which yielded in shear and failed in flexure. Correlation for the E Series is shown in Table 12. Again correlation is good between theoretical and measured maximum applied shear. Since the loading was just sufficient to cause failure, the beams acted in a nearly elastic manner through most of the loading and response history up to times equal to about one-half the natural period. Therefore, again yielding in shear did not greatly alter the maximum applied shear. The data in Table 12 are given in both dimensional and nondimensional form for convenience. The nondimensional forms are used in the charts developed by Keenan[1] (Figure 13).

Table 11. Stirrup Effectiveness

Beam No.	Stirrup Spacing (in.)	Stirrup Effectiveness, ψ		
		Measured [1] (%)	Computed [2] (%)	Ratio
Dynamic Tests				
WE1	5	33	16	2.1
WE2	5	38	15	2.5
WE3	5	21	15	1.4
WE5	3	19	22	0.9
WE6	3	28	22	1.3
WE12	3	30	23	1.3
Static Tests				
WE7	5	15	13	1.2
WE8	5	9	13	0.7
WE9	5	15	13	1.2
WE10	3	31	18	1.7
WE11	3	23	19	1.2

[1] $\psi = 100\left(1 - V_c'/V_u'\right)$, obtained from measured shear at the support.

[2] $\psi = 100\,C_2\left(Krf_y\right)/v_u$, obtained from computed unit shear at the critical section and from properties of the stirrups.

The test for beam WE6 is of particular interest. This beam contained the largest amount of web reinforcement and received the smallest load. The load was sufficient to cause early stages of crushing in the concrete at the top surface of the beam at the head of the diagonal tension crack, but did not cause heavy damage or collapse. Theoretically, with a step load and elastic response, the dynamic load required to cause a given deflection is one-half the static load causing that deflection. Since about 6% damping could be expected in the beam, the dynamic load would have to be slightly larger than one-half the static load to cause the same deflection. In the test for beam WE6, the maximum deflection of the beam was precisely equal to the static flexural yield deflection of similar beams (WE10 and WE11), the ratio of the dynamic load to the dynamic yield resistance (w/r_{dy}) was slightly greater than one-half, and the time to maximum deflection was one-half the natural period. All values are precisely as predicted by the theory for elastic response with a small amount of damping. Further, the predicted and measured maximum applied shears were the same within the accuracy of the measurements. Also, the times shown in Table 12 indicate that failure in shear occurred a short time prior to maximum shear, which in turn occurred a short time prior to maximum deflection. Strains at midspan approached dynamic yield values, and the extent of flexural cracking at midspan was advanced, as can be seen in Figure 7. All this evidence strongly indicates beam WE6 under its dynamic load was a balanced beam in the sense that it had equal probability of failing in either shear or flexure.
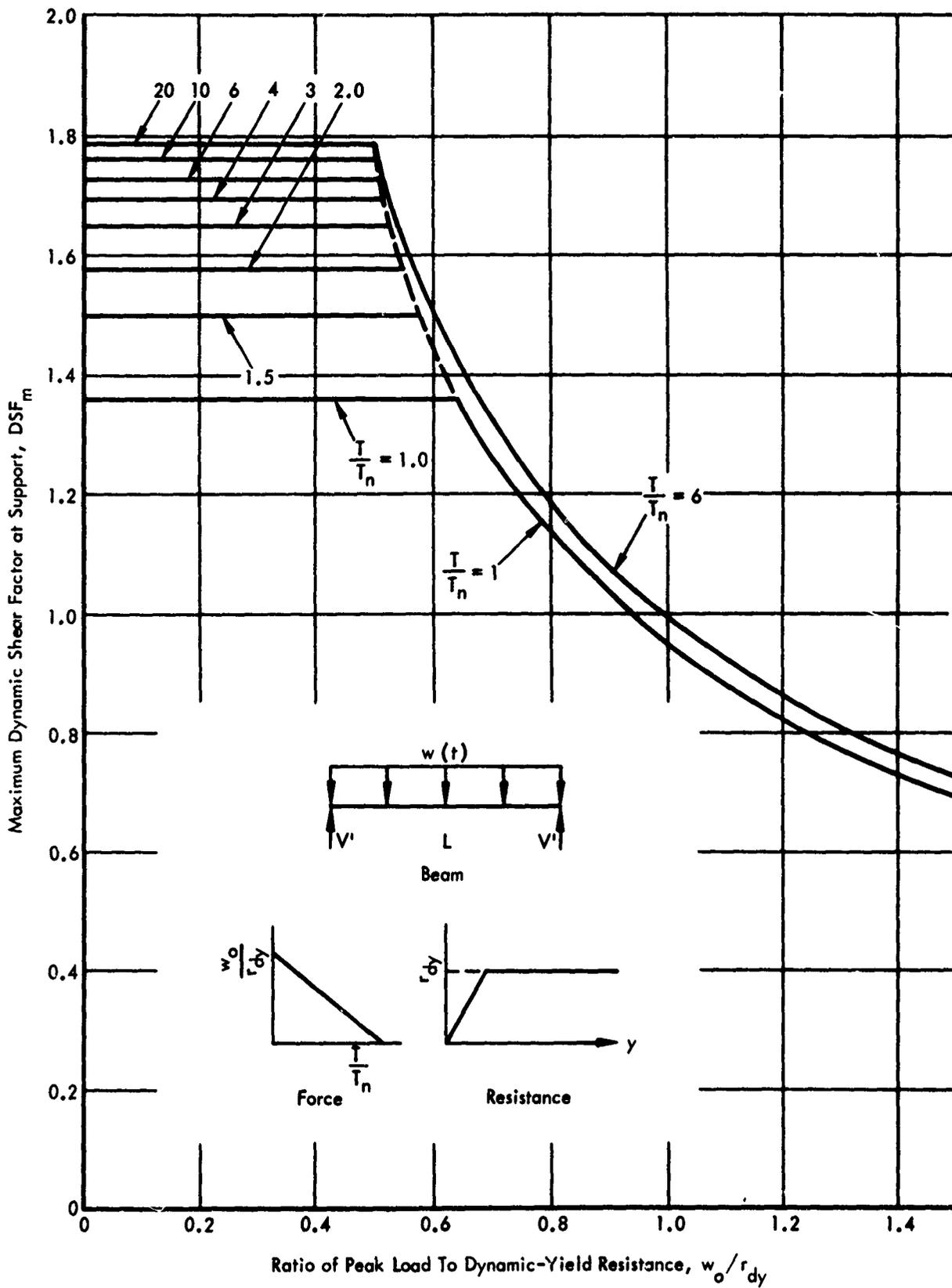
Figure 13. Maximum shear at supports of simple beam under uniformly distributed dynamic load.

Table 12. Dynamic Loadings and Responses

Beam No.	Equivalent Dynamic Step Load [1]			Midspan Deflection				Shear at East Support								Time to Shear Failure	
				Maximum		Time to Maximum		Computed Maximum [6]			Measured Maximum			Time to Maximum			
	w (lb/in.)	$\frac{w}{r_y}$ [2]	$\frac{w}{r_{dy}}$ [3]	y_m (in.)	$\frac{y_m}{y_y}$ [4]	t_m (msec)	$\frac{t_m}{T_n}$ [5]	V_m' (kips)	$\frac{V_m'}{V_y}$ [7]	DSF_m	V_m' (kips)	$\frac{V_m'}{V_y}$ [7]	DSF_m	t_m (msec)	$\frac{t_m}{T_n}$	t_f (msec)	$\frac{t_f}{T_n}$
WE1	577	0.925	0.740	--	--	--	--	53.0	1.18	1.27	57.2	1.27	1.37	15.25	0.42	13.50	0.37
WE2	436	0.699	0.559	1.14	1.24	21.50	0.60	50.4	1.12	1.60	47.6	1.06	1.52	14.75	0.41	11.25	0.31
WE3	450	0.721	0.577	--	--	--	--	50.4	1.12	1.55	57.3	1.27	1.76	14.00	0.39	11.50	0.32
WE5	441	0.706	0.565	1.09	1.18	19.50	0.54	50.8	1.13	1.60	50.3	1.12	1.59	17.00	0.47	11.25	0.31
WE6	430	0.689	0.551	0.92	1.00	18.75	0.52	50.4	1.12	1.62	49.2	1.09	1.58	14.75	0.41	12.50	0.35
WE12	558	0.894	0.715	--	--	--	--	53.0	1.18	1.32	56.7	1.26	1.41	11.75	0.33	11.75	0.33
OE2	454	0.727	0.582	--	--	--	--	50.8	1.13	1.55	40.5	0.90	1.24	10.25	0.28	12.50	0.35

1/ $T/T_n = \infty$.
2/ $r_y' = 624$ lb/in. (see Figure 10).
3/ $r_{dy} = 1.25\,r_y'$ (see Figure B-3 and Table 9).
4/ $y_y = 0.32$ in. (see Figure 10).
5/ $T_n = 36$ msec (measured natural period).
6/ Based on Figure 13 and the procedure discussed in Reference 1.
7/ $V_y' = 45.0$ kips (see Figure 10).

Limitations of the Test Program

Concrete strength varied more than expected between beams. This variation limited statistical confirmations and comparisons.

A definite value for the dynamic increase coefficient, C_2, could not be predicted. It was found that its value depends on the strain rate in the stirrups which in turn can be measured but not predicted. A relationship is needed between strain rate in stirrups and some dynamic flexural parameter before a practical design procedure can be completed.

The discovery in this series of tests that compression-type shear failures are more probable in dynamically loaded beams as compared to statically loaded beams indicates that the use of stirrup yielding to define usable ultimate shearing strength may not be a good criterion for the design of reinforced concrete beams.

Accuracy of Measurements

In any experiment, there is always a certain degree of inaccuracy involved in recording or reducing measurements. The following table contains reasonable assumptions of accuracy in the reduced experiment data for these tests:

Static Loading		Dynamic Loading	
Data	Accuracy (%)	Data	Accuracy (%)
Load (overpressure)	2 to 3	Load (overpressure)	3 to 4
Reactions (force)	3 to 4	Reactions (force)	4 to 6
Deflection (distance)	2 to 3	Acceleration	6 to 8
Depth change (distance)	2 to 3	Deflection (distance)	3 to 5
Strain	2 to 3	Depth change (distance)	3 to 4
		Strain	3 to 5

CONCLUSIONS

The conclusions listed refer to simply supported reinforced concrete beams both with or without web reinforcement, unless otherwise stated.

1. The shear strength, the flexural strength, the applied shear at the critical section, and the applied moment increase under dynamic load with respect to the same load applied statically; both the shear strength contributions from the concrete and the web reinforcement increase.

2. The applied shear and applied moment increase in about the same proportion with respect to type of loading - changing the load from static to dynamic.

3. The usable shear strength and the flexural strength increase in different proportions. Further, the contributions to the usable shear strength from the concrete and the web reinforcement increase in different proportions, depending mainly on the material used for stirrups and the rate of strain in the stirrups. Therefore, the characteristics of the dynamic load influence the relative increases in the flexural strength, shear strength from the concrete, and shear strength from stirrups.

4. Beams may or may not have shear resistance beyond yielding in shear; this additional resistance, if any, is less under dynamic than under static loading.

5. A beam containing adequate web reinforcement to force flexural failure under static conditions might not have sufficient web reinforcement to force flexural failure under dynamic conditions.

6. It is possible for a beam to fail in flexure after the usable ultimate shearing resistance has been exceeded. In other words, the additional shear resistance beyond yielding in shear might be enough to force flexural failure.

7. In beams which fail in diagonal tension, collapse might be retarded or prevented by dowel action.

8. A beam which fails in shear-compression under static loading might fail in compression under dynamic loading. In other words, if failure occurs after yielding of the web reinforcement under static loading, it might occur before yielding of the web reinforcement under dynamic loading. In the beams tested, this difference in behavior under dynamic loading was caused by a large increase in stirrup contribution which was not accompanied by a comparable increase in the flexural capacity of the cross section reduced by propagation of the diagonal tension crack. In this type of compression failure in the high shear zone, the ratio of applied moment to resisting moment becomes greater in the region of high shear than in the region of high moment.

9. In beams with web reinforcement, the critical diagonal tension crack at yielding in shear might be a different crack from the one which is critical at first shear cracking.

10. The location of the critical section is predictable using the method given in Appendix A.

11. In the beams tested, the location of the critical diagonal tension crack was about the same for static and dynamic loads, and for various stirrup spacings.

12. The shear and moment distributions along the span are a function of position and time under dynamic loads. However, for the beams tested, the difference between these distributions for static and dynamic conditions was small. Therefore, it is concluded that the static distributions can be used in designing beams of these general proportions to withstand dynamic loads.

13. Under laboratory controls, the usable ultimate shear strength of the beams tested was predicted by the ACI-ASCE Committee 326 formula as modified by Keenan[1] and in this report with accuracy of ±12% for static conditions and ±15% for dynamic conditions. Therefore, it is concluded that the formula is satisfactory and the capacity reduction factor (ϕ) value of 0.85 given in the safety provisions of the ACI Building Code[4] is adequate.

14. Stirrups with a value of Krf_v equal to 32.2 psi were effective where a minimum value of 54 psi would be required by the ACI Building Code.[4] Therefore, it is concluded that the ACI Building Code is conservative in regard to this limit.

15. For the beams tested, the method developed by Keenan[1] was adequate for predicting the maximum applied shearing force at the supports.

DESIGN RECOMMENDATIONS

The following design recommendations are based on the test results presented in both Part I and Part II of the continuing program. These recommendations will be revised as new information is obtained.

Dynamic Shear Design Procedure

Beams should be designed to resist the applied flexural forces first. Then the cross section should be checked for shear, and web reinforcement added if necessary. Under some conditions, it might be necessary to change the cross section. The following procedure is recommended for dynamic shear design after a flexural cross section has been established:

1. Determine the maximum applied shear at the support.

2. Locate the critical section.

3. Determine the maximum applied unit shear at the critical section.

4. Determine the shear-moment ratio at the critical section.

5. Determine the usable ultimate shear strength without web reinforcement at the critical section.

6. Compare the maximum applied unit shear with the usable ultimate shear strength without web reinforcement to determine whether web reinforcement is needed.

7. Compute the amount of web reinforcement, if needed, and check the limits placed on the minimum contribution from stirrups and the maximum contribution from the concrete. Increase the amount of web reinforcement if required. If it is necessary to change the cross section, repeat steps 2 through 7.

Maximum Applied Shear at the Support

The method developed by Keenan which is discussed on page 25 of Part I[1] and in Appendix G there can be used to determine the maximum applied shear at the support.

Location of the Critical Section

The distance from the support to the critical section can be approximated by using the method given in Appendix A. However, this distance should not be taken as less than the effective depth of the beam when designing simply supported beams subjected to uniformly distributed loads. This distance can be used to compute the maximum applied unit shear at the critical section if the shear at the support is known. It can also be used to compute the shear-moment ratio at the critical section if the shear and moment distributions are known. For simple supports and uniformly distributed loads

$$ v = \left(\frac{L - 2x_c}{L} \right) \left(\frac{V'}{bd} \right) \tag{10} $$

$$ \left(\frac{V}{M} \right)_c = \frac{L - 2x_c}{Lx_c - x_c^2 - z^2} \tag{11} $$

where v = unit shearing stress at critical section

$\left(\dfrac{V}{M}\right)_c$ = shear-moment ratio at critical section

L = length of span, center to center of supports

x_c = distance from support to critical section

z = overhang distance

V' = total shear at support

b = width of beam

d = effective depth of beam

Usable Ultimate Shear Strength

The following formulas are recommended for computing the usable ultimate shear strength of reinforced concrete beams with or without web reinforcement, and subjected to static or dynamic uniformly distributed or concentrated loads:

$$v_c = C_1\left(1.9\sqrt{f_c'}\right) + 2,500\,pd\left(\dfrac{V}{M}\right)_c \qquad \leq C_3\left(3.5\sqrt{f_c'}\right) \tag{12}$$

$$v_u = \phi\left[v_c + C_2\left(Krf_y\right)\right] \qquad \leq C_4\left(10\sqrt{f_c'}\right) \tag{13}$$

where $\phi\left[C_2\left(Krf_y\right)\right] \geq 0.15\,v_u$

Equation 12 is for computing the contribution from the concrete, and a maximum limit has been placed on that contribution. For designing statically loaded beams, $C_1 = C_3 = 1$. For designing dynamically loaded beams, $C_1 = 1.7$, with the value of C_3 unknown. Until the value of C_3 is determined in dynamic tests, the designer will be conservative in assuming $C_3 = 1$ under all conditions.

Equation 13 is for computing the usable ultimate shear strength as the sum of the contributions from the concrete and the web reinforcement, and a minimum limit has been placed on the contribution from the web reinforcement based on a stirrup effectiveness, ψ, of 15%. In general, this limit will permit lower Krf_y values than the limit given in the ACI Building Code.[4] If the limit based on effectiveness is not satisfied, the contribution from the web reinforcement must be neglected. The coefficient C_2 is the dynamic increase coefficient for the contribution from the web reinforcement. For designing statically loaded beams, $C_2 = 1$. For dynamically loaded beams, its value depends on the mechanical properties of the material and the rate at which the material is strained. Values were determined in the D and E Series beam tests by measuring the strain rates in the beams and testing coupons of the stirrup material. At the present time, however, no relations have been developed to predict strain rates in the web reinforcement in beams under dynamic loading. For dynamic conditions, $C_2 = 1.3$ is considered a conservative value covering a wide range of materials and strain rates. The capacity reduction factor, ϕ, is the safety provision as given in the ACI Building Code. Its value is 0.85 for diagonal tension. A maximum limit must be placed on Equation 13 as was done to Equation 2. The Part II experiment indicates that under dynamic loads, C_4 might be less than unity. For static design, $C_4 = 1$.

For computing the required amount of web reinforcement in step 7 of the recommended design procedure, Equation 13 may be designated in the form

$$rf_y = \dfrac{v - v_c}{C_2 K} \geq 0.176\left(\dfrac{v_c}{C_2 K}\right)$$

ACKNOWLEDGMENTS

LIST OF SYMBOLS

A_s	Cross-sectional area of longitudinal tension steel (in.^{2})	r'	Static load or static flexural resist
A_s'	Cross-sectional area of compression steel (in.^{2})	r_{dy}	Dynamic flexural yield resistance
A_v	Cross-sectional area of one stirrup (in.^{2})	r_y'	Static flexural yield resistance (lb
b	Width of beam (in.)	S	Maximum expected strain reading
C_1	Dynamic increase coefficient for tensile strength of concrete	s	Spacing of stirrups, center to cent
C_2	Dynamic increase coefficient for tensile strength of web reinforcement	T	Duration of dynamic load (msec)
C_3	Coefficient limiting concrete contribution to shearing strength	t	Time (msec)
		t_f	Time to failure (msec)
D	Diameter (in.)	t_m	Time to maximum value (msec)
DSF_m	Maximum dynamic shear factor	T_n	Natural period of beam (msec)
d	Effective depth of beam (in.)	V	Total shear at critical section (lb)
d'	Distance from remote fiber in compression to center of compression steel (in.)	V_x	Shear at distance x from center o
		V'	Total shear at support (lb)
E	Modulus of elasticity of steel (psi)	v	Unit shearing stress at critical s
f_c'	Compressive strength of concrete at 28 days (psi)	v'	Unit shearing stress at support (p
f_t	Tensile strength of concrete at 28 days (psi)	V_c	Total shear resistance at critical contributed by concrete (lb)
$\dot{f}_t$	Tensile stress rate (psi/sec)	v_c	Shearing strength at critical secti by concrete (psi)
f_y	Static yield strength of steel (psi)	V_c'	Total shear resistance at support by concrete (lb)
G	Gage factor		
K	$(\sin \alpha + \cos \alpha) \sin \alpha$	v_c'	Unit shearing stress at support u in shear (psi)
Krf_y	Shearing strength at critical section contributed by web reinforcement (psi)	v_f'	Unit shearing stress at support u failure (psi)
L	Length: length of span, center to center of supports (in.)	V_m'	Maximum dynamic total shear at
M	Moment at critical section (in.-lb)	V_u	Usable total shear resistance at section (lb)
M_x	Moment at a distance x from center of support (in.-lb)	V_u'	Usable total shear resistance at
p	Ratio of cross-sectional areas of longitudinal tension steel and effective concrete (in.^{2}/in.^{2})	v_u	Usable ultimate shearing strength section (psi)
p'	Ratio of cross-sectional areas of compression steel and effective concrete (in.^{2}/in.^{2})	v_u'	Unit shearing stress at support u in shear (psi)
R	Gage resistance (ohms)	v_{x_c}	Applied unit shear at critical sec
R'	Reaction at support (lb)	V_y'	Total shear at support upon yield (kips)
RC	Calibration resistance (ohms)	$(V\,M)_c$	Ratio of shear to moment at dist support (in.$^{-1}$)
r	A_v/bs		

LIST OF SYMBOLS

r' — Static load or static flexural resistance (lb/in.)

r_{dy} — Dynamic flexural yield resistance (lb/in.)

r_y' — Static flexural yield resistance (lb/in.)

S — Maximum expected strain reading (μin./in.)

s — Spacing of stirrups, center to center (in.)

T — Duration of dynamic load (msec)

t — Time (msec)

t_f — Time to failure (msec)

t_m — Time to maximum value (msec)

T_n — Natural period of beam (msec)

V — Total shear at critical section (lb)

V_x — Shear at distance x from center of support (lb)

V' — Total shear at support (lb)

v — Unit shearing stress at critical section (psi)

v' — Unit shearing stress at support (psi)

V_c — Total shear resistance at critical section contributed by concrete (lb)

v_c — Shearing strength at critical section contributed by concrete (psi)

V_c' — Total shear resistance at support contributed by concrete (lb)

v_c' — Unit shearing stress at support upon cracking in shear (psi)

v_f' — Unit shearing stress at support upon shear failure (psi)

V_m' — Maximum dynamic total shear at support (kips)

V_u — Usable total shear resistance at critical section (lb)

V_u' — Usable total shear resistance at support (lb)

v_u — Usable ultimate shearing strength at critical section (psi)

v_u' — Unit shearing stress at support upon yielding in shear (psi)

v_{x_c} — Applied unit shear at critical section (psi)

V_y' — Total shear at support upon yielding in flexure (kips)

$(V/M)_c$ — Ratio of shear to moment at distance x_c from support (in.$^{-1}$)

$(V/M)_x$ — Ratio of shear to moment at distance x from center of support (in.$^{-1}$)

W — Load (lb/in.)

w — Uniformly distributed load (lb/in.)

$w(t)$ — Time-dependent uniformly distributed load (lb/in.)

w_o — Initial value of time-dependent uniformly distributed load (lb/in.)

x — Distance from center of support (in.)

x_1 — Distance from center of support to critical diagonal tension crack measured along longitudinal tension steel (in.)

x_2 — Distance from center of support to critical diagonal tension crack measured midway between longitudinal tension and compression steel (in.)

x_c — Distance from center of support to critical section (in.)

y — Midspan deflection (in.); head displacement (in./in.)

y_m — Maximum deflection (in.)

y_y — Static flexural yield deflection (in.)

z — Overhang distance (in.)

α — Angle of inclination of web reinforcement (rad)

α_1 — $C_1\left(1.9\sqrt{f_c'}\right)$

β — 2.500 pd

γ — β/α_1

ϵ — Strain (in./in.)

$\dot{\epsilon}$ — Strain rate (in./in./sec)

θ — Stress increase (%)

σ — Stress (ksi)

σ_{du} — Dynamic ultimate stress (ksi)

σ_{dyl} — Dynamic lower yield stress (ksi)

σ_{dyu} — Dynamic upper yield stress (ksi)

σ_u — Average static ultimate stress (ksi)

σ_y — Average static yield stress (ksi)

ϕ — Capacity reduction factor

ψ — Stirrup effectiveness

Appendix A

COMPUTATION OF THE LOCATION OF THE CRITICAL SECTION

OBJECT

The object of this appendix is to present a method for approximating the location of the critical section of reinforced concrete beams in order to determine the shear-moment ratio, V/M, at the critical section. The ratio is needed to obtain values for the second term of Equation A-1 which is recommended for predicting the unit shearing resistance at the critical section corresponding to formation of a critical diagonal tension crack.

$$v_c = C_1 \left(1.9 \sqrt{f_c'}\right) + 2.500\, pd \left(\frac{V}{M}\right)_c \qquad (A-1)$$

where C_1 = 1.0 for static loading

C_1 = 1.7 for dynamic loading

SCOPE

Equation A-1 is used with assumptions regarding shear distribution to determine the location of the critical section for dynamic and static loading. The equation, which is developed in this appendix for the distance from the center of a support to the critical section, applies only to uniformly distributed loads and simple supports. The equation does apply to beams with overhangs.

ASSUMPTIONS

The assumptions are: (1) Equation A-1 for predicting shear resistance is adequate for approximating the location of the critical section both for static and dynamic loads; (2) the shear distribution along the span for dynamic loading is the same as for static loading. Thus, for uniformly distributed loads, the shear distribution is assumed to be linear for both static and dynamic loadings.

APPROACH

At the critical section, the applied shear expressed as a function of position x along the span is tangent to the resisting shear expressed as a function of position x. Therefore, the slopes of the two functions are equal and the shear values are equal. By equating the slopes and values of the two functions at that point (x_c), a polynomial equation in x_c is obtained. The fourth order equation obtained for the beams tested is solved by the method of finite difference on the IBM-1620 II computer.

DEVELOPMENT OF THE EQUATION

Shear-Moment Ratio Along the Span

If the shear distribution along the span is linear, the slope of the applied shear with respect to position x is

$$\frac{dV_x}{dx} = -\frac{V_x}{\frac{L}{2} - x}$$

and the moment at position x is equal to the area of the shear diagram to that point as shown in Figure A-1. If z is taken as the overhang distance, the moment at x is

$$M_x = \frac{1}{2} z \left[z \left(-\frac{V_x}{\frac{L}{2} - x} \right) \right] - \frac{1}{2} x \left[V_x + \frac{L}{2} \left(-\frac{V_x}{\frac{L}{2} - x} \right) \right]$$

$$M_x = V_x \left(\frac{Lx - x^2 - z^2}{L - 2x} \right)$$

Thus, the shear-moment ratio can be expressed as a function of position x:

$$\left(\frac{V}{M} \right)_x = \frac{L - 2x}{Lx - x^2 - z^2} \tag{A-2}$$
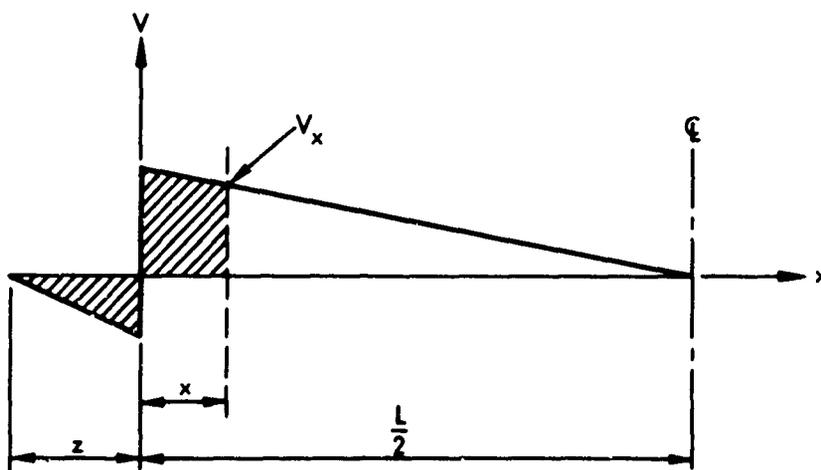
Figure A-1. Assumed applied shear diagram.

Resisting Unit Shear Function

By substituting Equation A-2 into Equation A-1, the resisting unit shear at critical diagonal cracking may be expressed as a function of position x:

$$v_c = f(x) = C_1 \left(1.9 \sqrt{f_c'} \right) + 2,500 \, pd \left(\frac{L - 2x}{Lx - x^2 - z^2} \right)$$

Let

$$\alpha_1 = C_1 \left(1.9 \sqrt{f_c'} \right) \quad \text{and} \quad \beta = 2,500 \, pd$$

then

$$v_c = \alpha_1 + \beta \left(\frac{L - 2x}{Lx - x^2 - z^2} \right) \tag{A-3}$$

and the slope is

$$\frac{dv_c}{dx} = \beta \left[\frac{-2x^2 + 2Lx - L^2 + 2z^2}{\left(Lx - x^2 - z^2 \right)^2} \right] \tag{A-4}$$

Conditions at the Critical Section

From the unit shear diagram (Figure A-2), it can be seen that at the critical section

$$x = x_c$$

$$v_c = v_{x_c}$$

$$\frac{dv_c}{dx} = -\frac{v_{x_c}}{\frac{L}{2} - x_c}$$
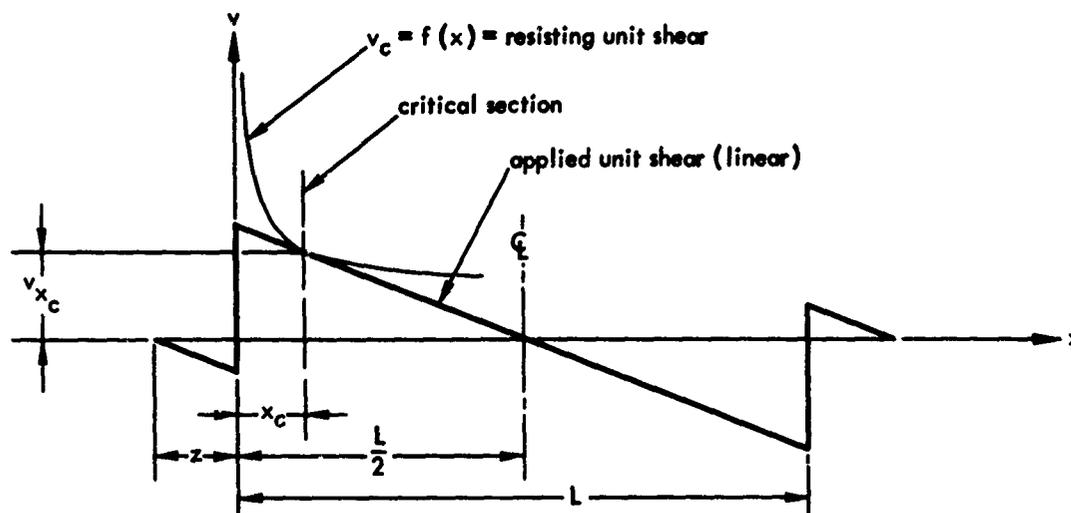
Figure A-2. Applied and resisting unit shear diagram.

Distance to the Critical Section

Applying the conditions at the critical section to Equations A-3 and A-4,

$$\frac{dv_c}{dx} = -\frac{v_c}{\frac{L}{2} - x_c} = \frac{v_c}{x_c - \frac{L}{2}}$$

Therefore

$$\beta \left[\frac{-2x_c^2 + 2Lx_c - L^2 + 2z^2}{\left(Lx_c - x_c^2 - z^2\right)^2} \right] = \left(\frac{1}{x_c - \frac{L}{2}}\right) \left[\alpha + \beta \left(\frac{L - 2x_c}{Lx_c - x_c^2 - z^2} \right) \right]$$

By cross-multiplication and letting

$$\gamma = \frac{\beta}{\alpha_1}$$

$$x_c^4 + x_c^3\left(4\gamma - 2L\right) + x_c^2\left(L^2 - 2z^2 - 6\gamma L\right) + x_c\left(3\gamma L^2 - 2z^2 L\right) + z^4 - \frac{1}{2}\gamma L^3 = 0$$

Thus, the equation for approximating the distance to the critical section for simply supported beams with overhangs under uniformly distributed loads is

$$x_c = \frac{x_c^4 + x_c^3\left(4\gamma - 2L\right) + x_c^2\left(L^2 - 2z^2 - 6\gamma L\right) + z^4 - 0.5\gamma L^3}{2z^2 L - 3\gamma L^2} \tag{A-5}$$

where $\qquad \gamma = \dfrac{\beta}{\alpha_1} = \dfrac{2,500\,pd}{C_1\left(1.9\sqrt{f_c'}\right)}$

Computer Program

A digital computer was used to solve Equation A-5 by the finite difference method. FORTRAN statements, sample input, and sample output are shown in Figure A-3.

46

```
            FORTRAN STATEMENTS

C     DYNAMIC SHEAR STUDIES ON REINFORCED CONCRETE BEAMS
C     DISTANCE TO THE CRITICAL SECTION
 9999 READ 1,FL,D,Z,FCP,P,C1
    1 FORMAT(6F10.0)
      PUNCH 2,EL,D,Z
    2 FORMAT(2HL=,F5.0,4H IN.,4X,2HD=,F6.2,4H IN.,4X,2HZ=,F6.2,4H IN.)
      PUNCH 3,FCP,P,C1
    3 FORMAT(4HFCP=,F6.0,5H PSI.,4X,2HP=,F5.3,4X,3HC1=,F5.2)
      SR=SQRTF(FCP)
      BETA=2500.*P*D
    4 ALPHA=C1*1.9*SR
      G=BETA/ALPHA
      X=D/2.-.1
    5 X=X+.1
      Y=X**4+X**3*(4.*G-2.*EL)+X*X*(EL*EL+2.*Z*Z-6.*G*EL)+Z**4-G*EL**3/2
     1.
      Y=Y/(2.*EL*Z*Z-3.*G*EL*EL)
      IF(X-Y)5,7,6
    6 Y=(Y+X)/2.
    7 IF(C1-1.)8,10,8
    8 PUNCH 9,Y
    9 FORMAT(/,20HFOR DYNAMIC LOADING,,39H THE DISTANCE TO THE CRITICAL
     1SECTION =,F5.1,4H IN.)
      C1=1.
      GO TO 4
   10 PUNCH 11,Y
   11 FORMAT(/,19HFOR STATIC LOADING,,39H THE DISTANCE TO THE CRITICAL S
     1ECTION =,F5.1,4H IN.,//)
      GO TO 9999
      END

          SAMPLE INPUT

144.       12.94       5.         3700.      0.02       1.7

          SAMPLE OUTPUT

L= 144. IN.     D= 12.94 IN.     Z=  5.00 IN.
FCP= 3700. PSI.     P= .020     C1= 1.70

FOR DYNAMIC LOADING, THE DISTANCE TO THE CRITICAL SECTION = 12.7 IN.

FOR STATIC LOADING, THE DISTANCE TO THE CRITICAL SECTION = 15.7 IN.
```

Figure A-3. Computer program for determining the distance to the critical section.

Appendix B

STRENGTH PROPERTIES OF MATERIALS

INTRODUCTION

To study the strength and behavior of structural elements, it is necessary to determine the strength and behavior of the structural materials from which the elements are made. The object of the work reported in this appendix was to determine both the static and dynamic strength of the materials used in the 15 reinforced concrete beams under study. These were composed of concrete, longitudinal reinforcing bars, and vertical wire stirrups. Both static and dynamic tests were made on samples of each material.

CONCRETE

Mix

The concrete mix was a 3,000-psi mix made from Type I Portland cement, 3/4-inch maximum size San Gabriel aggregate, and San Gabriel sand having a fineness modulus of 2.82. Mix proportions were 1.00 : 3.82 : 3.66 by weight, with a water-cement ratio of 0.71 by weight or 7.98 gallons per sack. The cement factor was 4.7 sacks per cubic yard. A slump of 2 inches was specified.

Static Tests

At the time each beam was cast, six standard 6-inch-diameter by 12-inch-long cylinders were cast from the same batch of concrete. The cylinders were cured under wet burlap along with the beam until two days before testing. Three cylinders were used to determine the concrete compressive strength, and three the tensile splitting strength. The results are given in Table B-1. The average static compressive strength at 28 days was 3,660 psi, and the average static splitting tensile strength was 410 psi.

Dynamic Tests

The dynamic tensile splitting strength of the concrete is discussed in Part I.[1] The effect of stress rate on the tensile splitting strength is shown in Figure B-1. Data in the figure are the results of rapid load tests on a series of 4-inch-diameter by 8-inch-long cylinders cast from the same mix used in the beams, but not from the same batch. The mode of failure was the same under static and dynamic loading. However, the tensile splitting strength of the cylinders increased with an increase in loading rate. The tensile splitting strength increased about 70% when the concrete was stressed at a rate of 300,000 psi per second.

LONGITUDINAL REINFORCING STEEL

Material

The longitudinal reinforcing steel in each beam consisted of two No. 9 bars in tension and two No. 7 bars in compression. All bars were from the same lot and satisfied the strength requirements of Specification A432 and the deformation requirements of Specification A305-56T of the American Society for Testing and Materials.
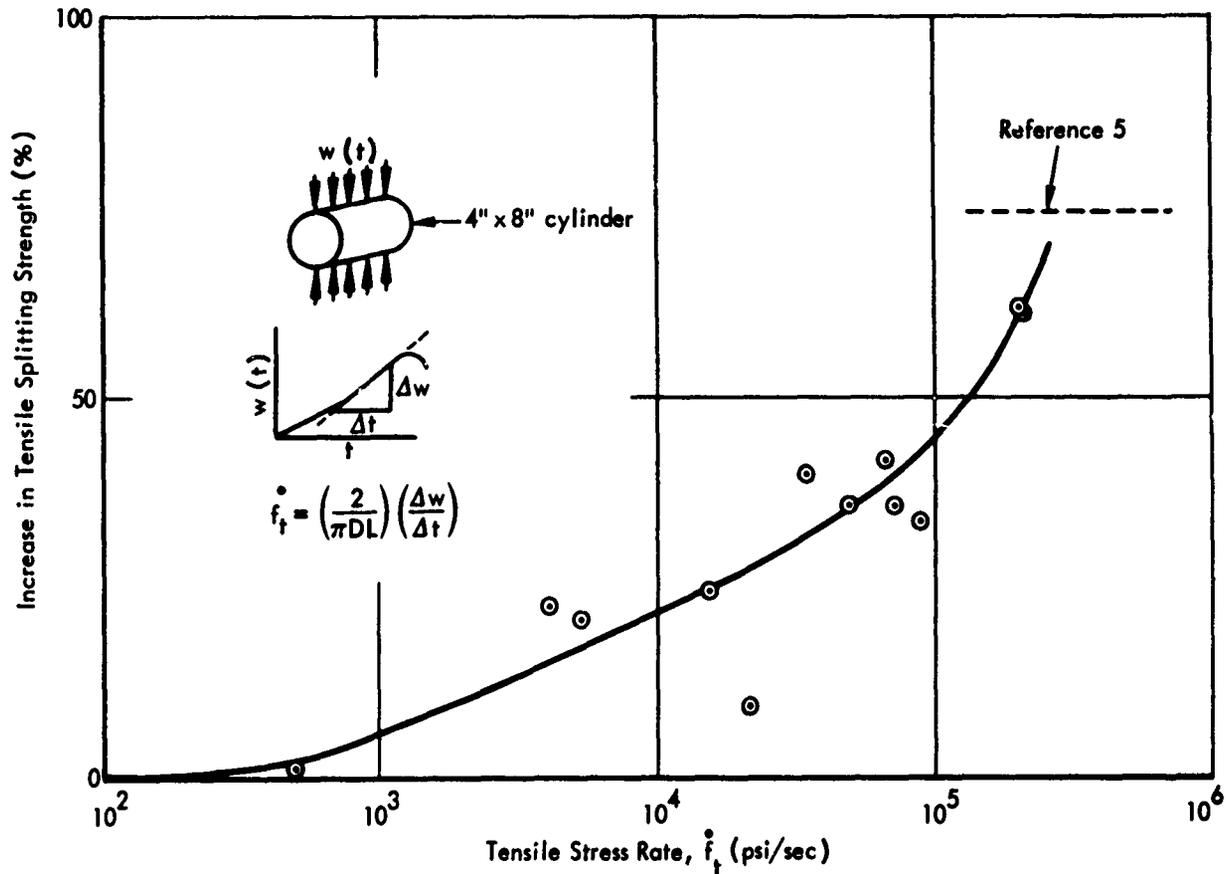
Figure B-1. Increase in tensile splitting strength versus tensile stress rate.

Table B-1. Static Compressive and Tensile Strength of Concrete

Beam No.	Slump (in.)	Age (days)	Compressive Strength, f_c' (psi)				Tensile Strength, f_t (psi)			
			Cyl 1	Cyl 2	Cyl 3	Average	Cyl 4	Cyl 5	Cyl 6	Average
WE1	2	32	3,080	3,010	2,950	3,013	380	370	345	365
WE2	1-3/4	30	3,940	4,210	4,120	4,090	385	400	385	390
WE3	2-1/4	35	3,360	3,430	3,570	3,453	380	415	415	403
WE4	1-3/4	27	3,570	3,610	3,570	3,583	415	400	455	423
WE5	2-1/2	30	3,800	3,960	3,960	3,907	445	340	400	395
WE6	2	33	4,070	4,000	4,280	4,117	425	455	475	452
WE7	2-3/8	26	3,540	3,110	-1/	3,325	370	370	370	370
WE8	2	28	3,710	3,640	3,820	3,723	410	440	470	440
WE9	2-1/2	23	3,960	3,870	3,930	3,920	420	450	470	447
WE10	2-1/4	27	3,980	4,100	3,710	3,930	460	385	420	422
WE11	2-1/4	20	3,310	3,610	3,340	3,420	410	420	360	397
WE12	2-1/2	27	3,430	3,410	3,290	3,377	370	420	390	393
OE1	2	28	3,680	3,080	3,450	3,403	405	405	405	405
OE2	2	27	3,890	3,080	3,940	3,637	435	455	405	432
OE3	2	28	3,940	3,990	4,080	4,003	--	--	--	--
Average of all values						3,660				410

1/ Not tested.

49

Static Tests

Standard tension tests to determine the upper yield point were made on coupons from all the tension bars and more than half the compression bars. The results are given in Table B-2. The average upper yield stress was 67,600 psi for No. 9 bars and 65,900 psi for No. 7 bars. One No. 9 and one No. 7 bar were tested to rupture, and the stress-strain curves are shown in Figure B-2. For both bar sizes, the proportional limit was about 50,000 psi, the tangent modulus of elasticity 29×10^6 psi, and the secant modulus taken to the upper yield point was approximately 27×10^6 psi. All bars had a well-defined yield point, but the larger diameter bars had higher yield strengths.

Table B-2. Static Yield Strength of Longitudinal Reinforcing Bars

Tension Steel No. 9 Bars			Compression Steel No. 7 Bars		
Bar No.	Beam in Which Used	Upper Yield Stress (psi)	Bar No.	Beam in Which Used	Upper Yield Stress (psi)
9-37	WE1	70,600	7-37	WE1	-- 2/
9-38	WE1	70,600	7-38	WE1	65,300
9-39	WE2	66,400	7-39	WE2	64,100
9-40	WE2	71,000	7-40	WE2	67,500
9-41	WE3	66,200	7-41	WE3	--
9-42	WE3	63,900	7-42	WE3	66,600
9-43	WE4	70,400	7-43	WE4	--
9-44	WE4	64,500	7-44	WE4	64,100
9-45	WE5	69,700	7-45	WE5	--
9-46	WE5	66,900	7-46	WE5	67,700
9-47 1/	WE7	70,900	7-47	WE7	--
9-48	WE7	68,100	7-48	WE7	64,000
9-49	OE2	68,400	7-49	OE2	--
9-50	WE6	66,000	7-50	WE6	68,300
9-51	WE8	71,100	7-51	WE8	--
9-52	WE8	64,500	7-52	WE8	64,900
9-53	WE10	66,000	7-53	WE10	--
9-54	WE10	66,400	7-54	WE10	65,100
9-55	WE11	70,800	7-55 1/	WE11	65,600
9-56	WE11	63,400	7-56	WE11	68,000
9-57	OE1	71,400	7-57	OE1	--
9-58	OE1	66,200	7-58	OE1	66,000
9-59	WE12	64,500	7-59	WE12	--
9-60	WE12	71,400	7-60	WE12	64,400
9-61	WE9	62,000	7-61	WE9	66,900
9-62	WE9	71,100	7-62	WE9	67,100
9-63	OE2	63,500	7-63	OE2	--
9-64	WE6	66,600	7-64	WE6	64,500
Lowest value		62,000	Lowest value		64,000
Highest value		71,400	Highest value		68,300
Average value		67,600	Average value		65,900

1/ Tested to rupture and plotted in Figure B-2.
2/ Not tested.
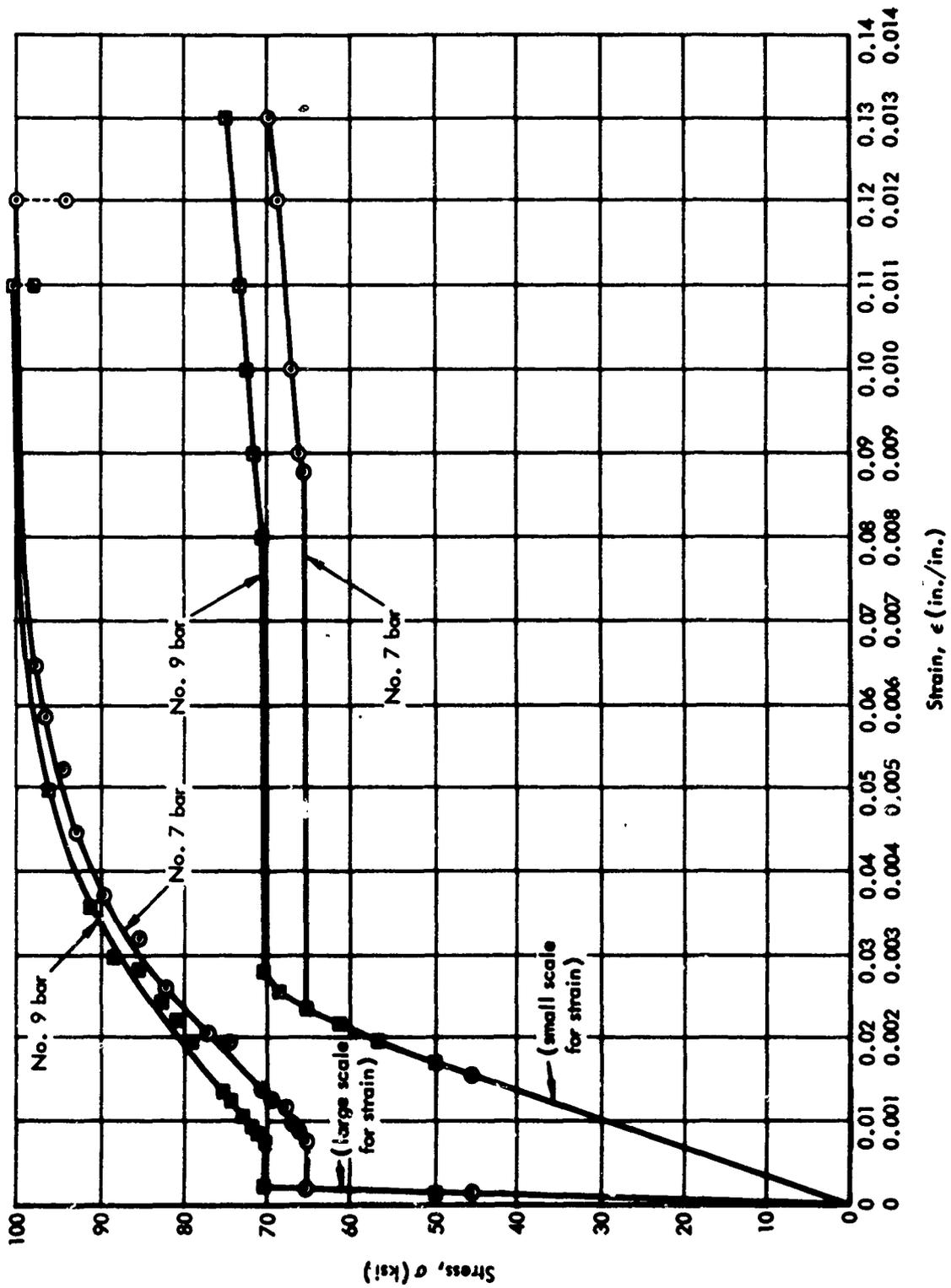
Figure B-2. Tension tests on longitudinal reinforcing bars.

Dynamic Tests

The dynamic yield strength of the bars used is discussed in Part I.[1] A plot of increase in upper yield stress with respect to increase in strain rate for No. 9 bars is shown in Figure B-3. The average strain rate for the No. 9 bars in the beam tests is about 0.3 in./in./sec. The corresponding increase in yield stress, from Figure B-3, is 24%.

STIRRUPS

Material

The stirrups were made from 9-gage bright annealed plain wire. The chemical composition included 0.12% carbon, 0.49% manganese, 0.014% phosphorus, 0.017% sulfur, and 0.19% silicon. The cross-sectional area of 9-gage wire is 0.0172 square inch.

Static Tests

Nine samples of the wire were tested. The yield point was obtained for all samples and the ultimate stress for three of them. The wire, received in a 2-foot-diameter coil, was carefully straightened by pulling it through a hole in a wooden block by hand. Specimens 10 inches long were cut from the straightened wire and a strain gage applied at midlength to measure strain in the longitudinal direction. A tension testing machine was used to apply the load, and an "M" indicator to take strain readings. The specimen was preloaded to about 150 pounds to seat the wire grips and associated parts. Then the load was relieved to 30 pounds and the test started. A plot of load versus indicator reading was made to determine the reading for zero load.

The results of the tests are given in Table B-3, and the stress-strain curve for specimen number 6 is shown in Figure B-4. The stress-strain curve is linear to a proportional limit of about 28,000 psi. The upper yield point was not well defined and no lower yield point was observed. The wire was very ductile and had a long interval of relatively constant load before strain hardening commenced. An idealized straight-line stress-strain relationship, shown in the figure, was constructed using the average yield stress of the nine specimens (36,000 psi) and a secant modulus of elasticity of 29×10^6 psi. The average ultimate stress was 52,300 psi.

Dynamic Tests

Seventeen specimens of stirrup wire 10 inches long were strained in tension with the NCEL dynamic materials testing machine[6] and continuous measurements recorded of tensile strain and force in each specimen. The strain was measured with one SR-4 foil resistance strain gage (EA-05-500 BH) placed midway between the ends of the specimen. Force was measured with an NCEL strain gage-type tension link. A typical oscillogram is shown in Figure B-5.

The results are given in Table B-4 and plotted in Figure B-6. The wire had a diameter of 0.146 inch and a cross-sectional area of 0.0167 square inch. The increase in upper yield strength varied logarithmically with respect to strain rate from 50% at a strain rate of 0.2 in./in./sec to 100% at 3.0 in./in./sec. The increase in ultimate strength varied logarithmically from 10% at 0.2 in./in./sec to 16% at 3.0 in./in./sec. Both yield strength and ultimate strength increased with increasing strain rate, but the strain rate had a much greater influence on yield strength. Most of the stirrups in the beam tests were strained at a rate of about 1 in./in./sec. The corresponding increase in upper yield strength is 80%, and the corresponding increase in ultimate strength 14%. The material had well-defined upper and lower yield points under dynamic load.
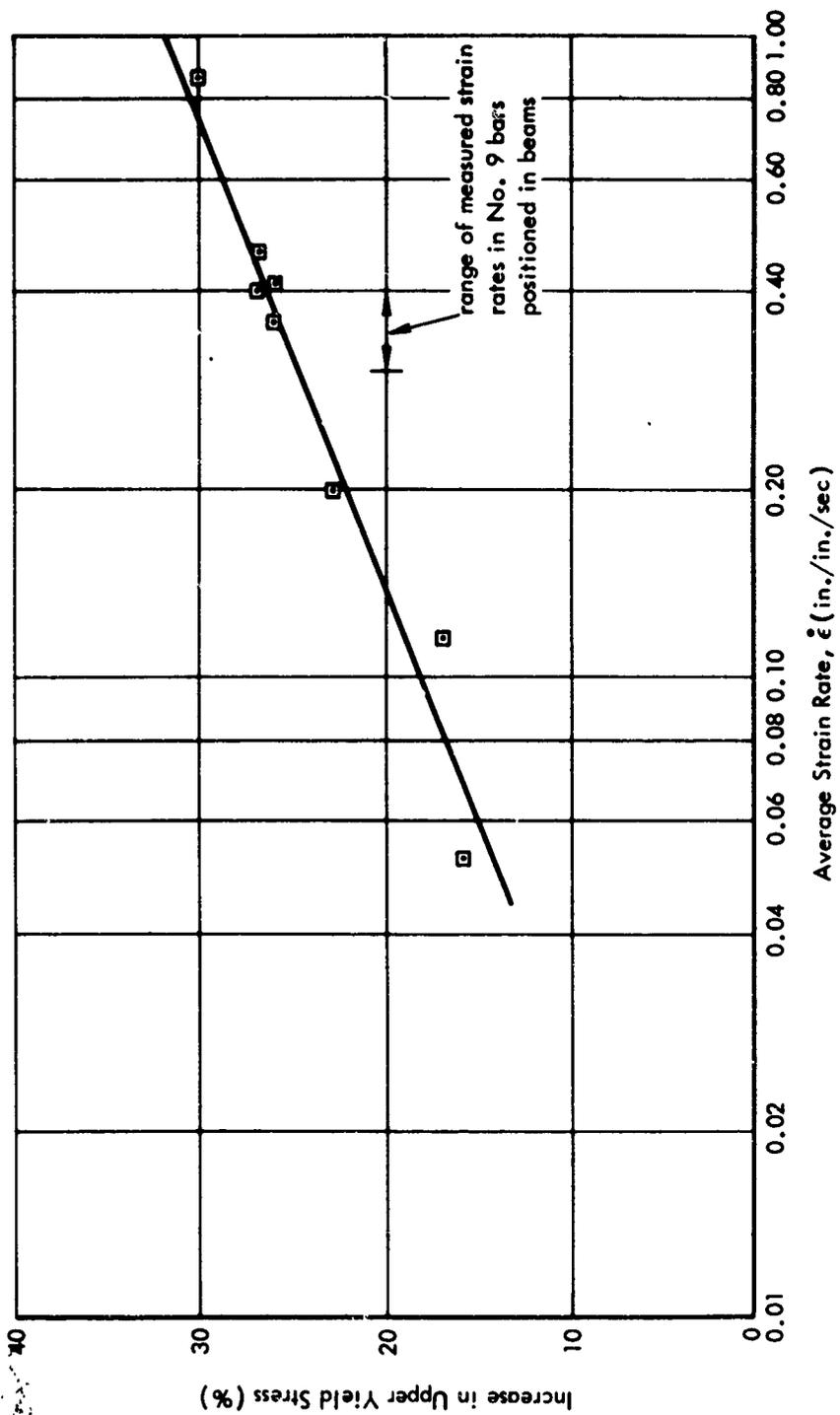
Figure B-3. Increase in upper yield stress versus strain rate curve for No. 9 bars.

The figure shows a plot of Increase in Upper Yield Stress (%) (y-axis, ranging 0 to 40) versus Average Strain Rate, $\dot{\epsilon}$ (in./in./sec) (x-axis, logarithmic scale from 0.01 to 1.00). Data points are marked with squares, and a line is fitted through them. An annotation indicates the "range of measured strain rates in No. 9 bars positioned in beams."
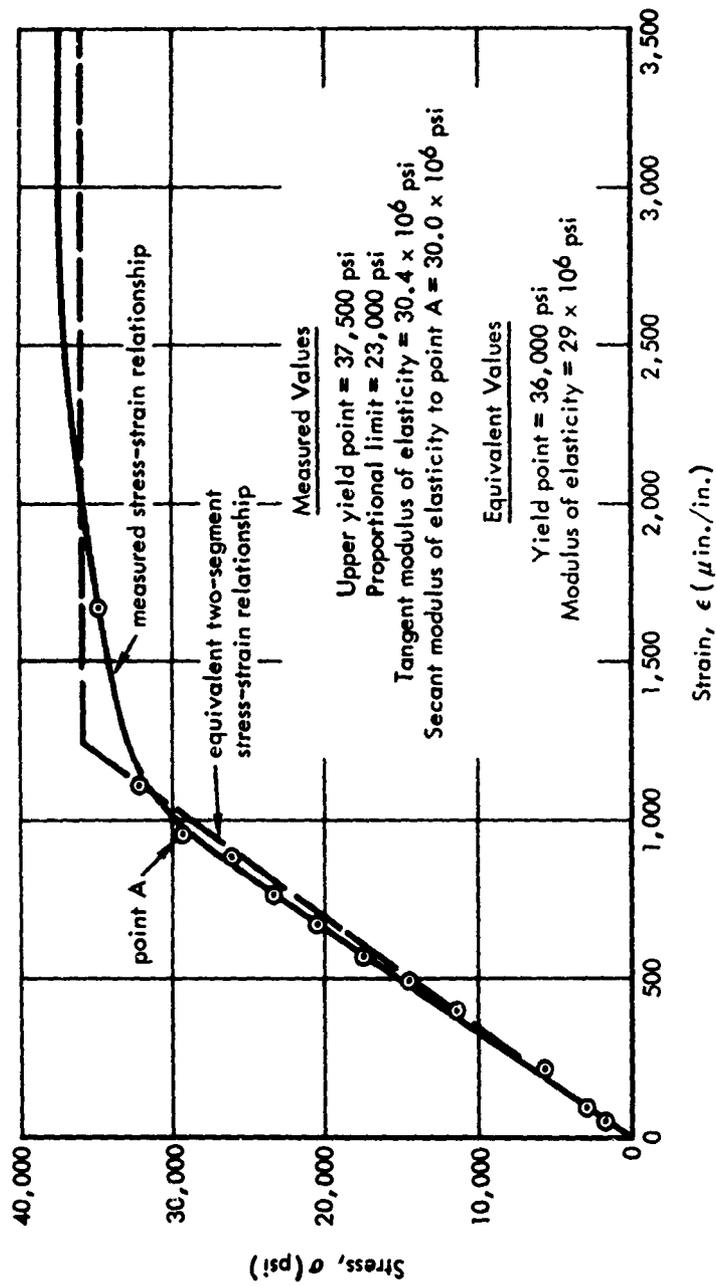
Figure B-4. Tension test of 9-gage wire used for stirrups.

54
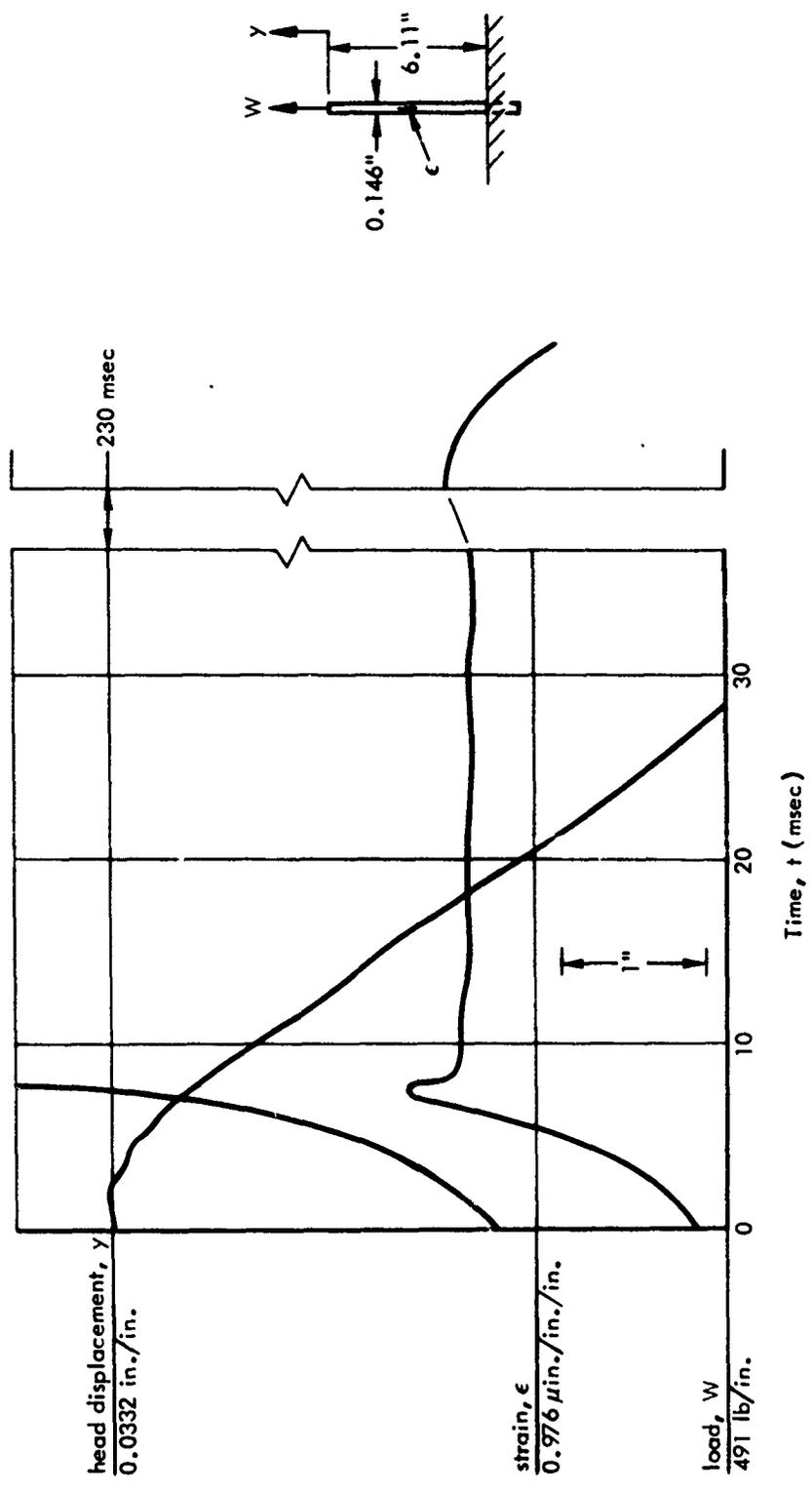
Figure B-5. Typical oscillogram, rapid load test on 9-gage wire.

55
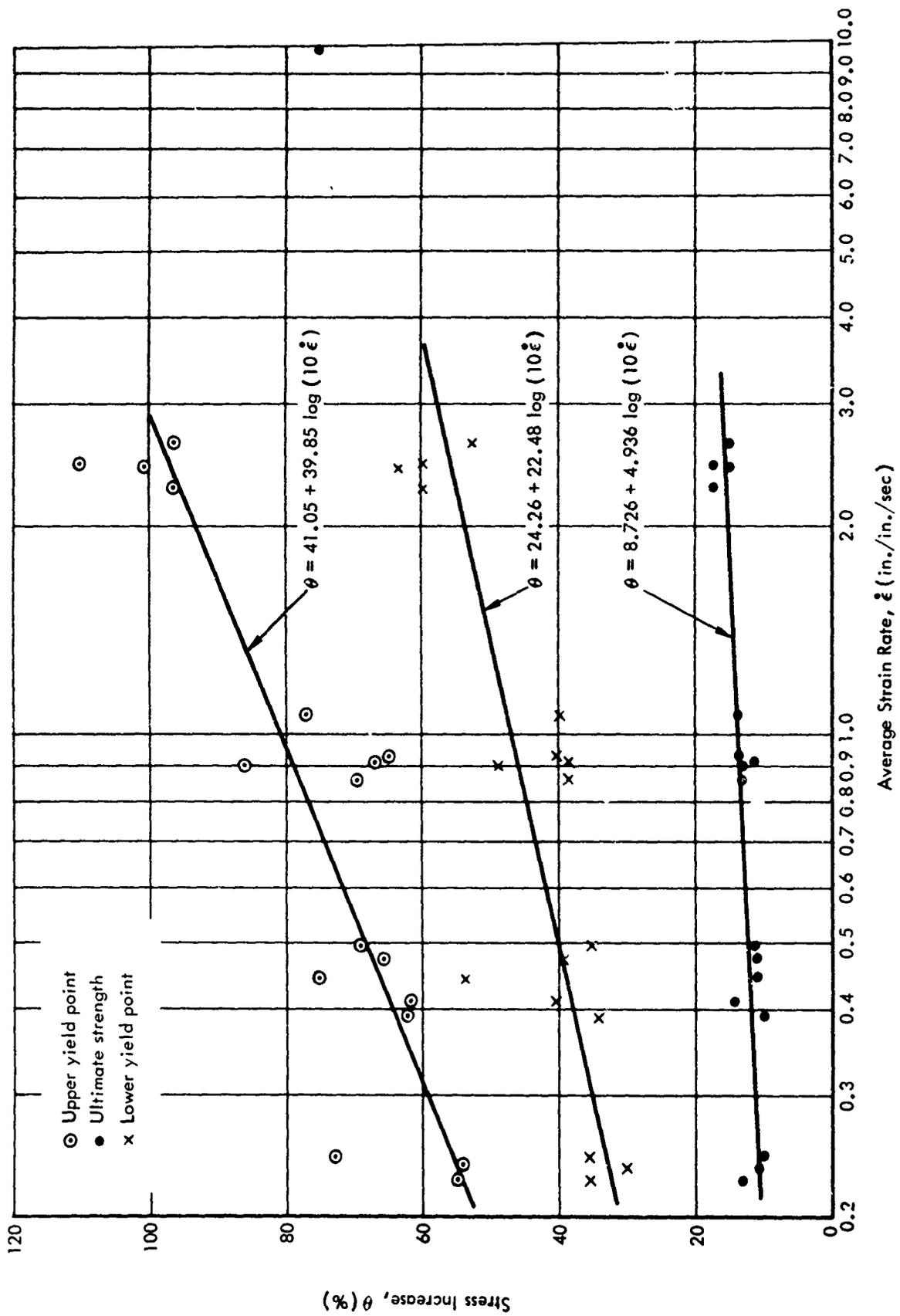
Figure B-6. Increase in strength of 9-gage wire versus strain rate.

$\theta = 41.05 + 39.85 \log (10\dot{\epsilon})$

$\theta = 24.26 + 22.48 \log (10\dot{\epsilon})$

$\theta = 8.726 + 4.936 \log (10\dot{\epsilon})$

⊙ Upper yield point
● Ultimate strength
✕ Lower yield point

Average Strain Rate, $\dot{\epsilon}$ (in./in./sec)

Stress Increase, θ (%)

Table B-3. Tension Tests on 9-Gage Wire

Specimen No.	Yield Stress (psi)	Ultimate Stress (psi)
1	36,300	-- [2]
2	37,200	--
3	37,500	--
4	35,800	--
5	36,100	--
6 [1]	37,500	--
7	35,200	52,400
8	35,400	52,600
9	34,600	52,000
Average value	36,000	52,300

[1] Stress-strain curve shown in Figure B-4.
[2] Not tested.

Table B-4. Results of Rapid Load Tests on 9-Gage Wire

Specimen No.	Diameter (in.)	Area (in.²)	Gage Length (in.)	Average Strain Rate, $\dot{\epsilon}$ (in./in./sec)	Dynamic Upper Yield Stress, σ_{dyu} (ksi)	Increase in Upper Yield Stress, $\frac{\sigma_{dyu}}{\sigma_y}$ 1/	Dynamic Lower Yield Stress, σ_{dyl} (ksi)	Increase in Lower Yield Stress, $\frac{\sigma_{dyl}}{\sigma_y}$ 1/	Dynamic Ultimate Stress, σ_{du} (ksi)	Increase in Ultimate Stress, $\frac{\sigma_{du}}{\sigma_u}$ 2/
1	0.147	0.0170	6.08	0.391	58.4	1.62	48.3	1.34	57.6	1.10
2	0.146	0.0167	5.98	0.236	55.6	1.55	46.8	1.30	58.0	1.11
3	0.145	0.0165	--	0.226	55.6	1.55	48.8	1.36	59.3	1.13
4	0.146	0.0167	5.92	0.244	62.3	1.73	48.8	1.36	57.6	1.10
5	0.146	0.0167	6.12	0.443	63.1	1.75	55.4	1.54	58.1	1.11
6	0.146	0.0167	6.04	0.473	59.6	1.66	50.2	1.39	58.1	1.11
7	0.145	0.0165	6.08	0.410	58.2	1.62	50.5	1.40	59.8	1.14
8	0.146	0.0167	6.14	0.496	60.7	1.69	48.7	1.35	58.4	1.12
9	0.146	0.0167	5.96	0.914	60.0	1.67	49.8	1.38	58.3	1.11
10	0.146	0.0167	6.08	0.860	61.0	1.70	49.8	1.38	59.2	1.13
11	0.146	0.0167	--	1.31	63.6	1.77	50.3	1.40	59.6	1.14
12	0.145	0.0165	--	0.903	67.0	1.86	53.5	1.49	59.1	1.13
13	0.146	0.0167	6.06	0.928	59.3	1.65	50.5	1.40	59.6	1.14
14	0.146	0.0167	6.14	2.46	75.6	2.10	57.5	1.60	61.4	1.17
15	0.146	0.0167	6.16	2.28	70.5	1.96	57.5	1.60	61.4	1.17
16	0.146	0.0167	6.02	2.63	70.5	1.96	54.9	1.52	60.1	1.15
17	0.146	0.0167	6.12	2.42	73.4	2.04	58.8	1.63	60.1	1.15

1/ σ_y = 36.0 ksi = average static yield stress.
2/ σ_u = 52.3 ksi = average static ultimate stress.

58

Appendix C

INSTRUMENTATION

by

O. M. Wilsey

INTRODUCTION

This appendix describes the electronic recording equipment, control equipment, and transducers, and the instrumentation procedures used during calibration and testing of the 15 reinforced concrete beams of the study. In tests on eight beams loaded dynamically, 24 channels of instrumentation were provided to measure acceleration, deflection, overpressure, force, and strain; in tests on seven beams loaded statically, only 23 channels were provided, since the acceleration measurement was not needed. A diagram of the system used in the dynamic tests is given in Figure C-1.

RECORDING EQUIPMENT FOR DYNAMIC TESTS

A Honeywell Model LAR 7300 Laboratory Recorder was used to record all 24 channels at a speed of 60 ips. This is a seven-track, direct-record, multiple-speed tape recorder.

The data gathering system, Model FMT 290, made by Vector Manufacturing Company, consisted of seven racks (modules) of low-level voltage control oscillators with four channels per rack. Each rack contained four standard IRIG frequencies. The center frequencies were 70, 52.5, 40, and 30 kcps with a linear bandwidth of ±7.5% of the center frequency. The four frequencies were multiplexed onto one track of the seven-track magnetic recorder. The components and their specifications are shown in Table C-1.

CONTROL EQUIPMENT FOR DYNAMIC TESTS

An electromechanical sequential timer manufactured by Artisan Electronics, Model EPC 70068, was used to control the sequence of events during each test. The times of the events and the corresponding responses were as follows:

Time (msec)	Event Response
-5000	Timer on
-4990	Tape recorder start
-1500	Rotating drum start
- 100	Key and calibrate
0	Detonate charge
+ 100	Valve series "C" open
+ 900	Valve series "A" open
+1500	Tape recorder stop
+2500	Timer stop and reset to zero

The key, listed in the response column, is a timing code put on the tape to activate the analog-to-digital converter during data reduction. The key is an eight-cycle burst at a rate of 1 kcps at 2 volts (pp). The burst is supplied by a General Radio Company Tone Burst Generator, Model 1369A, and a Hewlett-Packard Audio Oscillator, Model 2048.
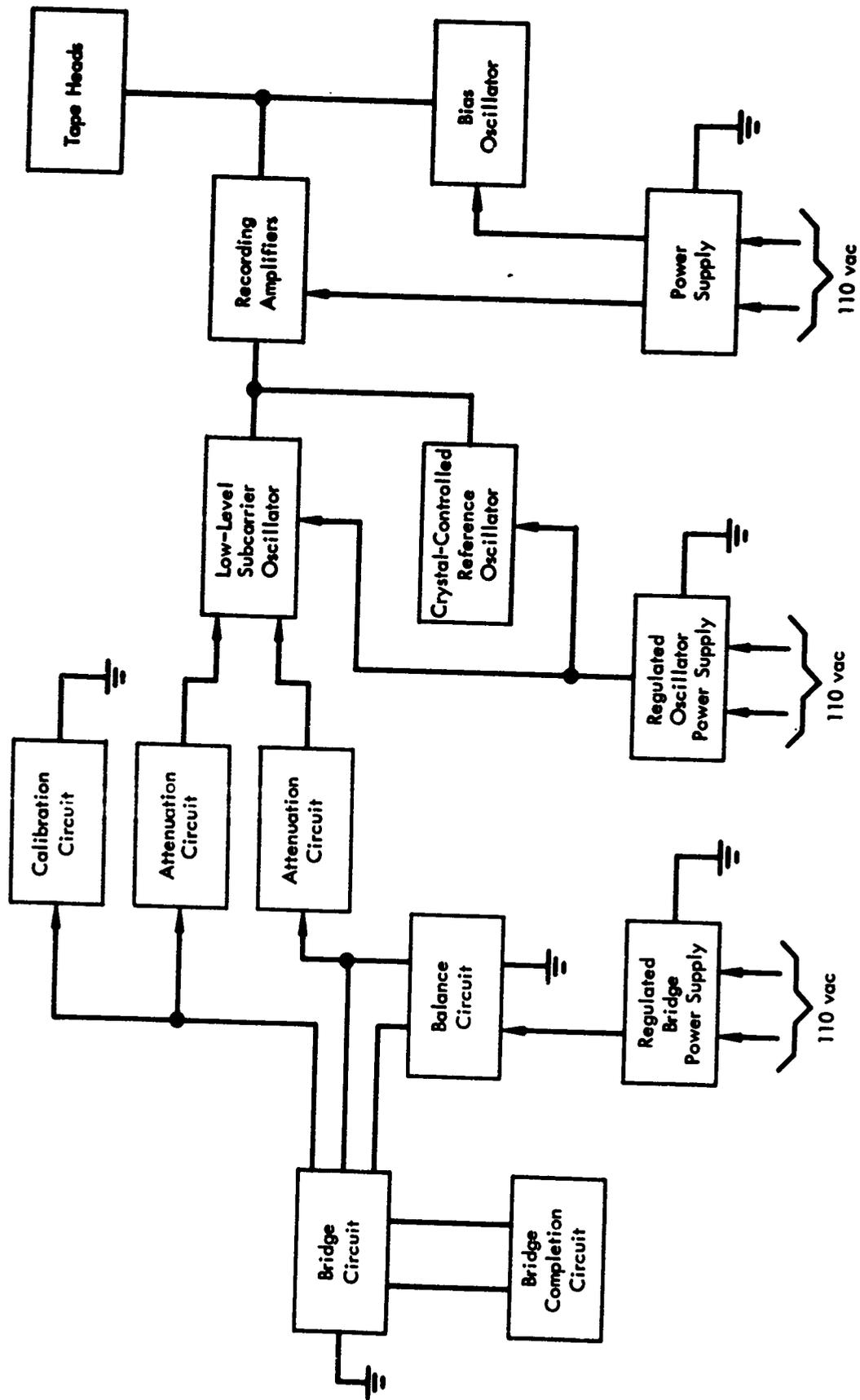
Figure C-1. Block diagram of instrumentation used in dynamic tests.

Table C-1. Component Specifications for the Voltage Control Oscillators

Component	Specifications
Full-scale FM output	±7. 5% of center frequency
Input	Differential ±1 mv adjustable from ±3 mv with no attenuation to ±100 mv with full attenuation
Input attenuator	Four steps, adjustable in step 　0-3 mv not attenuated 　3-10 mv 　10-30 mv 　30-100 mv
Input impedance	1, 000 ohms
Bridge balance	Capable of accommodating: 　(a) Any four-arm bridge of resistive elements 　　　with maximum bridge unbalance of 5% 　(b) Single or double strain gages
Controls	Input attenuator Bridge balance Bridge voltage adjustment (0-10 vdc) Bandwidth adjustment Center frequency adjustment FM output gain adjustment (0-1 v) Manual calibrate switch
Linearity	Output frequency proportional to input voltage within 0. 5% of full scale
Frequency response	0. 9 kcps at 30 kcps 1. 2 kcps at 40 kcps 1. 6 kcps at 52. 5 kcps 2. 1 kcps at 70 kcps
Output impedance	1, 000 ohms

RECORDING EQUIPMENT FOR STATIC TESTS

All static test data were recorded in digital form with the use of Budd Instruments Switch and Balance Units, Series C-10LTC; Budd Instruments Digital Strain Indicator, Model A-110; and Vector Manufacturing Company Printer Control Unit, Model E-140. The capacity of the system used is 30 channels of static test measurements. The switch and balance units provide automatic step-switching and manual bridge balance. The digital strain indicator has an automatic servo-driven balance unit and a balance time of 4 seconds from zero to full scale. The printer control unit uses standard 2-inch adding machine tape for data printout. The printout information includes channel number, reading with three significant figures, and attenuation setting.

TRANSDUCERS AND STRAIN GAGES

Purpose and Location

Twenty-four measurements were taken with transducers or strain gages in the dynamic tests. All except the acceleration measurement were taken in the static tests. The transducers and strain gages are listed in Table C-2 of this appendix, and the locations are shown on Figures 1, 2, and 3 of the report.

Accelerometer

The accelerometer was a Statham Accelerometer, Model A5-100-350, ±100 g, used with a four-active-arm bridge-sensing element which has unbonded strain gages. The specifications are:

1.	Bridge resistance	350 ohms
2.	Overload range	300% full scale
3.	Output	±50 mv
4.	Nonlinearity and hysteresis	Less than 1% of full scale
5.	Transverse acceleration	Less than 0.02 g/g of rated range
6.	Natural frequency	600 cps
7.	Ambient temperature limits	$-40°F$ to $+200°F$

Linear Potentiometers

One Model 156 Bourns Align-O-Pot and three Bourns Model 108 linear potentiometers were used. The Model 156 has nonlinearity of ±0.5%, displacement of 0-4 inches, and resolution of 0.001 inch. The Model 108 has nonlinearity of ±0.75%, displacement of 1.31 inches, and resolution of 0.0016 inch.

Load Cells

Kulite-Bytrex 0-60,000-pound load cells were used. The full-scale output is 30 mv. The nonlinearity is less than 1% of full scale and the bridge resistance is 700 ohms.

Pressure Cells

Statham Instrument Model PA208TC-150-350 pressure cells were used. Specifications of these gages are:

1.	Bridge resistance	350 ohms
2.	Overload range	200% full scale
3.	Output	56 mv at 7 volts input
4.	Nonlinearity and hysteresis	Less than 0.75% of full scale
5.	Transduction	Resistive, balanced, unbonded strain gage bridge
6.	Natural frequency	12.5 kc
7.	Ambient temperature limits	$-60°F$ to $+250°F$

Table C-2. Transducers and Strain Gages

Quantity	Type	Designation	Measurement
1	Accelerometer	MA	Midspan acceleration
1	Linear potentiometer	MD	Midspan deflection
3	Linear potentiometer	DC	Depth change
1	Load cell	RE	Reaction, east
1	Load cell	RW	Reaction, west
3	Pressure cell	PC	Overpressure
9	Strain gage	WS	Web steel strain
2	Strain gage	TS	Tension steel strain
1	Strain gage	CS	Compression steel strain
2	Strain gage	C	Concrete strain
24			

Strain Gages

Three types of strain gages were used. The first, manufactured by Baldwin-Lima-Hamilton, Type FA-100-12-S6, was used on the longitudinal reinforcing bars, Type ASTM A-432, No. 7 and No. 9. These gages have a resistance of 120 ±0.2 ohms, with a gage factor of 2.09 ±1%. They are self-compensated for ASTM A-432 steel and were applied with Baldwin-Lima-Hamilton EPY-150 epoxy cement. The second type, manufactured by Allegheny Instruments Incorporated, Type EA-05-500BH, was used on the 9-gage-wire stirrups. The resistance is 120 ±0.2 ohms, with a gage factor of 2.08 ±0.5%. They were applied to the stirrups with Eastman 910 cement. The third type, Type A-9-2 manufactured by Baldwin-Lima-Hamilton, was used on the concrete. These gages have a resistance of 200 ±2.0 ohms, with a gage factor of 2.13 ±1%, and were applied to the concrete with Baldwin-Lima-Hamilton EPY-150 epoxy cement.

All strain gages were used in a four-arm bridge circuit. The FA-100-12-S6 type was wired with two active gages (in opposite arms of the bridge) and two dummy gages. The other types employed one active gage and three dummies. All dummies were mounted on the same kind of material as the active gages, in order to obtain the same coefficient of expansion and temperature compensation. All active gages were waterproofed with Petrocene wax and a layer of electrical tape, both of which were then covered with a sealing compound, Ten-X, manufactured by Electro Cote Company.

CALIBRATIONS FOR DYNAMIC TESTS

Accelerometer

The accelerometer was calibrated to 100 g in 10-g increments by using a Schaevitz rotary accelerometer and the Vector voltage control oscillators (VCO). A resistor was selected and placed across one arm of the bridge. A frequency deviation of approximately 70% of full scale was achieved. This was recorded and compared to the calibration during the test to determine any change in system sensitivity between the time of the initial calibration and the test.

Linear Potentiometers

The 4-inch displacement gage was calibrated to full scale in quarter-inch increments with a 4-inch micrometer on the Vector voltage control oscillators. A resistor was selected and placed across one arm of the bridge. A frequency deviation of 82% of full scale was achieved. This was recorded and compared to the calibration during the test to determine any change in system sensitivity.

The 1.31-inch gages were calibrated to 0.300 inch, in successive increments of 0.002 inch up to 0.020 inch, 0.020 inch up to 0.100 inch, and finally 0.050 inch up to 0.300 inch. A resistor was selected and placed across one arm of the bridge. A frequency deviation of 85% of full scale was achieved. This was recorded and compared to the calibration during the test to determine any change in system sensitivity.

Load Cells

The load cells were calibrated on the voltage control oscillators to full scale by loading them on a 60,000-pound Baldwin load machine in 5,000-pound increments. A resistor was selected and placed across one arm of the bridge. A frequency deviation of 80% was achieved. This was recorded and compared to the calibration during the test to determine any change in system sensitivity.

Pressure Cells

The pressure cells were calibrated to 150 psi in 15-psi increments in a static pressure calibrator, using nitrogen as a pressure source. A resistor was selected and placed across one arm of the bridge. A frequency deviation of 85% was achieved. This was recorded and compared to the calibration during the test to determine any change in system sensitivity.

Strain Gages (Single Active Arm)

The calibration resistors chosen for the strain gages were derived by the following formulas. First, to find the approximate resistance value required, the formula used was

$$RC = R\left(\frac{1 - GS}{GS}\right)$$

where   RC = calibrate resistor

   R = gage resistance

   G = gage factor

   S = maximum expected strain (μin./in.)

Second, the required resistance having been found, a resistor was selected as near to the computed value as possible. Then it was measured on a precision bridge, and by using the measured value and the formula

$$S = \frac{1}{G}\left(\frac{R}{R + RC}\right)$$

the exact value of the resistor in μin./in. was determined.

If the value of the resistor corresponds to approximately the maximum strain expected, the calibration resistor can be used to adjust the band limits.

Strain Gages (Two Active Arms)

When using two active arms on opposite sides of the bridge, the maximum strain expected may be multiplied by two and the same procedure used as with the single arm type.

CALIBRATION FOR STATIC TESTS

The accelerometer was not calibrated or used in the static tests. Calibrations for the static tests were identical to those for dynamic tests except that the Budd digital recorder was used instead of the voltage control oscillators.

REDUCTION OF DATA FROM DYNAMIC TESTS

After the data was recorded on magnetic tape, it was played at the NCEL computer facility into an Ampex FR-100 reproducer, through a Data Control Systems Discriminator, Model GFD-2, to a Control Logic Incorporated Analog-to-Digital Converter, Model PH ADC-1, and finally into an IBM Data Processing System, IBM 1620-II.[7]

Appendix D

PLOTS OF MEASURED DATA

by

D. S. Harrington and R. H. Seabold

This appendix presents data from both dynamic and static tests. Data from the dynamic tests were recorded continuously on magnetic tape, then reduced and plotted by a digital computer at 0.25-msec intervals. Data from the static tests were recorded on a digital recorder or by hand at 5-psi intervals up to 30 psi, and at 2-psi intervals thereafter. In the test for beam OE3 only, data were recorded at 1-psi intervals after an overpressure of 40 psi was obtained.

The width of the load was 8.10 inches; therefore, the overpressures which are given in pressure units (psi) must be multiplied by 8.10 to obtain load per unit length (lb/in.).

Figures D-1 through D-7 are plots of dynamic load and reaction with respect to time. Although shear failures occurred at the east end, the reactions are given for both ends of the beam for comparison.

Figures D-8 through D-13 are plots of the motion at the center of the span during dynamic tests. Deflections computed from the acceleration measurements are plotted as well as the measured deflections. Values on the curves for deflection must be multiplied by 1/10 to obtain values in inches, and for acceleration by 10 to obtain values in gravity units (g).

Figures D-14 through D-27 are plots of the strains measured during dynamic tests at midspan and at the east end. The strains near the east end were measured in the region of the critical diagonal tension crack.

Figures D-28 through D-33 are plots of strain and deflection measured during the static tests. Each figure contains two sets of curves, one for the strains and deflection at midspan, the other for the strains in the region of the critical diagonal tension crack. Beam OE3 had no stirrups in the region of the critical diagonal tension crack; therefore, in Figure D-33, the change in the total depth of the critical section is plotted in lieu of stirrup strain.

The locations of the measurements are shown in Figures 1, 2, and 3 in the body of the report.

66
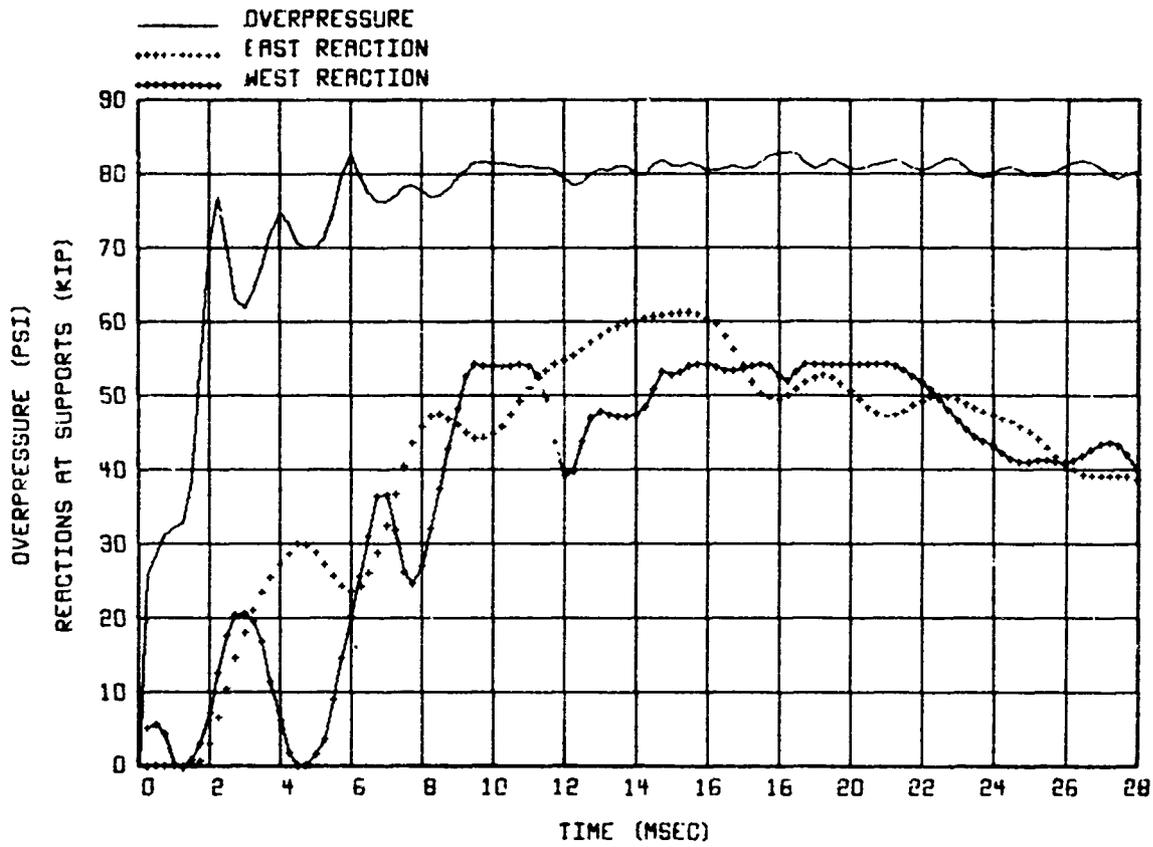
FIGURE D-1. LOAD AND REACTION VS. TIME, BEAM WE 1.
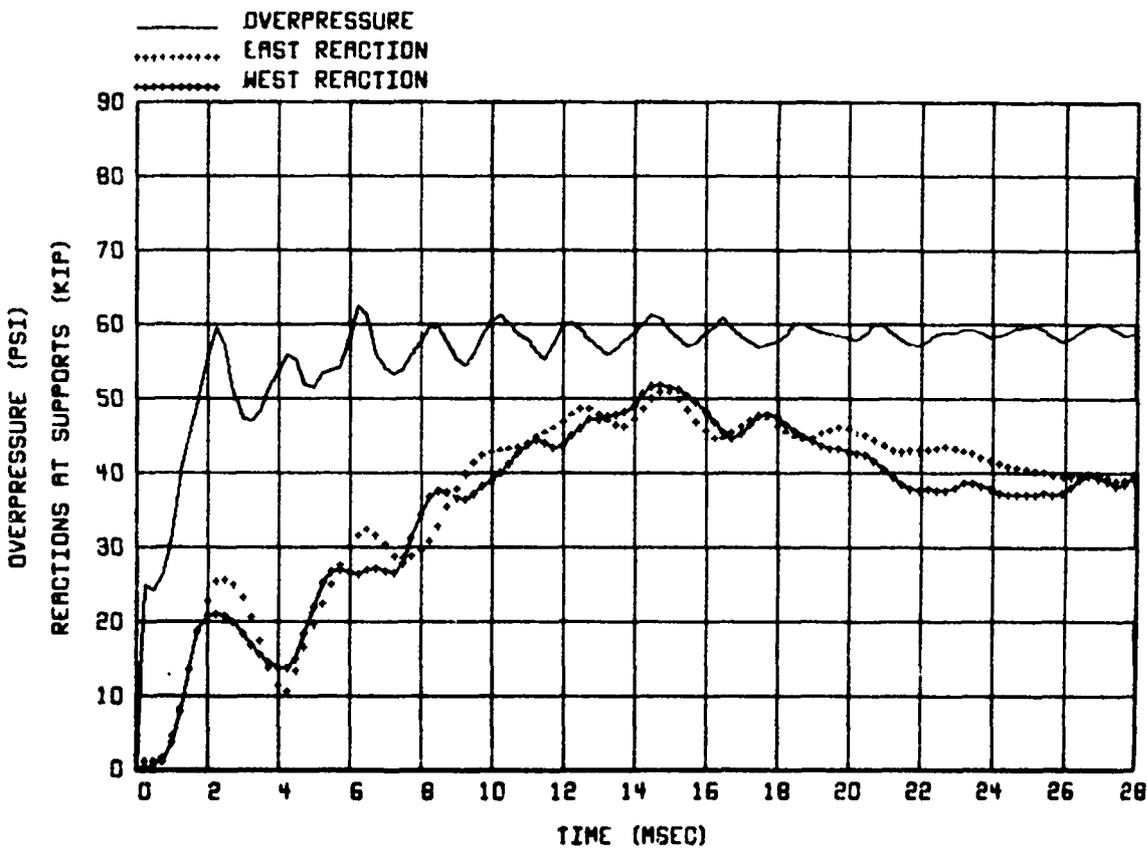
FIGURE D-2. LOAD AND REACTION VS. TIME, BEAM WE 2.
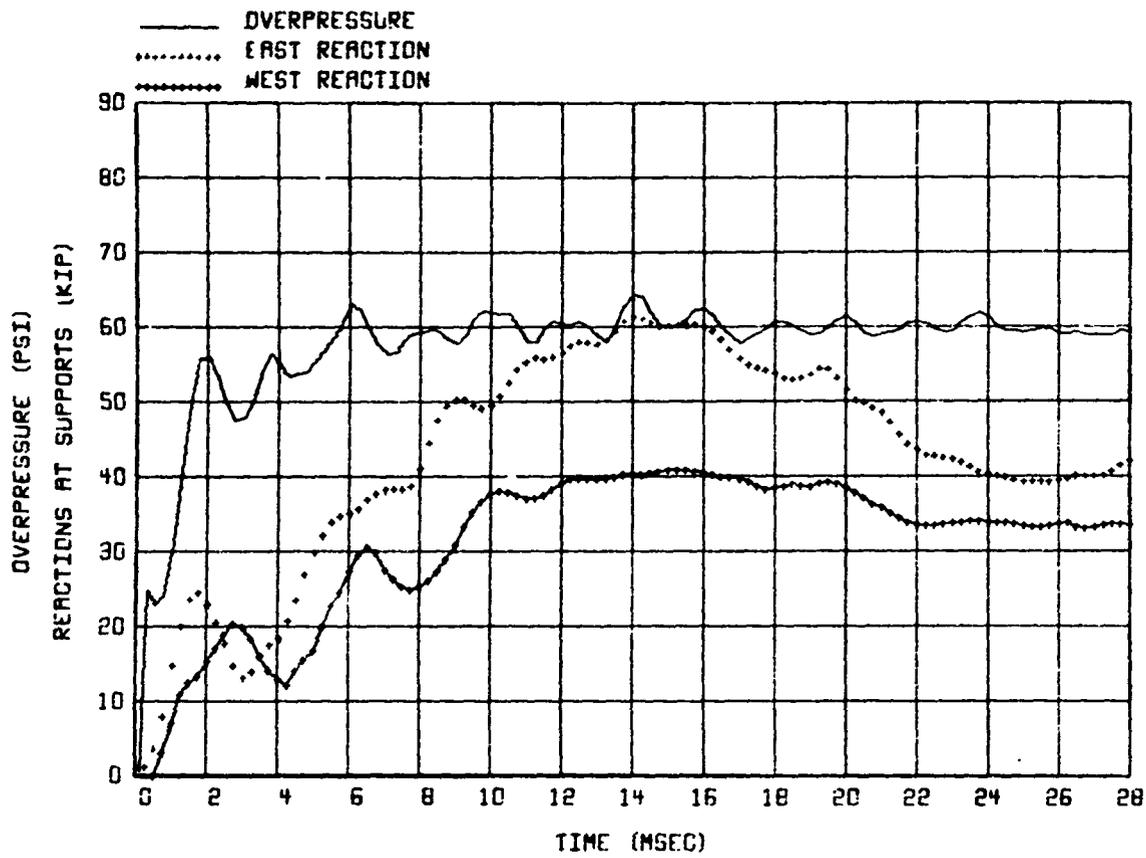
FIGURE D-3. LOAD AND REACTION VS. TIME, BEAM WE 3
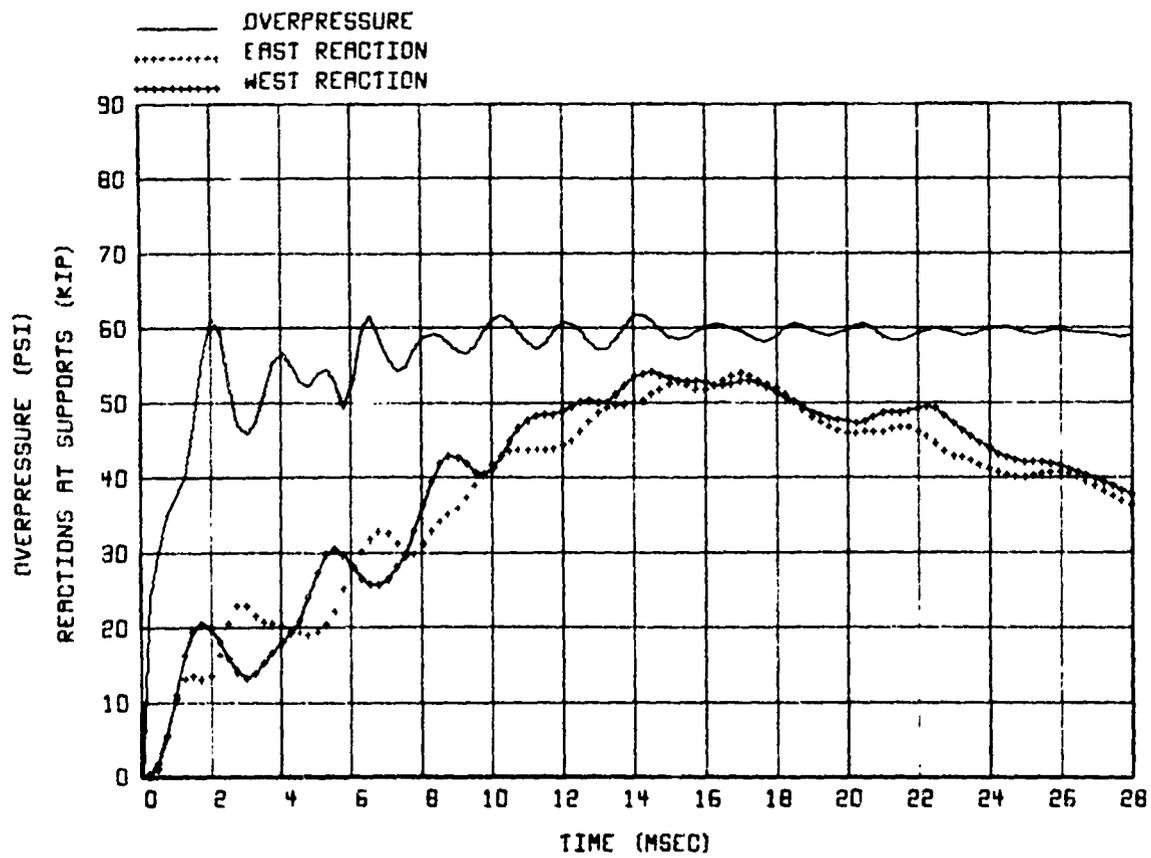
FIGURE D-4. LOAD AND REACTION VS. TIME, BEAM WE 5.

68
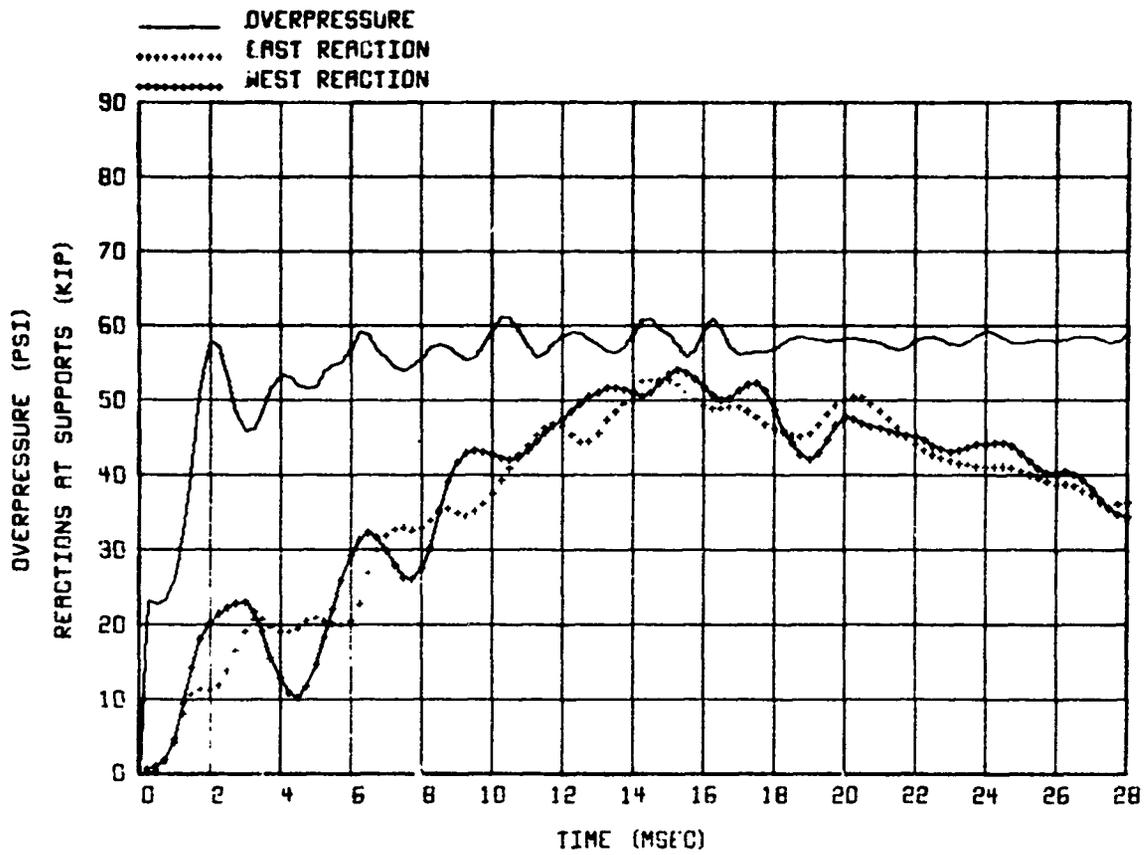
FIGURE C-5. LCAD AND REACTION VS. TIME, BEAM WE 6.
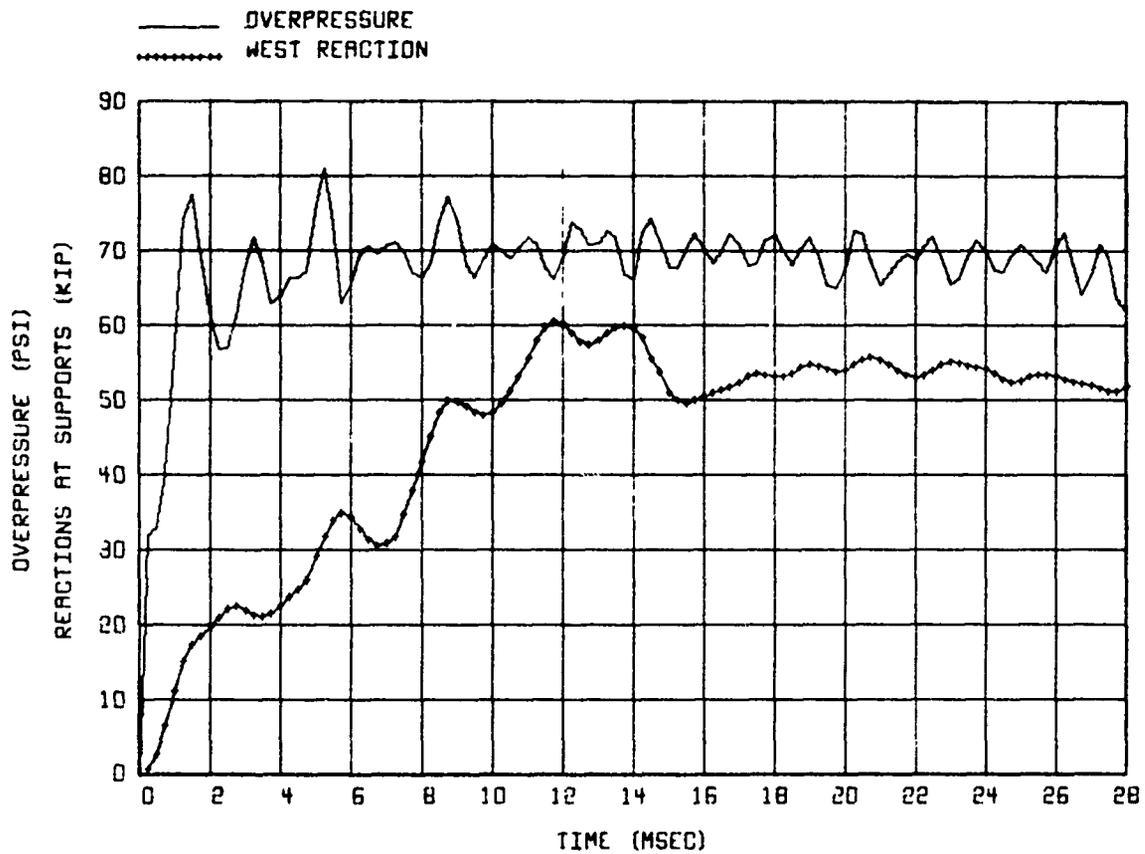
FIGURE C-6. LOAD AND REACTION VS. TIME, BEAM WE12.
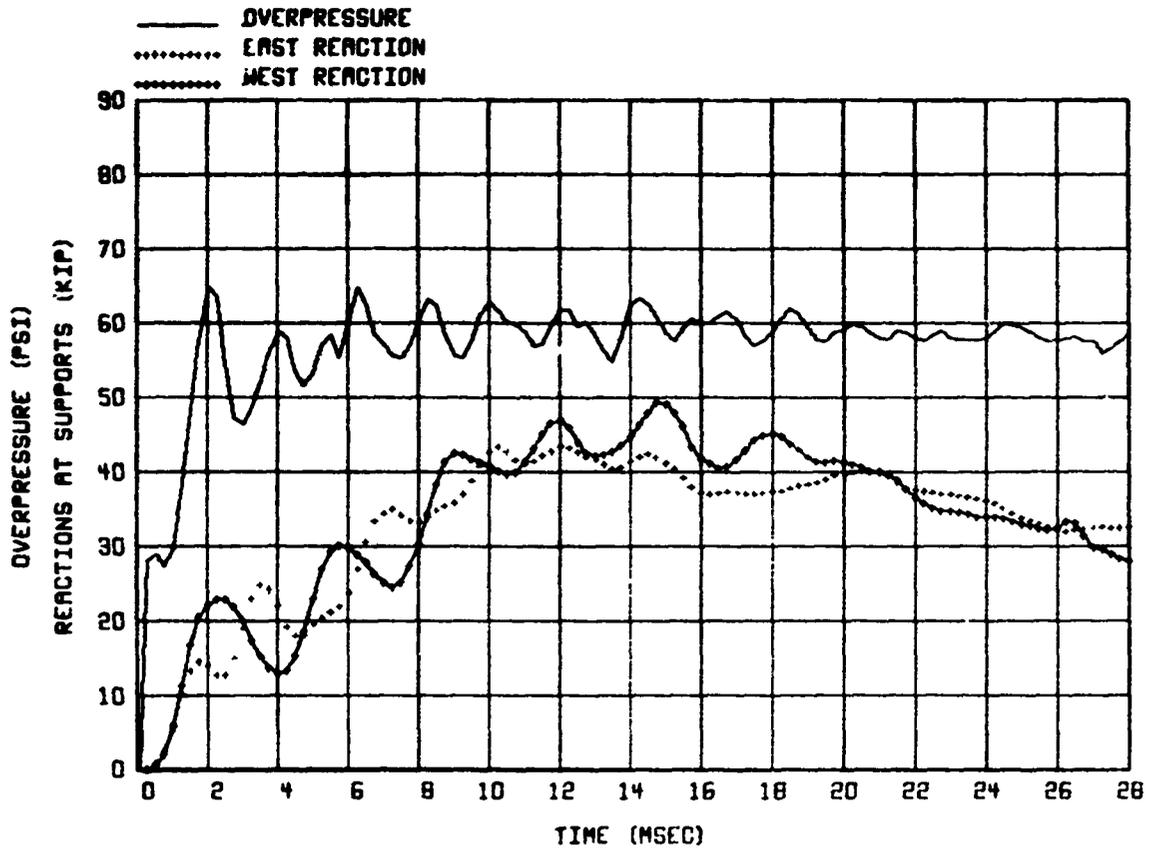
FIGURE D-7. LOAD AND REACTION VS TIME, BEAM DE 2.
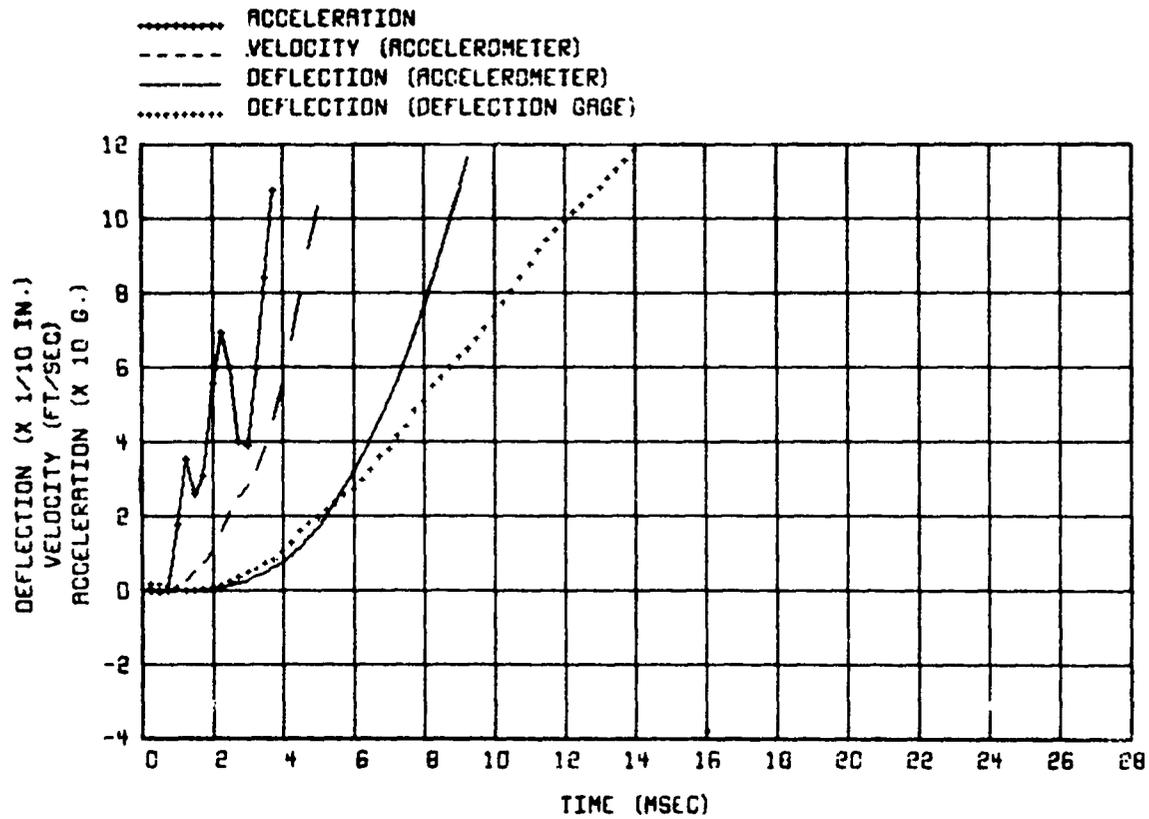
FIGURE D-8. MOTION AT THE CENTER OF THE SPAN, BEAM WE 1

70

ACCELERATION
VELOCITY (ACCELEROMETER)
DEFLECTION (ACCELEROMETER)
DEFLECTION (DEFLECTION GAGE)
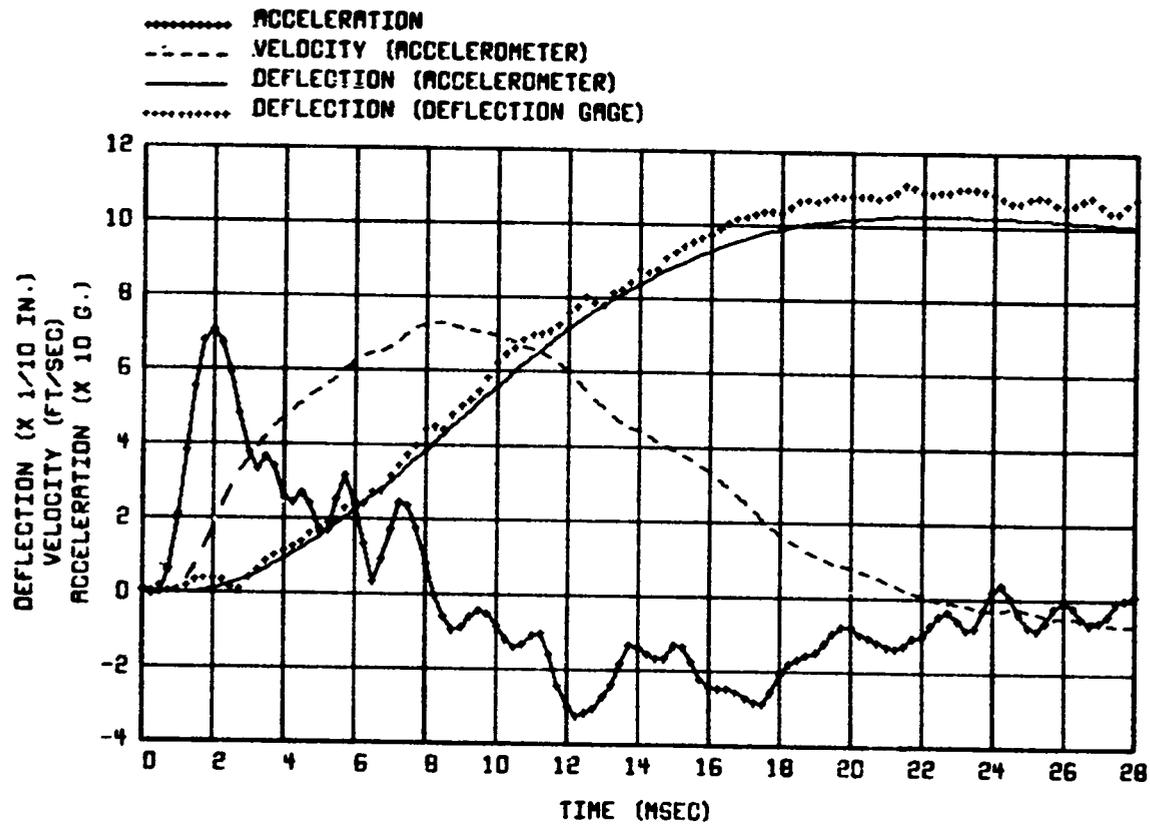
FIGURE D-9. MOTION AT THE CENTER OF THE SPAN, BEAM WE 2.

ACCELERATION
VELOCITY (ACCELEROMETER)
DEFLECTION (ACCELEROMETER)
DEFLECTION (DEFLECTION GAGE)
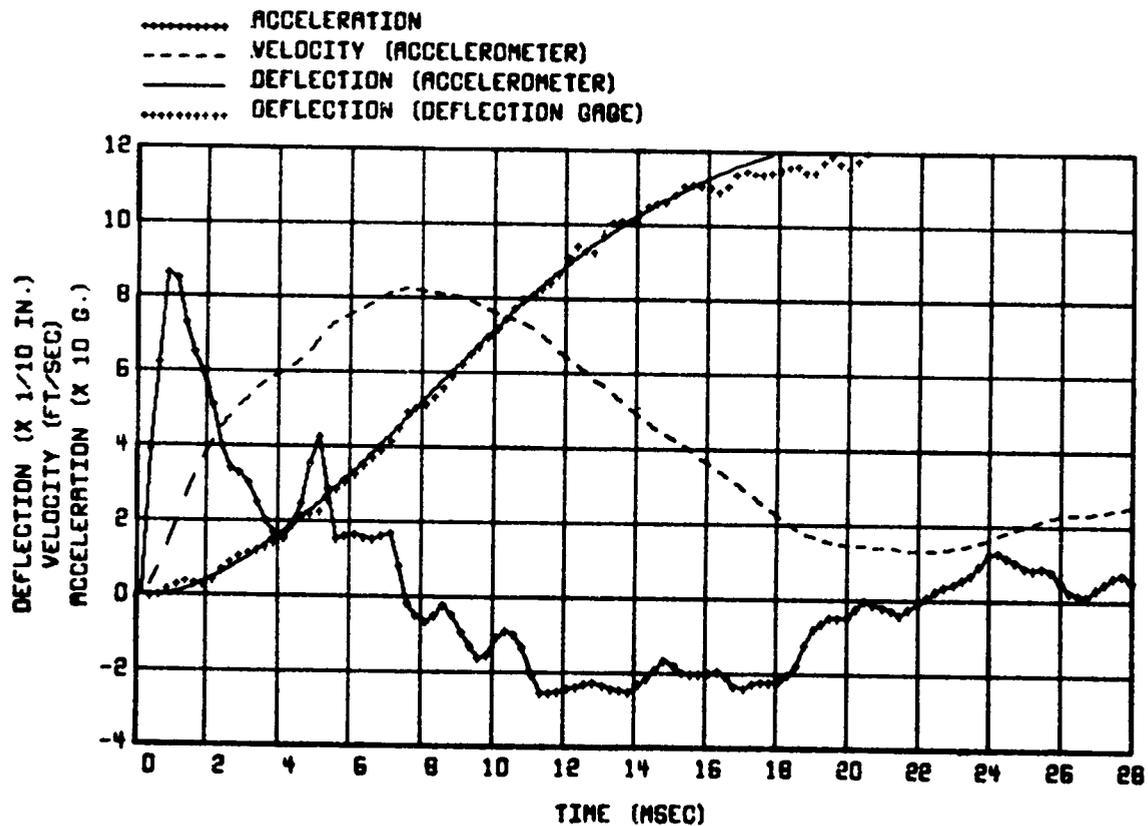
FIGURE D-10. MOTION AT THE CENTER OF THE SPAN, BEAM WE 3.

71
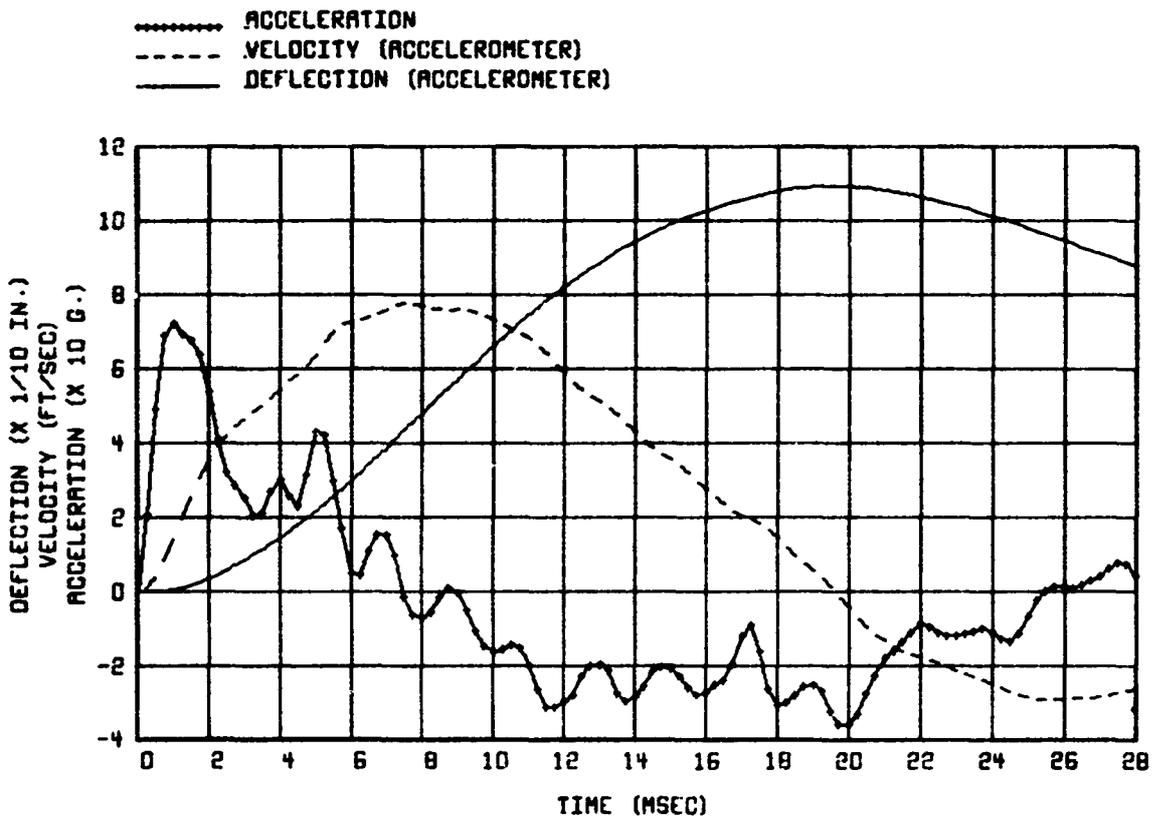
FIGURE D-11. MOTION AT THE CENTER OF THE SPAN, BEAM WE 5.
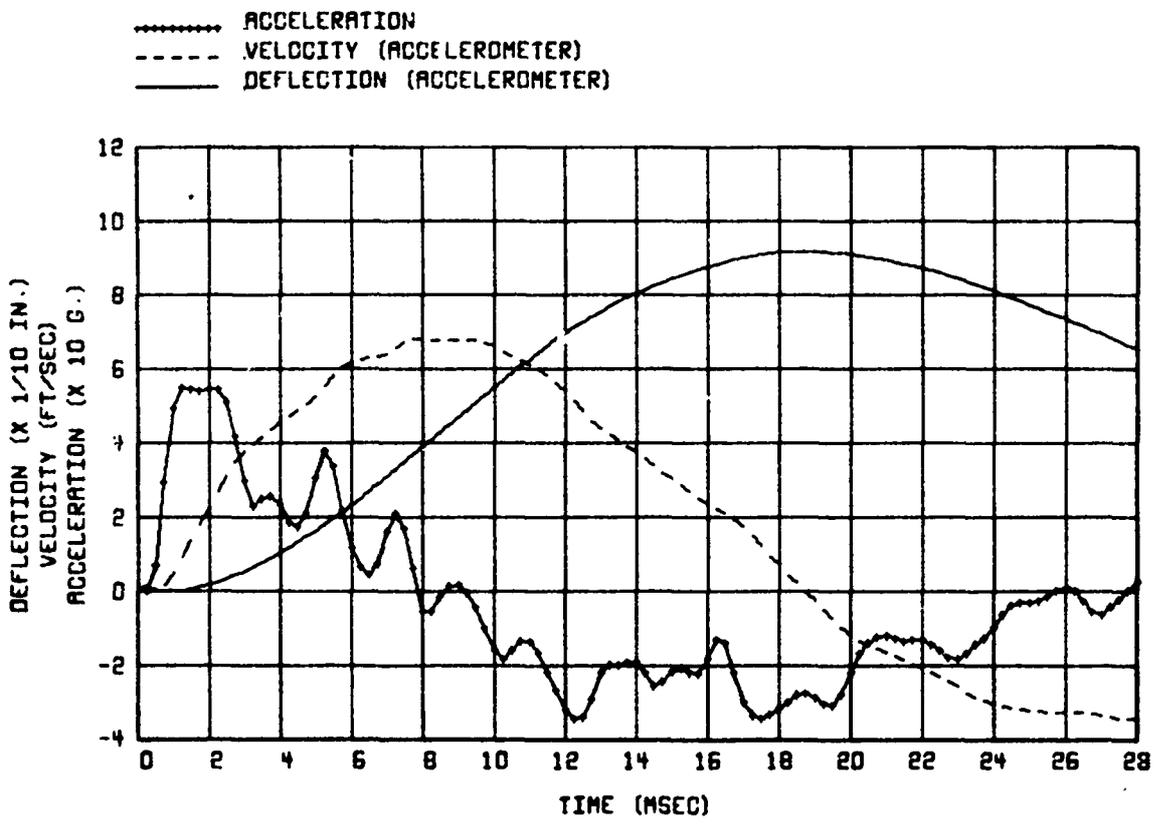
FIGURE D-12. MOTION AT THE CENTER OF THE SPAN, BEAM WE 6.
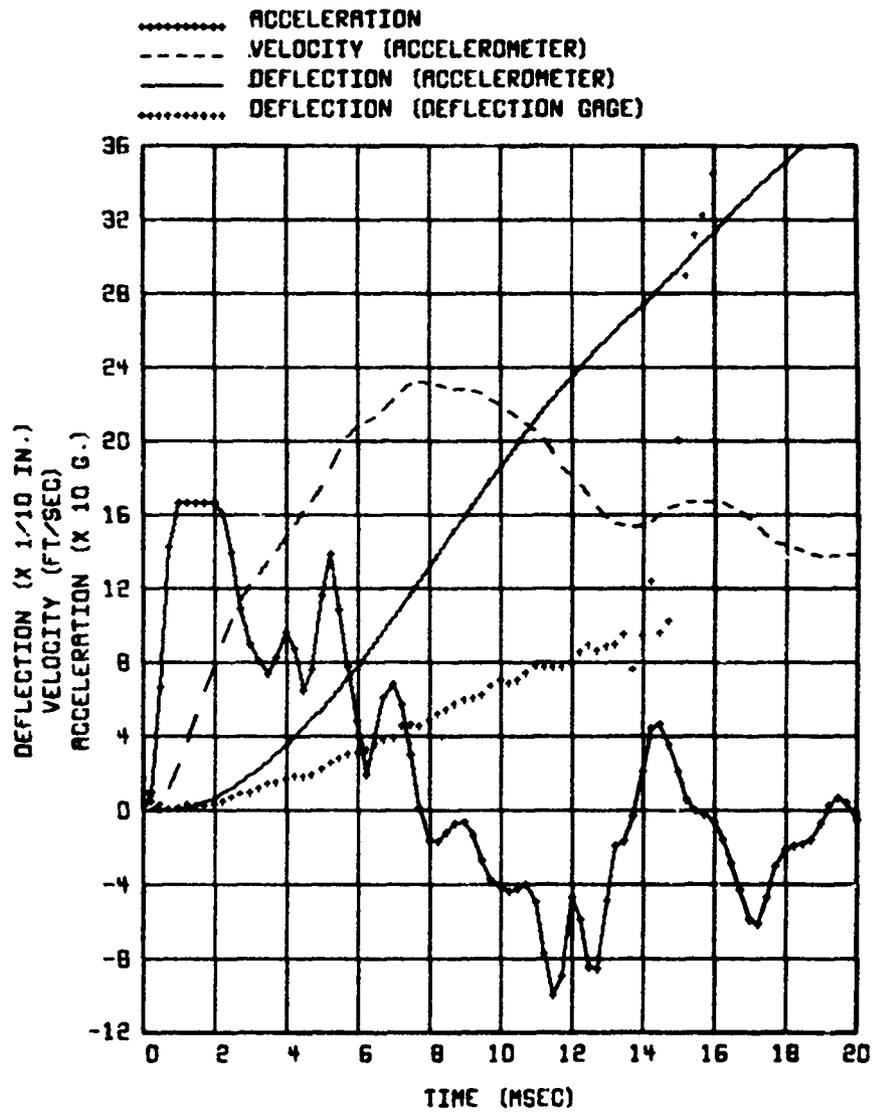
FIGURE D-13. MOTION AT THE CENTER OF THE SPAN, BEAM OE 2.
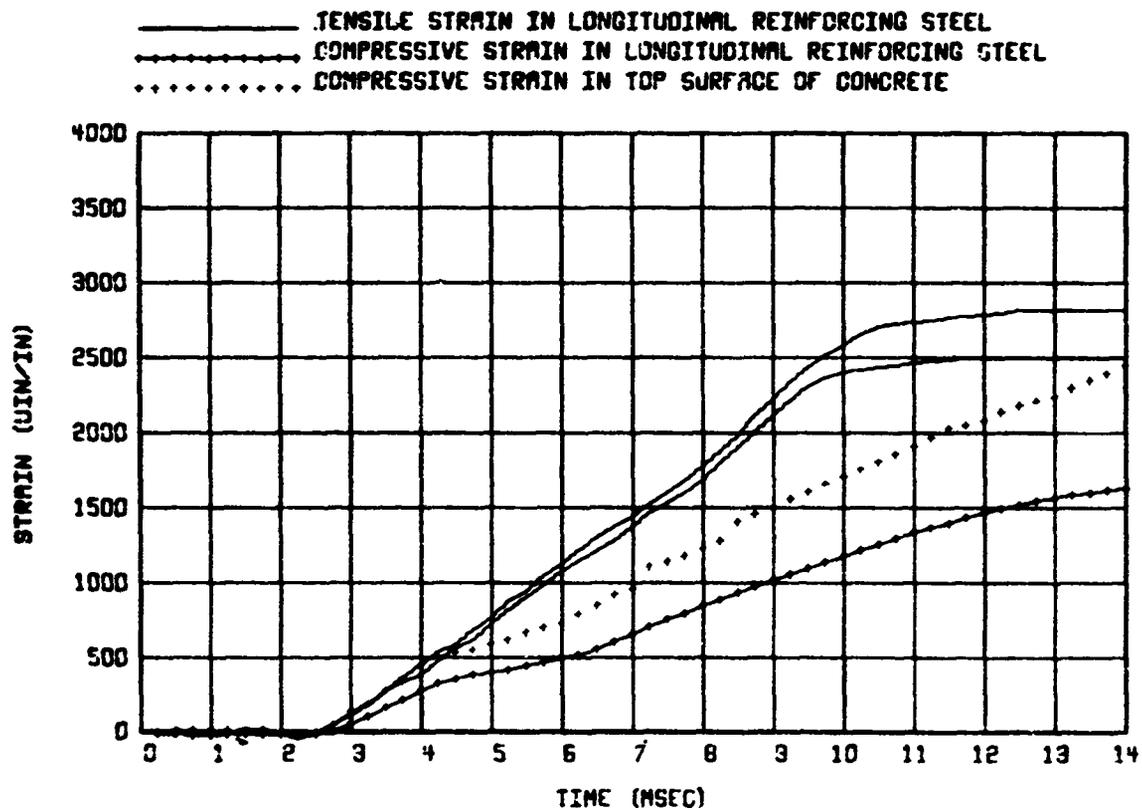
FIGURE D-14. STRAINS AT THE CENTER OF THE SPAN, BEAM WE 1.
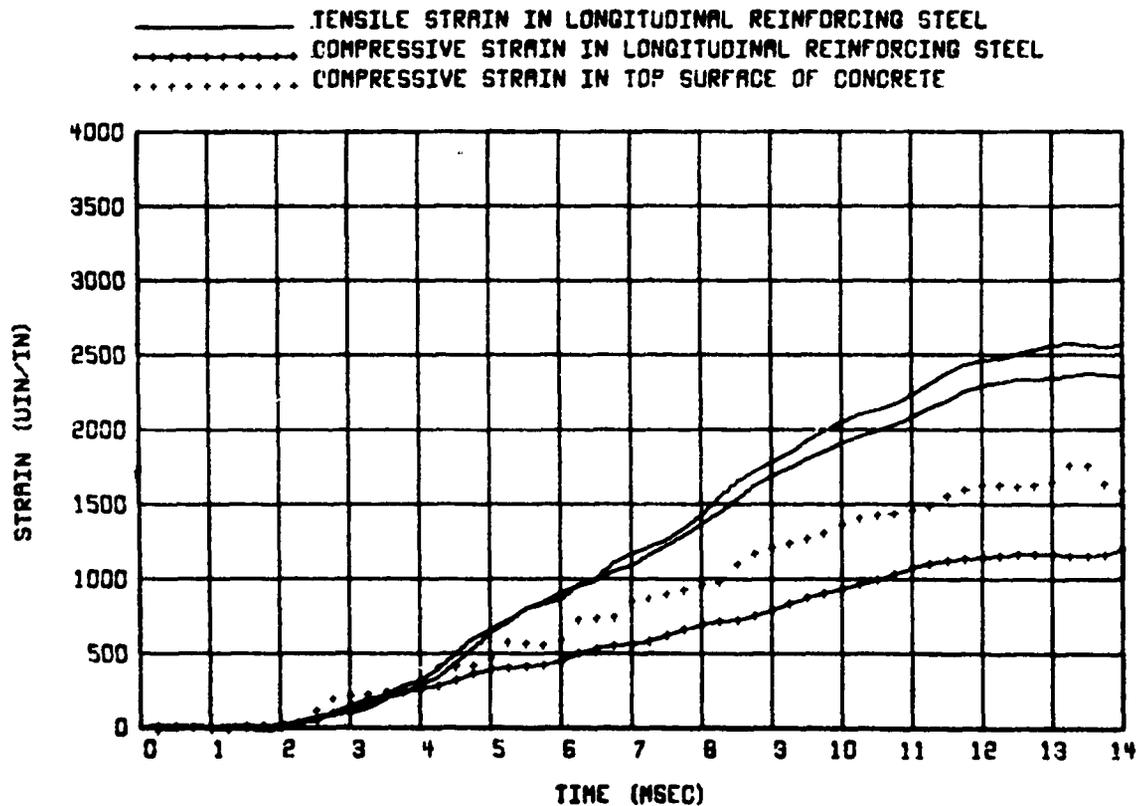
FIGURE D-15. STRAINS AT THE CENTER OF THE SPAN, BEAM WE 2.
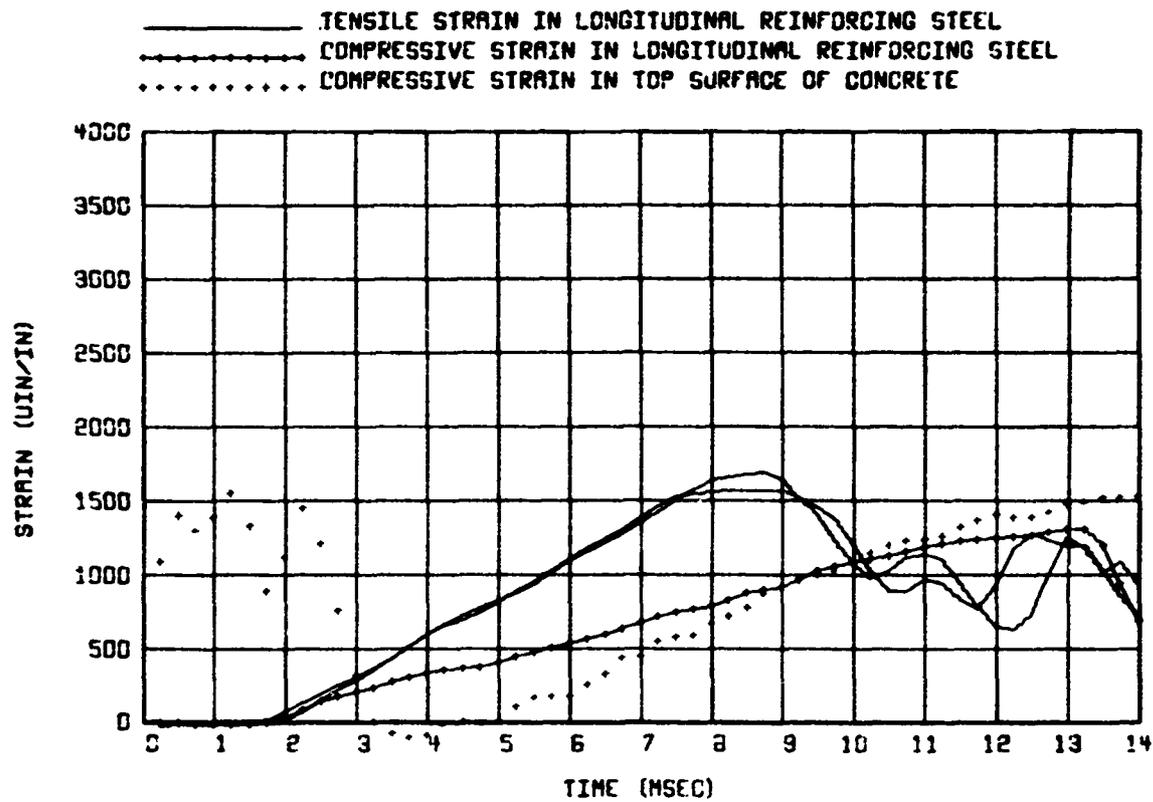
FIGURE D-16. STRAINS AT THE CENTER OF THE SPAN, BEAM WE 3.
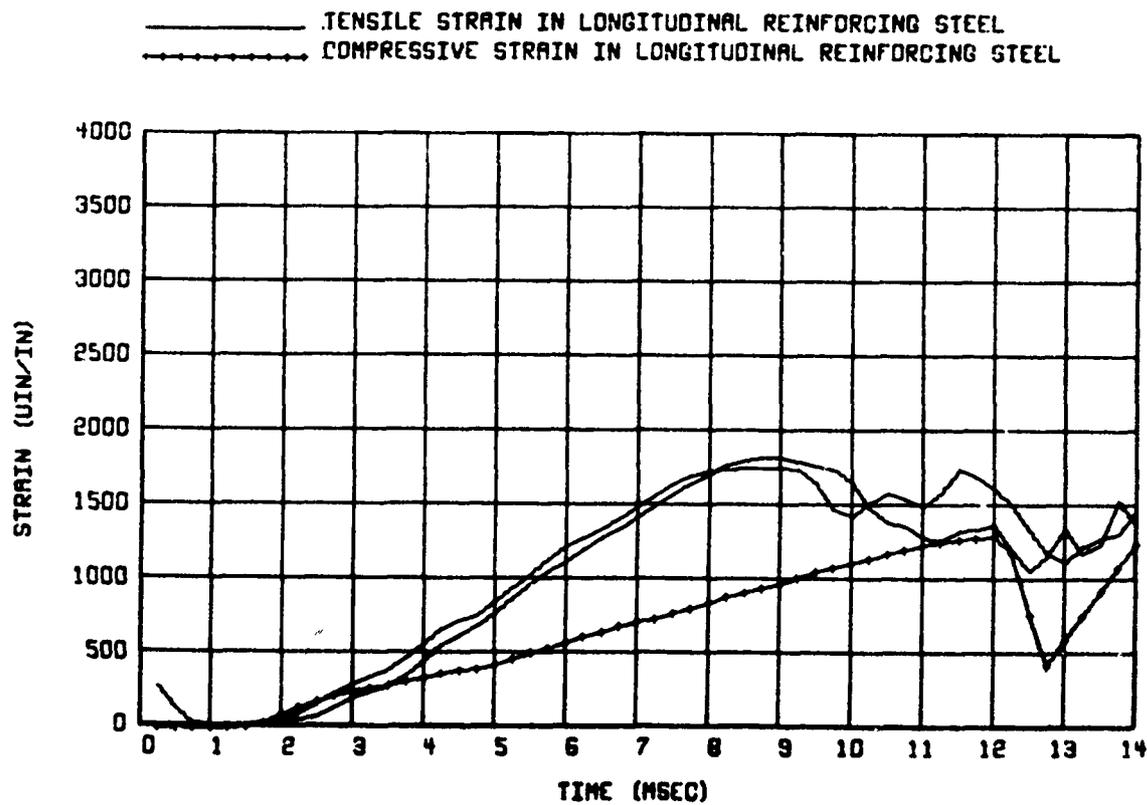
FIGURE D-17. STRAINS AT THE CENTER OF THE SPAN, BEAM WE 5.

TENSILE STRAIN IN LONGITUDINAL REINFORCING STEEL
COMPRESSIVE STRAIN IN LONGITUDINAL REINFORCING STEEL
COMPRESSIVE STRAIN IN TOP SURFACE OF CONCRETE
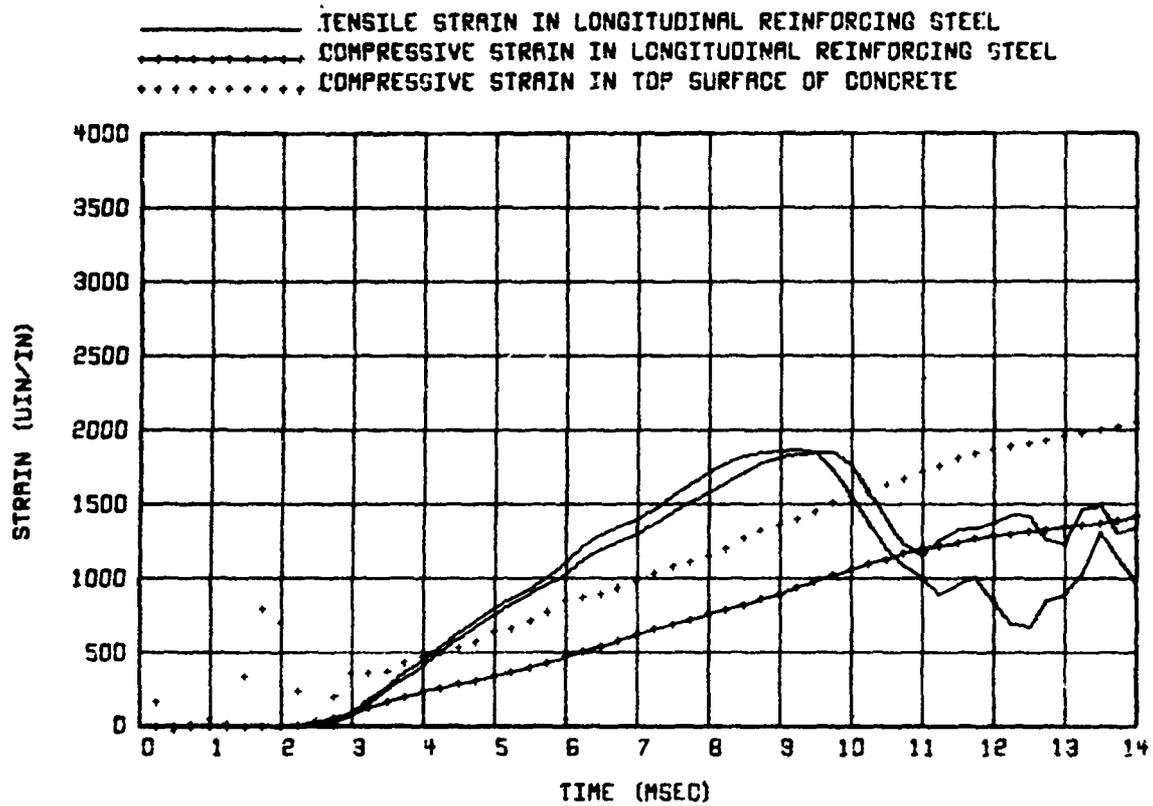
FIGURE D-18. STRAINS AT THE CENTER OF THE SPAN, BEAM WE 6.

TENSILE STRAIN IN LONGITUDINAL REINFORCING STEEL
COMPRESSIVE STRAIN IN LONGITUDINAL REINFORCING STEEL
COMPRESSIVE STRAIN IN TOP SURFACE OF CONCRETE
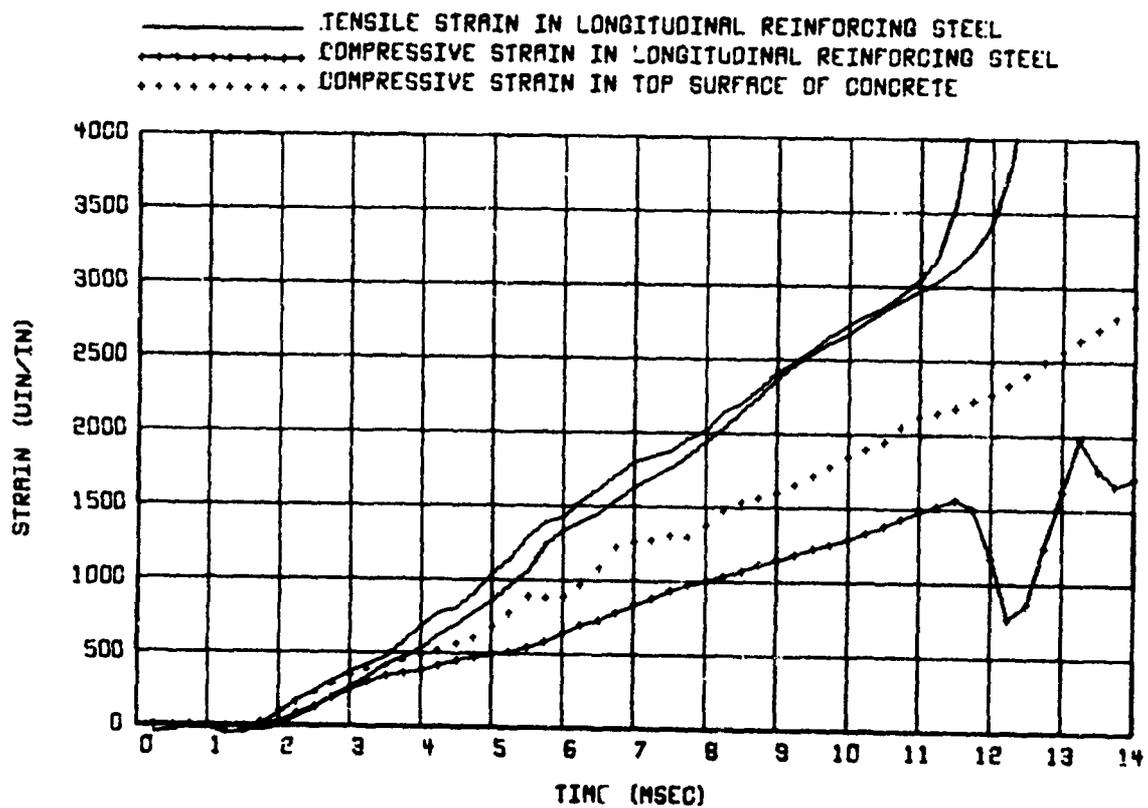
FIGURE D-19. STRAINS AT THE CENTER OF THE SPAN, BEAM WE 12.
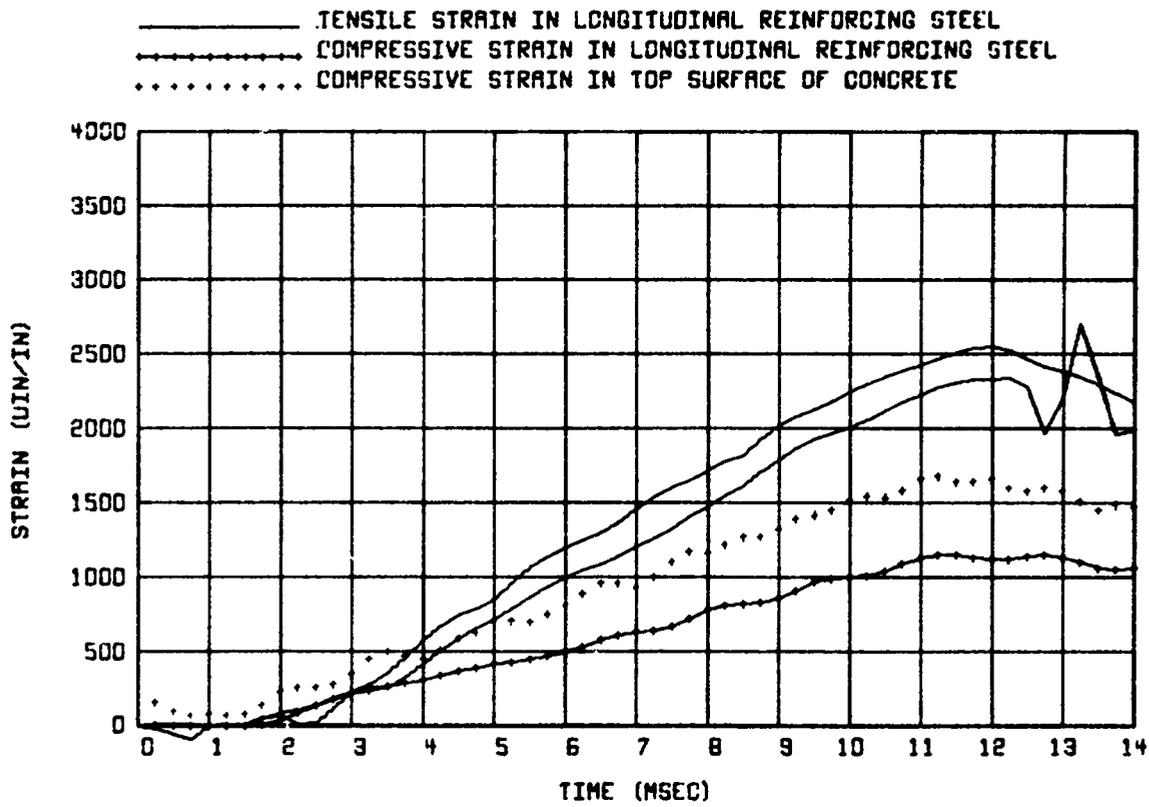
FIGURE D-20. STRAINS AT THE CENTER OF THE SPAN, BEAM DE 2.
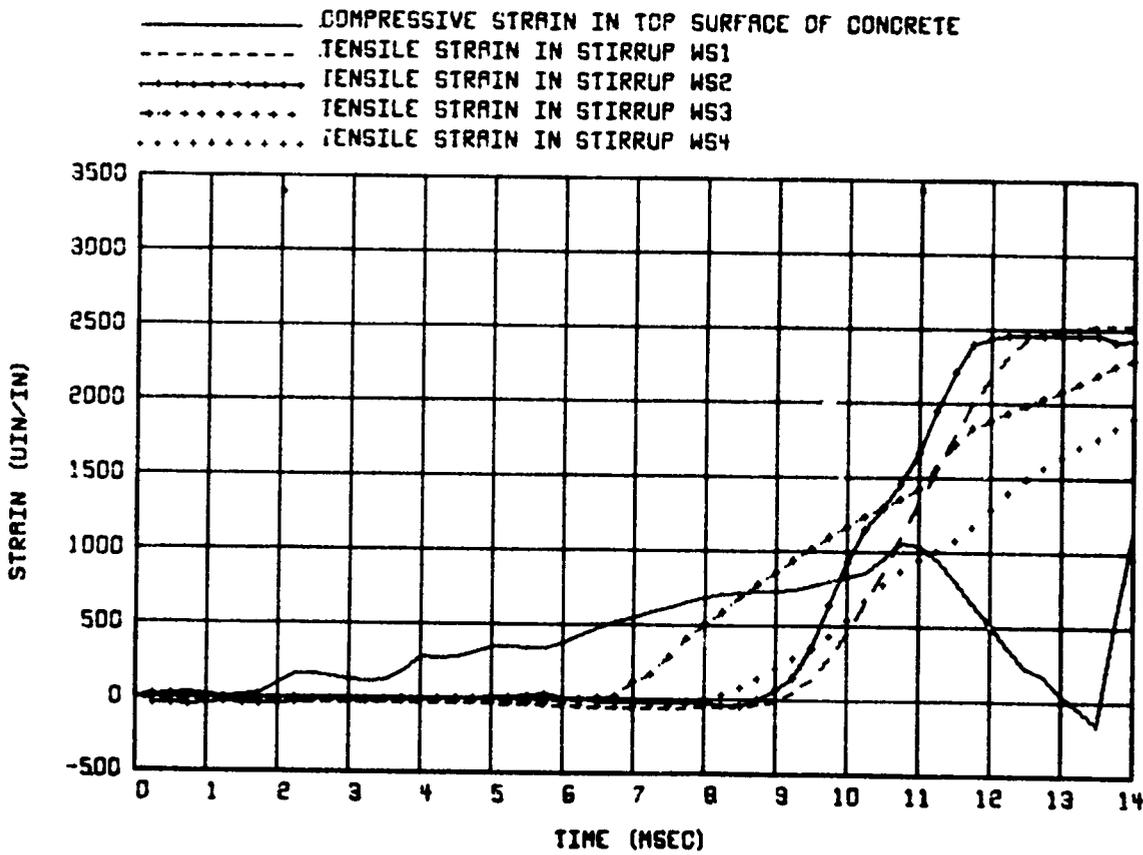
FIGURE D-21. STRAINS AT THE EAST END OF BEAM WE 1.

COMPRESSIVE STRAIN IN TOP SURFACE OF CONCRETE
TENSILE STRAIN IN STIRRUP WS1
TENSILE STRAIN IN STIRRUP WS2
TENSILE STRAIN IN STIRRUP WS3
TENSILE STRAIN IN STIRRUP WS4
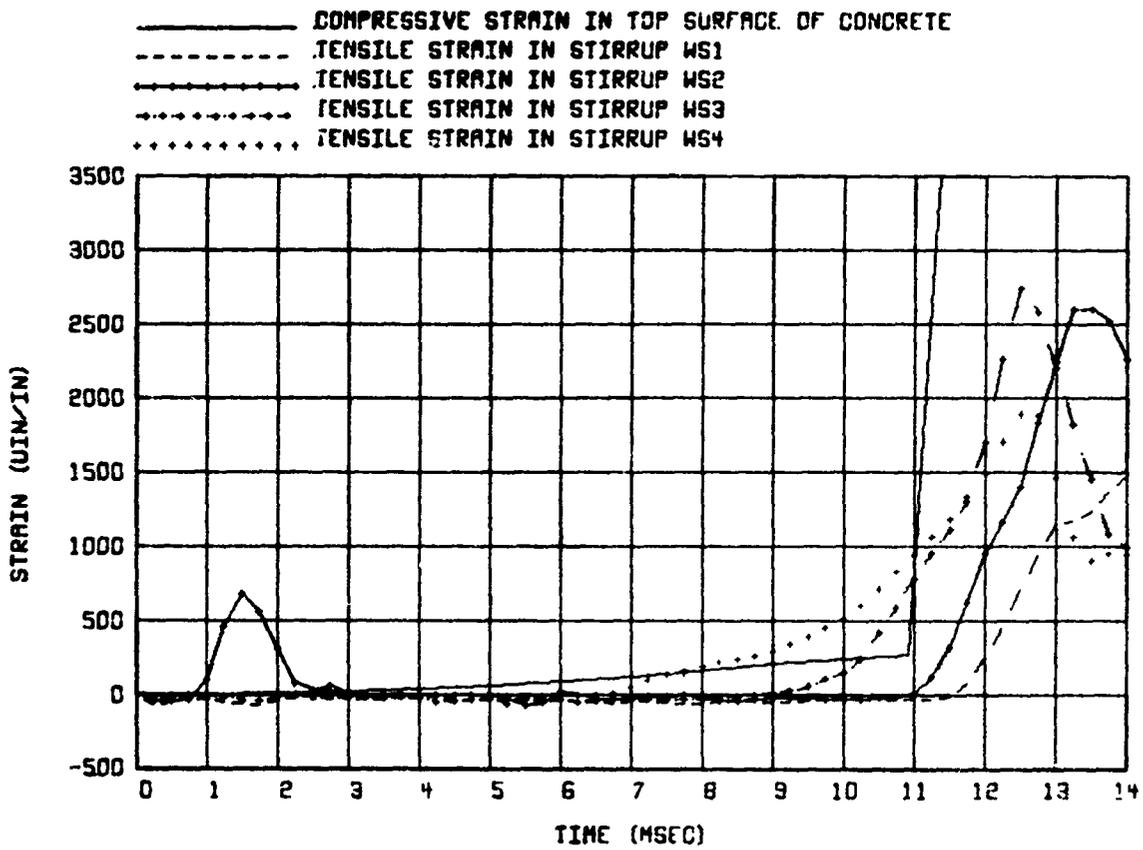
FIGURE D-22. STRAINS AT THE EAST END OF BEAM WE 2.

COMPRESSIVE STRAIN IN TOP SURFACE OF CONCRETE
TENSILE STRAIN IN STIRRUP WS1
TENSILE STRAIN IN STIRRUP WS2
TENSILE STRAIN IN STIRRUP WS3
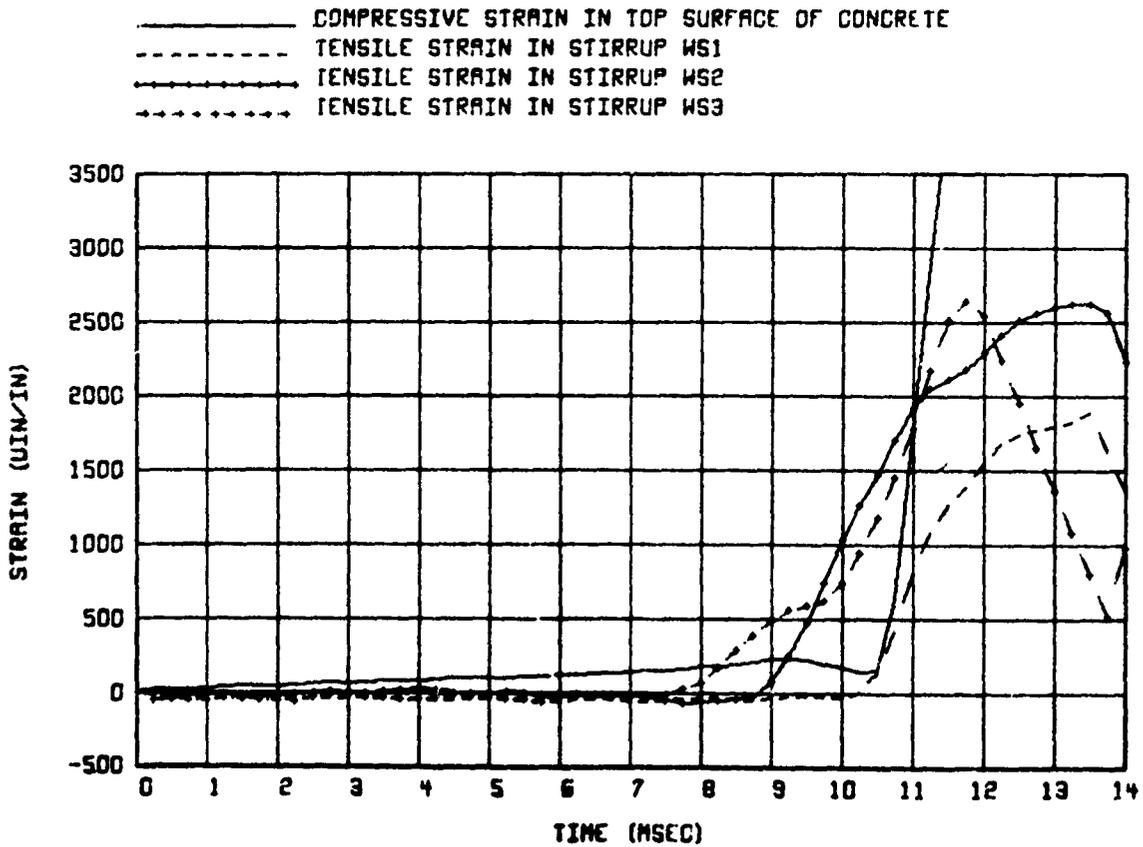
FIGURE D-23. STRAINS AT THE EAST END OF BEAM WE 3.

78
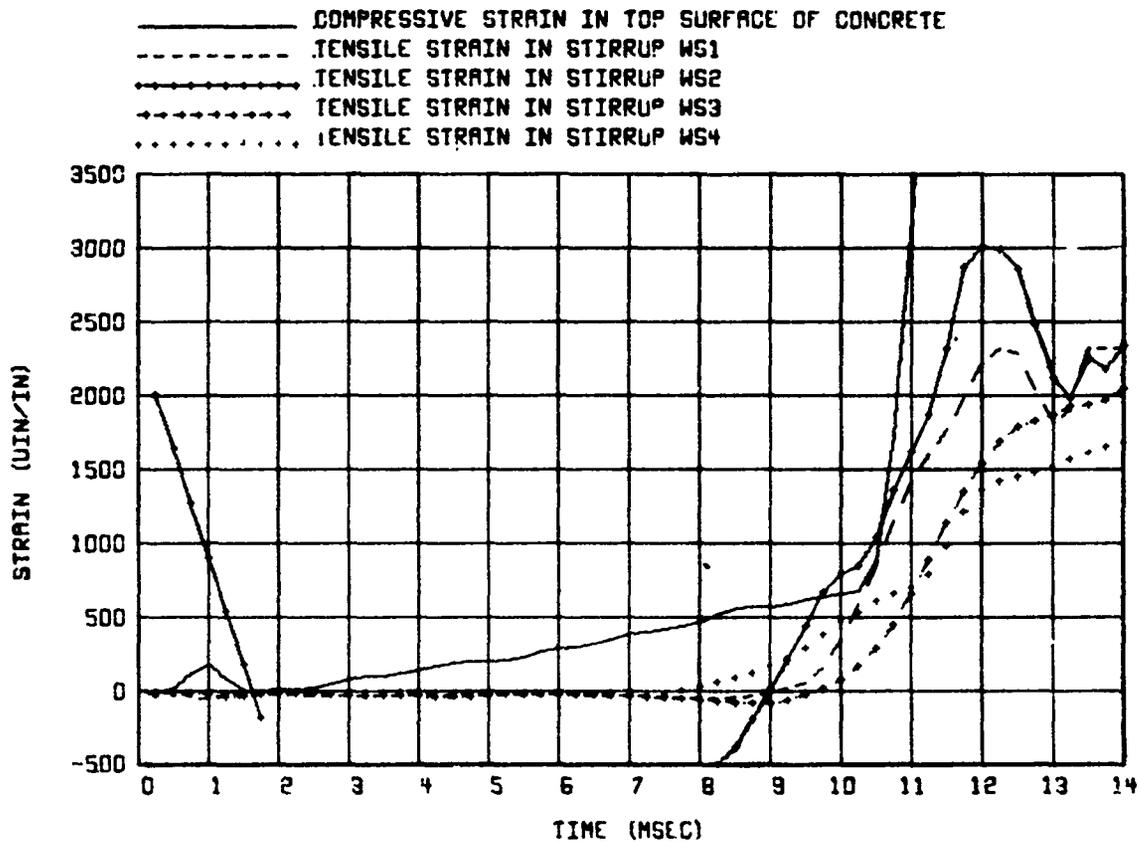
FIGURE D-24. STRAINS AT THE EAST END OF BEAM WE 5.
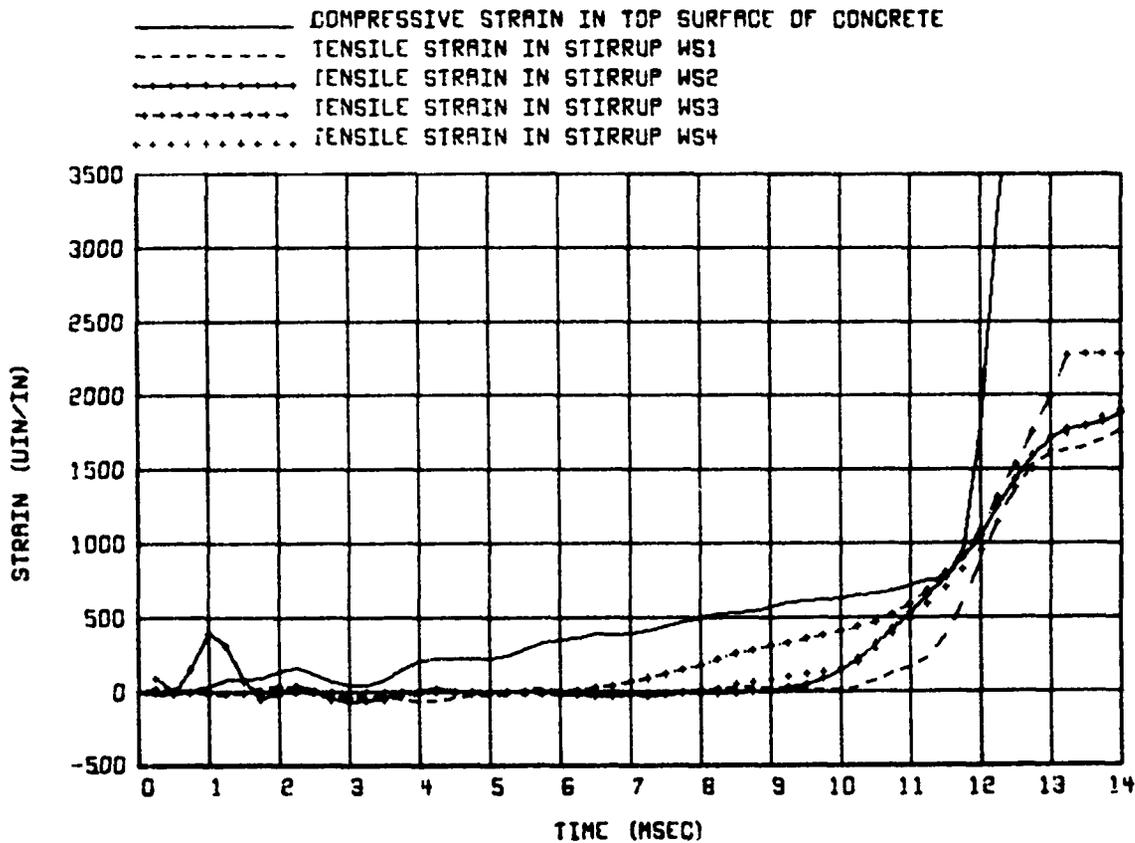
FIGURE D-25. STRAINS AT THE EAST END OF BEAM WE 6
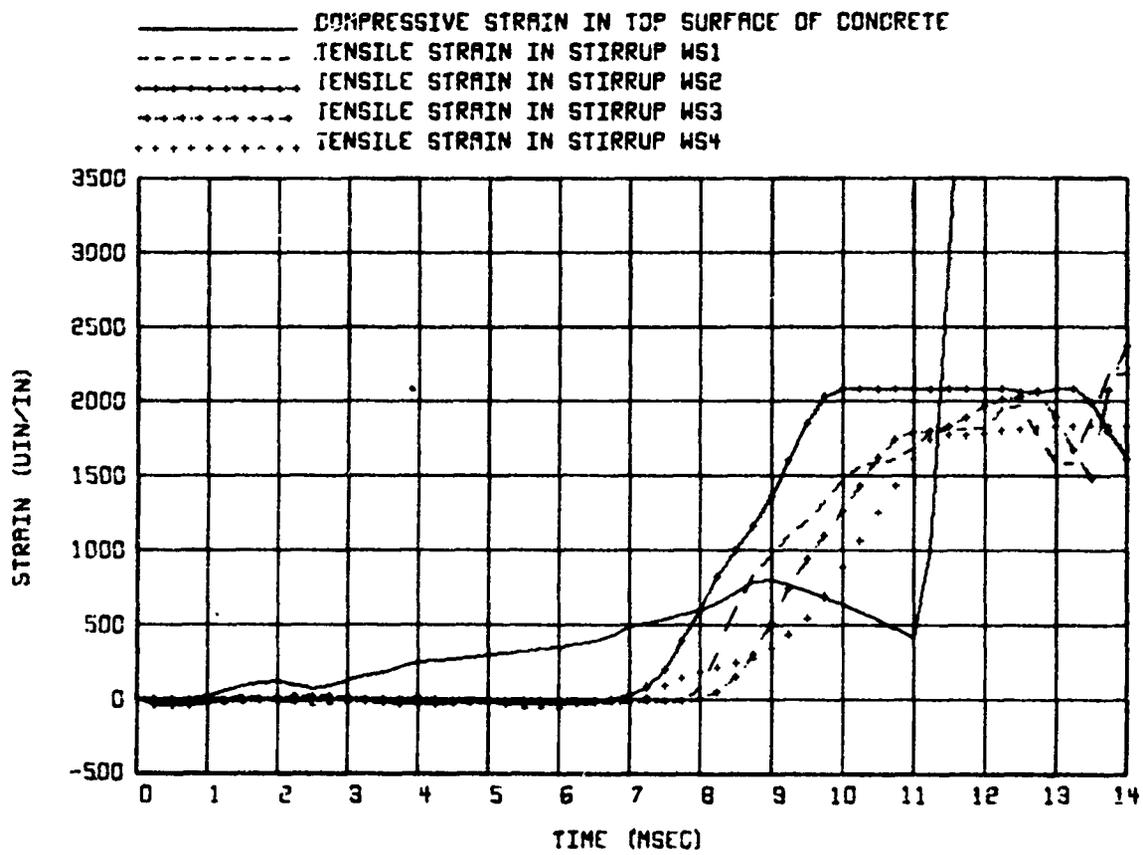
FIGURE D-26. STRAINS AT THE EAST END OF BEAM WE 12.

NOTE. THIS BEAM DID NOT HAVE ANY STIRRUPS NEAR
THE CRITICAL SECTION AT THE EAST END.
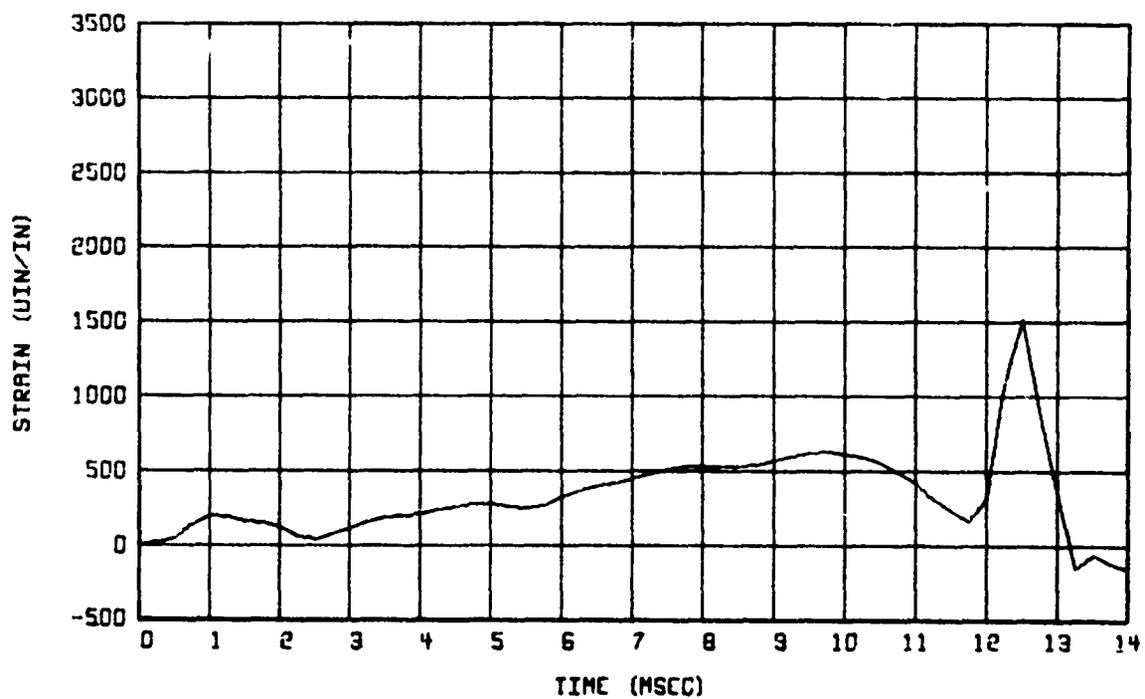
FIGURE D-27. COMPRESSIVE STRAIN IN THE TOP SURFACE
OF THE CONCRETE AT THE EAST END OF BEAM DE 2.

Legend

C Compressive strain in concrete at remote fiber   MD Midspan deflection
CS Compressive strain in compression steel   TS Tensile strain in tension steel
DC Change in total depth at critical section   WS Tensile strain in stirrup
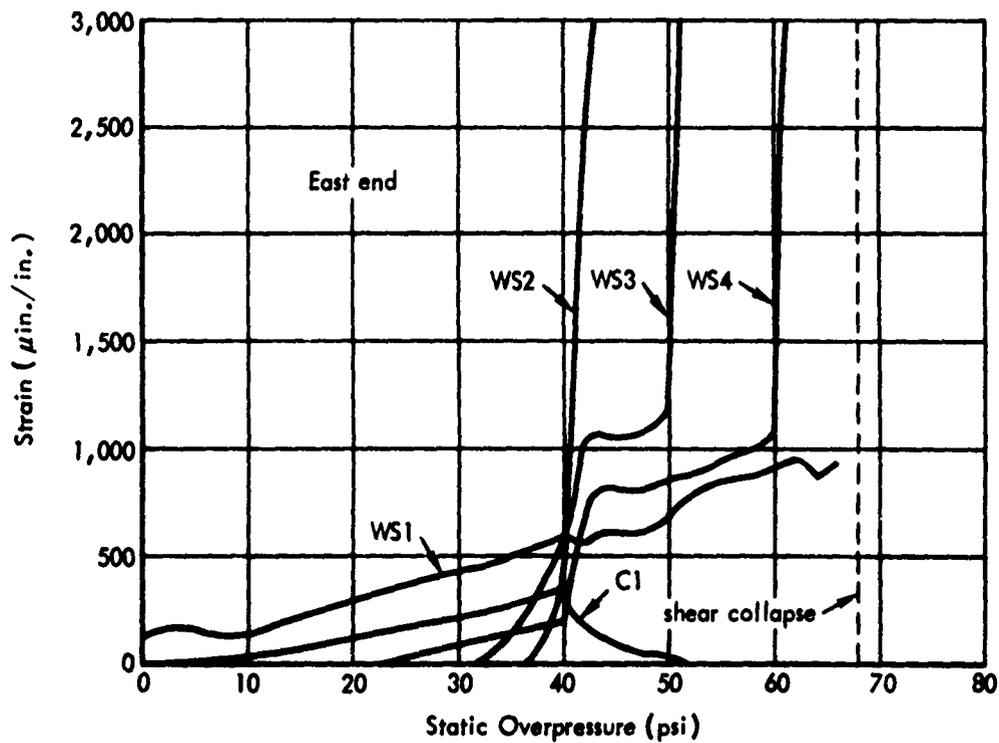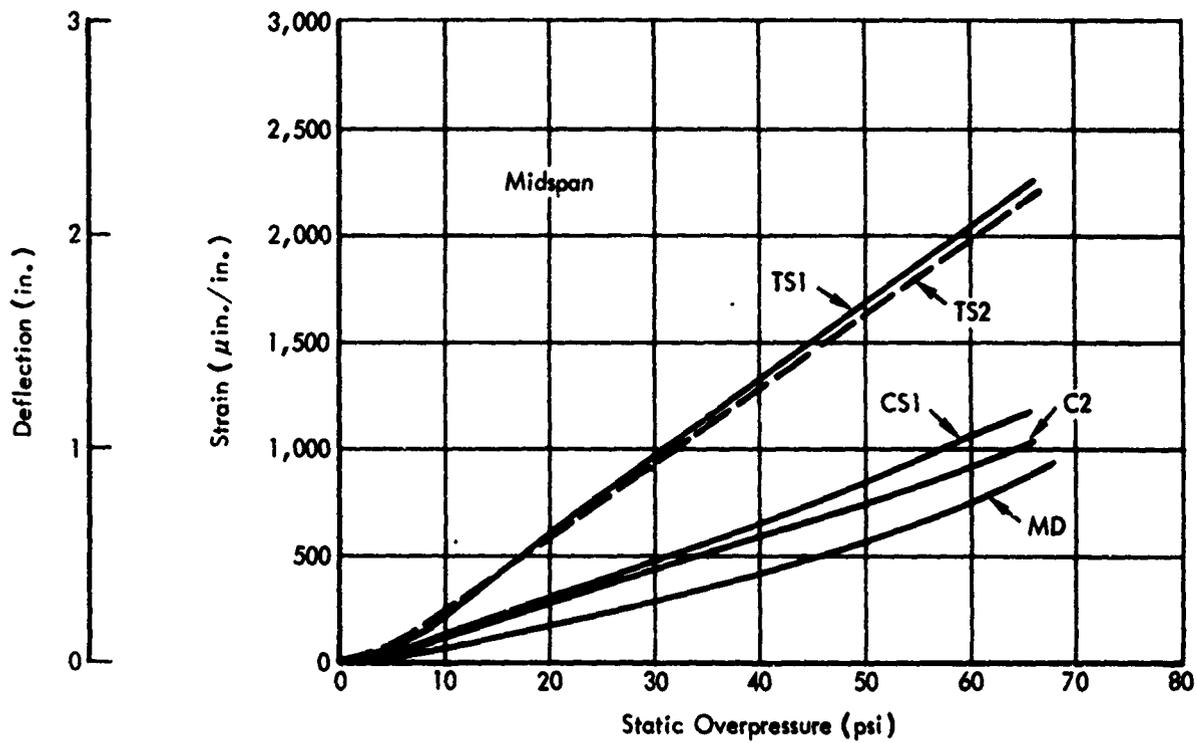
Figure D-28. Strain and deflection versus static overpressure, beam WE7.
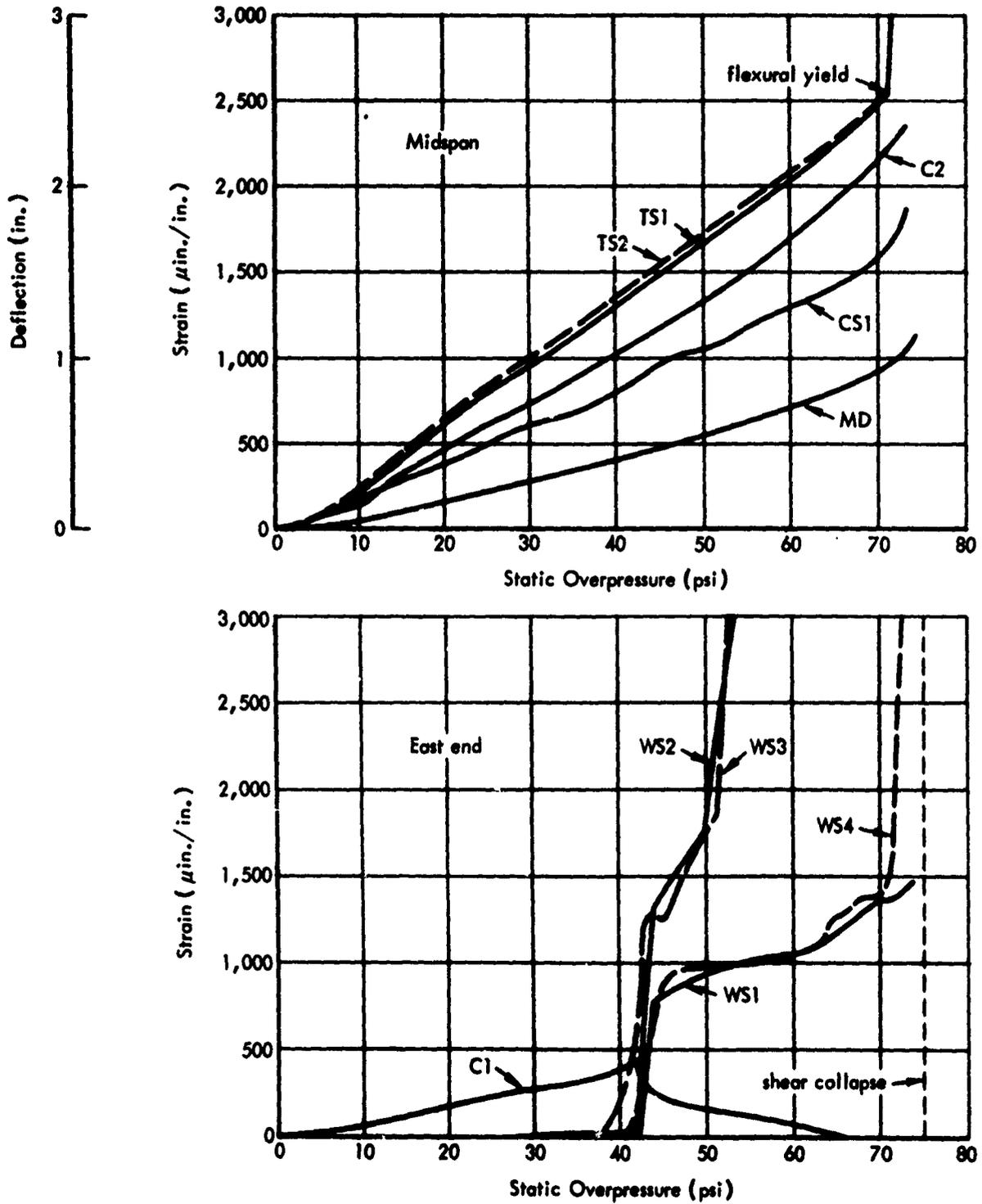
Figure D-29. Strain and deflection versus static overpressure, beam WE8.

Legend

C   Compressive strain in concrete at remote fiber   MD   Midspan deflection
CS Compressive strain in compression steel   TS   Tensile strain in tension steel
DC Change in total depth at critical section   WS   Tensile strain in stirrup
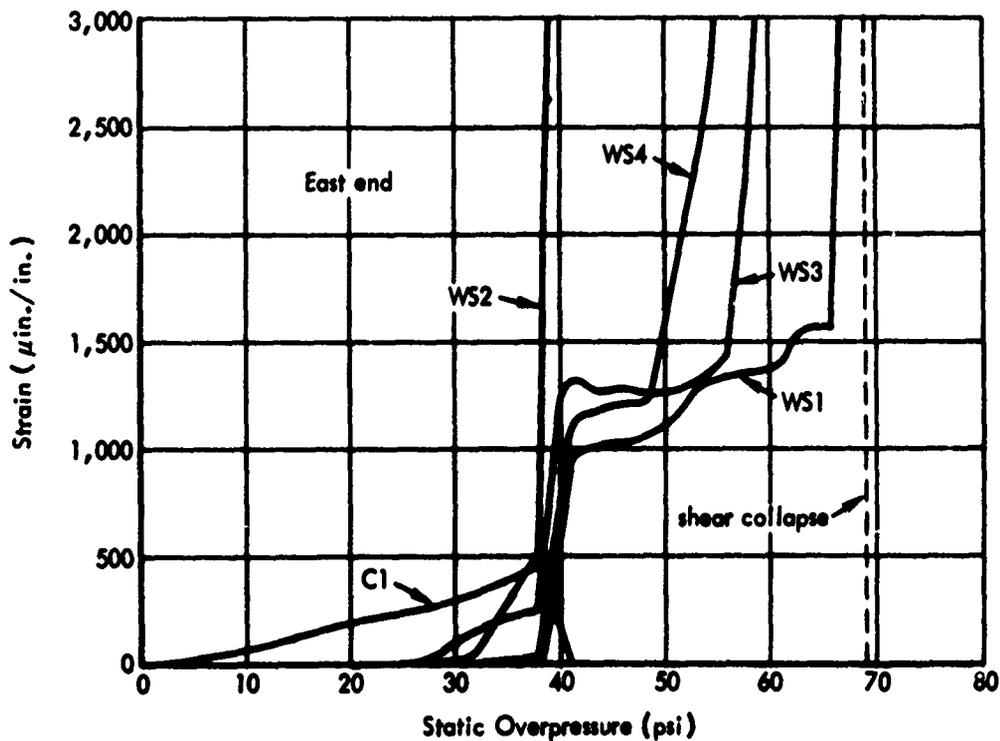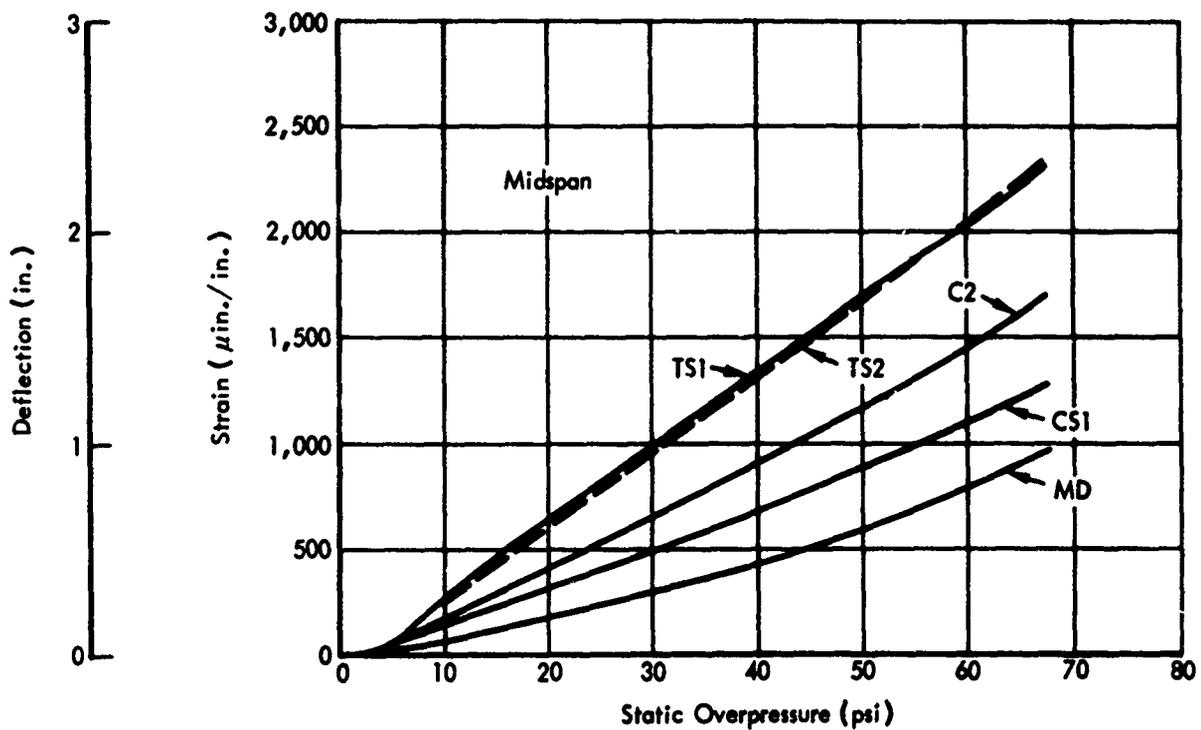
Figure D-30.   Strain and deflection versus static overpressure, beam WE9.

C   Compressive strain in concrete at remote fiber   MD   Midspan deflection
CS   Compressive strain in compression steel   TS   Tensile strain in tension steel
DC   Change in total depth at critical section   WS   Tensile strain in stirrup
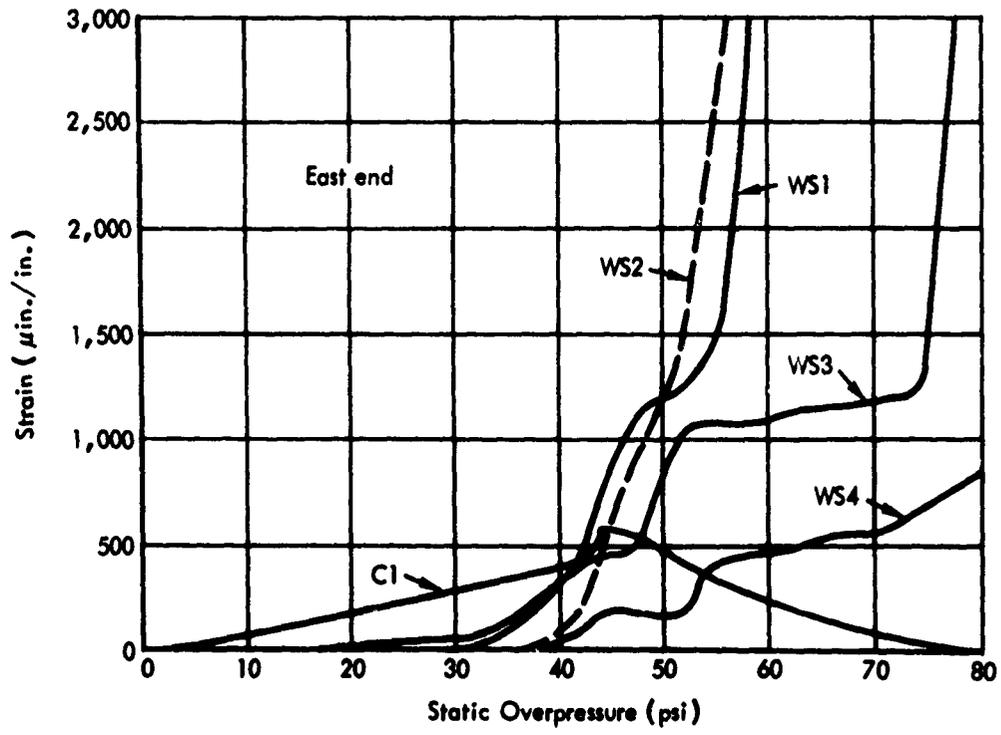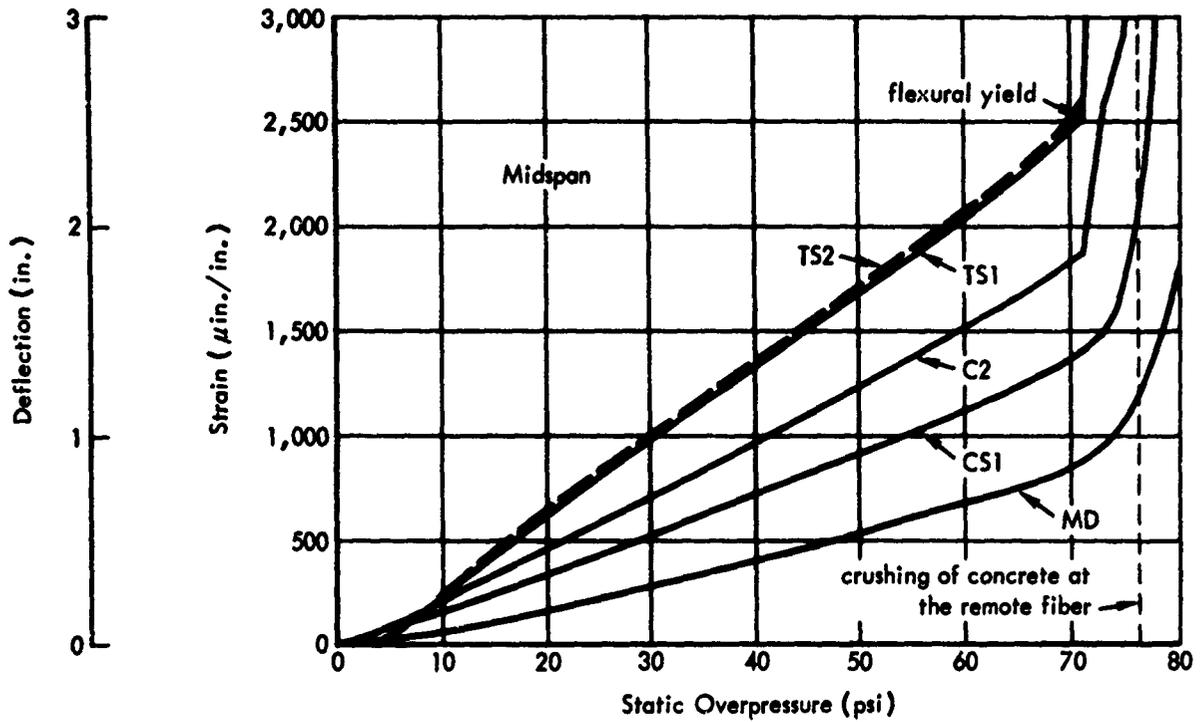
Figure D-31.   Strain and deflection versus static overpressure, beam WE10.

84

Legend

C   Compressive strain in concrete at remote fiber   MD Midspan deflection
CS Compressive strain in compression steel   TS Tensile strain in tension steel
DC Change in total depth at critical section   WS Tensile strain in stirrup
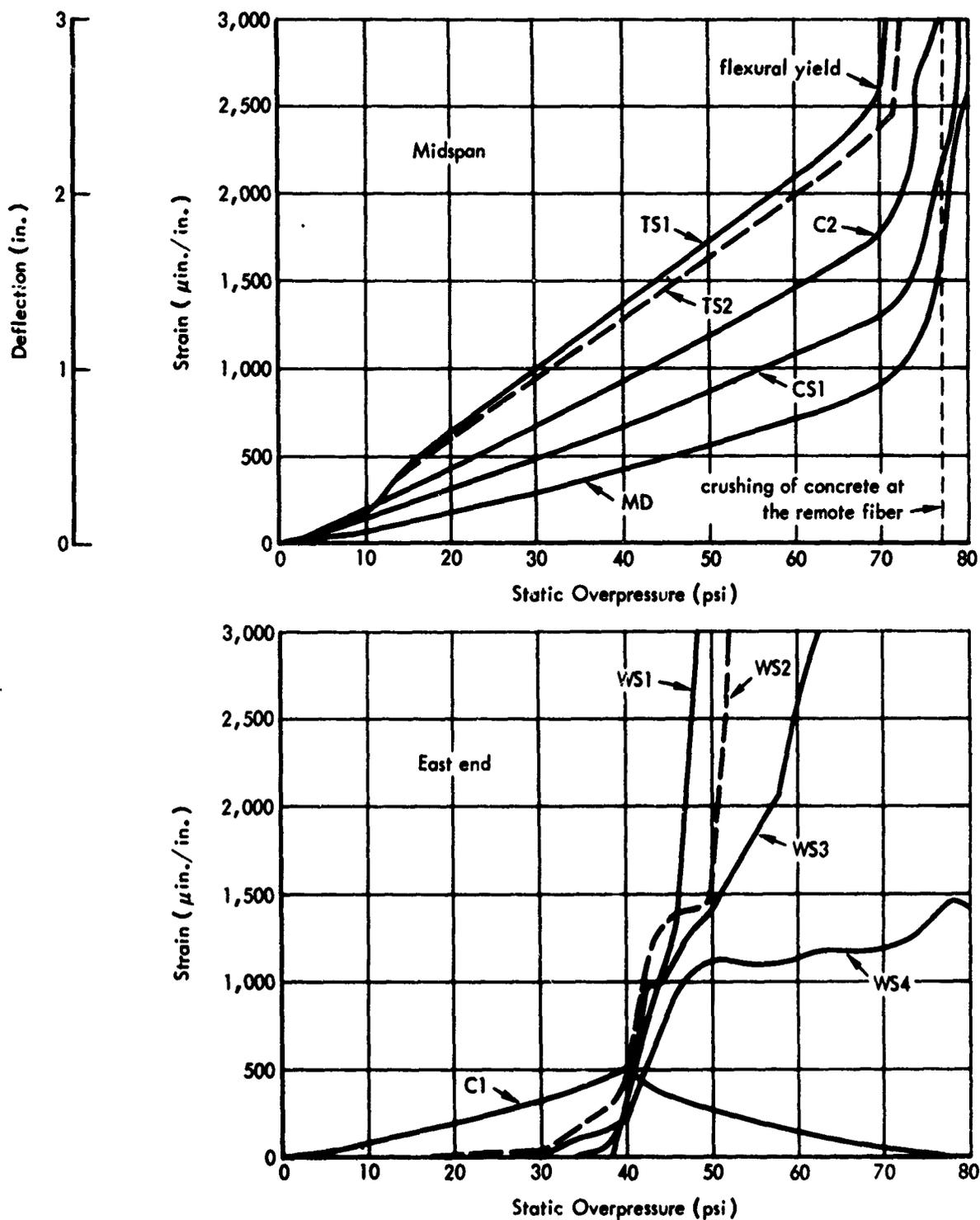
Figure D-32. Strain and deflection versus static overpressure, beam WE11.
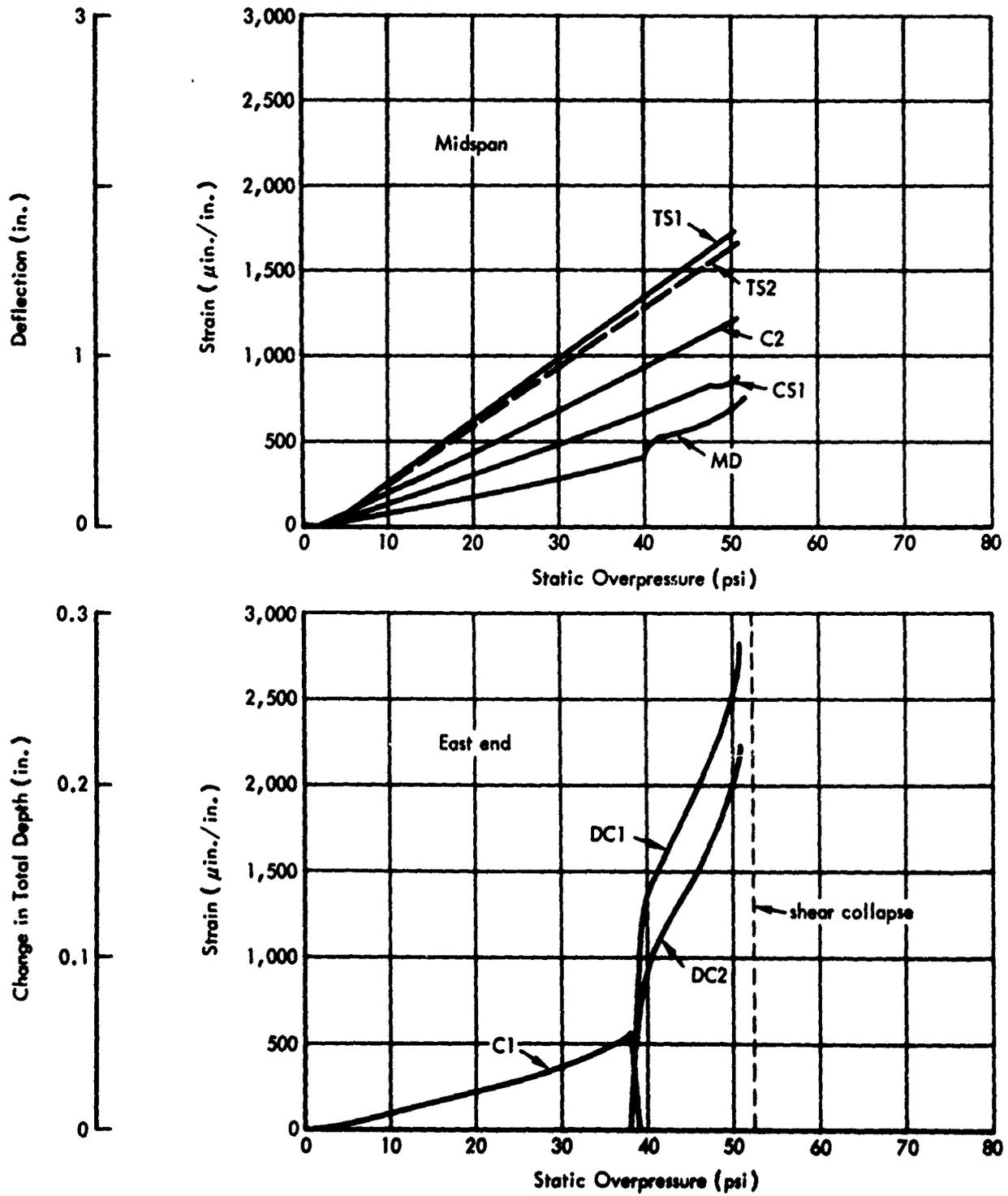
Figure D-33. Strain and deflection versus static overpressure, beam OE3.

REFERENCES

1. U. S. Naval Civil Engineering Laboratory. Technical Report R-395: Dynamic shear strength of reinforced concrete beams - Part I, by William A. Keenan. Port Hueneme, Calif., Dec. 1965.

2. ACI-ASCE Committee 326. "Shear and diagonal tension, Part 1," American Concrete Institute Journal, Proceedings, vol. 59, no. 1, Jan. 1962, pp. 1-30.

————. Part 2, American Concrete Institute Journal, Proceedings, vol. 59, no. 2, Feb. 1962, pp. 277-333.

————. Part 3, American Concrete Institute Journal, Proceedings, vol. 59, no. 3, Mar. 1962, pp. 353-395.

3. W. A. Shaw and J. R. Allgood. "An atomic blast simulator," Society for Experimental Stress Analysis, Proceedings, vol. 17, no. 1, 1959, pp. 127-134.

4. American Concrete Institute, Committee 318. Building code requirements for reinforced concrete. Detroit, Mich., American Concrete Institute, June 1963. (Also abridged in American Concrete Institute Journal, Proceedings, vol. 60, no. 7, July 1963, pp. 809-816.)

5. U. S. Army Engineer Waterways Experiment Station. Miscellaneous Paper no. 6-609: Dynamic and static tests of plain concrete specimens, by R. L. Lundeen. Vicksburg, Miss., Nov. 1963.

6. U. S. Naval Civil Engineering Laboratory. Technical Report R-331: NCEL dynamic testing machine, by W. L. Cowell. Port Hueneme, Calif., Oct. 1964.

7. ————. Data handling complex for the NCEL blast simulator, by W. Wilcoxson and A. Jackson. Port Hueneme, Calif. (Unpublished report)

DOCUMENT CONTROL DATA · R&D

(Security classification of title, body of abstract and indexing annotation must be entered when the overall report is classified)

1. ORIGINATING ACTIVITY (Corporate author)	2a. REPORT SECURITY CLASSIFICATION
U. S. Naval Civil Engineering Laboratory Port Hueneme, California 93041	Unclassified **2b GROUP**

3. REPORT TITLE

Dynamic Shear Strength of Reinforced Concrete Beams — Part II

4. DESCRIPTIVE NOTES *(Type of report and inclusive dates)*

Not final; January 1965 to June 1966

5. AUTHOR(S) *(Last name, first name, initial)*

Seabold, Richard H.

6. REPORT DATE	7a. TOTAL NO. OF PAGES	7b. NO OF REFS
January 1967	87	7

8a. CONTRACT OR GRANT NO. DASA-13.018	9a. ORIGINATOR'S REPORT NUMBER(S)
b. PROJECT NO. Y-F008-08-02-110	TR-502
c.	9b. OTHER REPORT NO(S) *(Any other numbers that may be assigned this report)*
d.	

10. AVAILABILITY/LIMITATION NOTICES

Distribution of this document is unlimited. Copies available at the Clearinghouse (CFSTI) $3.00

11. SUPPLEMENTARY NOTES	12. SPONSORING MILITARY ACTIVITY DASA-NAVFAC

13. ABSTRACT

A series of reinforced concrete beams was tested to study shear and diagonal tension in beams under dynamic load. The tests constitute the second phase of a continuing program to determine criteria for the minimum amount of web reinforcement required for developing the ultimate flexural resistance of beams, and to determine the difference between these criteria for static and dynamic loading.

The primary objectives of this Part II series of tests were (1) to determine the minimum amount of web reinforcement necessary to force flexural failures; (2) to confirm, under uniformly distributed loads, a formula for shear resistance recommended by a joint committee of the American Concrete Institute (ACI) and the American Society of Civil Engineers (ASCE), which is based on the analysis of data from tests with concentrated loads; (3) to confirm the coefficients suggested in Part I of this program for the dynamic increase in shearing strength; and (4) to study the influence of stirrup arrangement and type of loading on the location of the critical diagonal tension crack.

Fifteen beams were tested, eight loaded dynamically and seven statically. Each beam was simply supported and all loads were uniformly distributed. Twelve beams contained web reinforcement in the region of the critical section, and three had none there. Major variables were type of loading (static and dynamic), magnitude of dynamic load, and stirrup spacing.

It was found that the shear strength of reinforced concrete beams is greater under dynamic load than under static load, and that a formula for designing simply supported beams subjected to concentrated static loads recommended by the joint ACI-ASCE committee could be modified for designing simply supported beams subjected to uniformly distributed dynamic loads.

DD FORM 1473 0101-807-6800

14. KEY WORDS	LINK A		LINK B		LINK C	
	ROLE	WT	ROLE	WT	ROLE	WT
Dynamic tests						
Static tests						
Shear strength						
Reinforced concrete						
Beams (structural)						
Reinforcing steel						

INSTRUCTIONS

1. ORIGINATING ACTIVITY: Enter the name and address of the contractor, subcontractor, grantee, Department of Defense activity or other organization *(corporate author)* issuing the report.

2a. REPORT SECURITY CLASSIFICATION: Enter the overall security classification of the report. Indicate whether "Restricted Data" is included. Marking is to be in accordance with appropriate security regulations.

2b. GROUP: Automatic downgrading is specified in DoD Directive 5200.10 and Armed Forces Industrial Manual. Enter the group number. Also, when applicable, show that optional markings have been used for Group 3 and Group 4 as authorized.

3. REPORT TITLE: Enter the complete report title in all capital letters. Titles in all cases should be unclassified. If a meaningful title cannot be selected without classification, show title classification in all capitals in parenthesis immediately following the title.

4. DESCRIPTIVE NOTES: If appropriate, enter the type of report, e.g., interim, progress, summary, annual, or final. Give the inclusive dates when a specific reporting period is covered.

5. AUTHOR(S): Enter the name(s) of author(s) as shown on or in the report. Enter last name, first name, middle initial. If military, show rank and branch of service. The name of the principal author is an absolute minimum requirement.

6. REPORT DATE: Enter the date of the report as day, month, year; or month, year. If more than one date appears on the report, use date of publication.

7a. TOTAL NUMBER OF PAGES: The total page count should follow normal pagination procedures, i.e., enter the number of pages containing information.

7b. NUMBER OF REFERENCES: Enter the total number of references cited in the report.

8a. CONTRACT OR GRANT NUMBER: If appropriate, enter the applicable number of the contract or grant under which the report was written.

8b, 8c, & 8d. PROJECT NUMBER: Enter the appropriate military department identification, such as project number, subproject number, system numbers, task number, etc.

9a. ORIGINATOR'S REPORT NUMBER(S): Enter the official report number by which the document will be identified and controlled by the originating activity. This number must be unique to this report.

9b. OTHER REPORT NUMBER(S): If the report has been assigned any other report numbers *(either by the originator or by the sponsor)*, also enter this number(s).

10. AVAILABILITY/LIMITATION NOTICES: Enter any limitations on further dissemination of the report, other than those

imposed by security classification, using standard statements such as:

(1) "Qualified requesters may obtain copies of this report from DDC."

(2) "Foreign announcement and dissemination of this report by DDC is not authorized."

(3) "U. S. Government agencies may obtain copies of this report directly from DDC. Other qualified DDC users shall request through

_____ ."

(4) "U. S. military agencies may obtain copies of this report directly from DDC. Other qualified users shall request through

_____ ."

(5) "All distribution of this report is controlled. Qualified DDC users shall request through

_____ ."

If the report has been furnished to the Office of Technical Services, Department of Commerce, for sale to the public, indicate this fact and enter the price, if known.

11. SUPPLEMENTARY NOTES: Use for additional explanatory notes.

12. SPONSORING MILITARY ACTIVITY: Enter the name of the departmental project office or laboratory sponsoring *(paying for)* the research and development. Include address.

13. ABSTRACT: Enter an abstract giving a brief and factual summary of the document indicative of the report, even though it may also appear elsewhere in the body of the technical report. If additional space is required, a continuation sheet shall be attached.

It is highly desirable that the abstract of classified reports be unclassified. Each paragraph of the abstract shall end with an indication of the military security classification of the information in the paragraph, represented as *(TS), (S), (C), or (U)*.

There is no limitation on the length of the abstract. However, the suggested length is from 150 to 225 words.

14. KEY WORDS: Key words are technically meaningful terms or short phrases that characterize a report and may be used as index entries for cataloging the report. Key words must be selected so that no security classification is required. Identifiers, such as equipment model designation, trade name, military project code name, geographic location, may be used as key words but will be followed by an indication of technical context. The assignment of links, roles, and weights is optional.